Titre: Title:	A Novel Approach to Determine Harmonic Distortions in Unbalanced Networks and Harmonic Filter Planning in Industrial Systems
Auteur: Author:	Ahmad Hosseinimanesh
Date:	2015
Type:	Mémoire ou thèse / Dissertation or Thesis
Référence: Citation:	Hosseinimanesh, A. (2015). A Novel Approach to Determine Harmonic Distortions in Unbalanced Networks and Harmonic Filter Planning in Industrial Systems [Mémoire de maîtrise, École Polytechnique de Montréal]. PolyPublie. https://publications.polymtl.ca/1962/

UNIVERSITÉ DE MONTRÉAL

A NOVEL APPROACH TO DETERMINE HARMONIC DISTORTIONS IN UNBALANCED NETWORKS AND HARMONIC FILTER PLANNING IN INDUSTRIAL SYSTEMS

AHMAD HOSSEINIMANESH

DÉPARTEMENT DE GÉNIE ÉLECTRIQUE

ÉCOLE POLYTECHNIQUE DE MONTRÉAL

MÉMOIRE PRÉSENTÉ EN VUE DE L'OBTENTION

DU DIPLÔME DE MAÎTRISE ÈS SCIENCES APPLIQUÉES

(GÉNIE ÉLECTRIQUE)

NOVEMBRE 2015

UNIVERSITÉ DE MONTRÉAL

ÉCOLE POLYTECHNIQUE DE MONTRÉAL

Ce mémoire intitulé :

A NOVEL APPROACH TO DETERMINE HARMONIC DISTORTIONS IN UNBALANCED NETWORKS AND HARMONIC FILTER PLANNING IN INDUSTRIAL SYSTEMS

présenté par : HOSSEINIMANESH Ahmad

en vue de l'obtention du diplôme de : Maîtrise ès sciences appliquées

a été dûment accepté par le jury d'examen constitué de :

M. KARIMI Houshang, Ph. D, président

M. KOCAR Ilhan, Ph. D, membre et directeur de recherche

M. LACROIX Jean-Sebastien, M. Sc. A, membre

DEDICATION

To my beloved family Mohammad, Zahra, Hossein and Golriz

ACKNOWLEDGMENTS

Firstly, I am grateful to the God for the good health and wellbeing that were necessary to complete this thesis.

A special thanks to my family. Words cannot express how grateful I am to my mother and father for all of the sacrifices that you have made on my behalf. I am also thankful to my brother for supporting me spiritually throughout writing this thesis and my life in general.

My deepest gratitude is to Professor Ilhan Kocar, my Research Director, for the continuous support of my Master study and related research, for his patience, motivation, immense knowledge and providing me with an excellent atmosphere for doing research. His guidance helped me in all the time of research and writing of this thesis.

My sincere thanks also goes to Jean-Sebastien Lacroix, R&D Manager at CYME International T&D, who provided me an opportunity to join their team as intern, and who gave access to the research facilities. Without they precious support it would not be possible to conduct this research.

I take this opportunity to express gratitude to all of the Department faculty members for their help and support. Special thanks to Ming Cai for commenting on my thesis and guidance. I would also like to thank my friends in Polytechnique, particularly Thomas Kauffmann for debates and exchange of knowledge during my graduate program, which helped enrich the experience.

I also place on record, my sense of gratitude to one and all, who directly or indirectly, have lent their hand in this venture.

RÉSUMÉ

Ce mémoire présente une méthode d'analyse des harmoniques dans un réseau électrique à n phases. Cette méthode est basée sur l'analyse nodale modifiée augmentée (abrégée MANA en anglais). Elle peut être appliquée à des réseaux déséquilibrés avec plusieurs sources d'harmoniques et plusieurs charges déséquilibrées. Il n'y a pas de limites quant à la taille, la structure ou la topologie du réseau étudié.

L'algorithme développé ici peut être divisé en deux parties. Une première partie résous l'écoulement de puissance du réseau (load-flow en anglais) pour la fréquence fondamentale. La seconde partie est un calcul en régime permanent (basé sur la MANA) pour les différentes fréquences des harmoniques étudiés. Cette partie permet de calculer la propagation des harmoniques issus des éléments non-linéaires. Les éléments linéaires du réseau sont représentés par un modèle équivalent tandis que les éléments non-linéaires sont représentés par un modèle généralisé de l'équivalent de Norton. L'application de l'analyse nodale modifiée augmentée à l'étude des harmoniques est réalisée ici pour la première fois.

Cette méthode est appliquée ici à l'étude des filtres passifs qui réduisent la propagation des harmoniques. L'objectif de ces filtres est de maintenir la tension des harmoniques sous les niveaux présentés dans le standard IEEE 519. Les différents types de filtre et la variation de la fréquence de coupure de ceux-ci sont aussi considérés ici. De plus ce mémoire présente une analyse sur l'emplacement de ces filtres. En raison de la forte capacité de calcul des ordinateurs actuels ainsi que la petite taille des réseaux industriels, une méthode essai erreur est appliquée. Dans cette méthode, toutes les barres pouvant accueillir des filtres sont identifiées puis l'emplacement est déterminé en testant tous les cas possibles. Afin de réduire le nombre de filtres, la méthode proposée a aussi pour objectif de minimiser les coûts d'investissement de ces filtres.

Les principaux objectifs de cette étude sont (1) de résumer les modèles harmoniques pour les composants de réseau dans des conditions déséquilibrées, (2) de promulguer la formulation de MANA pour déterminer le courant / les distorsions de tension harmonique -, (3) de discuter des stratégies pratiques afin d'améliorer la compensation réactive des systèmes électriques industriels, tout en réduisant les problèmes de résonance et limitant les problèmes harmoniques.

Les modèles et algorithmes ont été testés avec différent systèmes de distribution et industriels. Les résultats montrent que les méthodes sont efficaces et adaptées aux ’analyses harmoniques et à la planification des filtres passifs dans des systèmes électriques de puissance.

ABSTRACT

A multiphase harmonic analysis solution technique using Modified Augmented Nodal Analysis (MANA) formulation is presented in this thesis. The solution technique can solve unbalanced networks with multiple unbalanced harmonic sources and unbalanced loads. There is no limitation in terms of network size, configuration and topology.

The algorithm developed in this work consists of two steps: A fundamental frequency load flow using the MANA formulation is carried out first. Then the second step is steady state computation based on MANA in frequency domain to calculate the harmonic propagation due to nonlinear devices. In this step, the linear elements of the network are represented with equivalent models while the nonlinear devices are represented with generalized Norton equivalents. The application of MANA for harmonic analysis is promulgated here for the first time.

A study on the application of passive harmonic filters is also presented in this thesis in relation with IEEE 519 requirements. The application of several types of passive harmonic filters are discussed and the tuned frequency deviation of the single tuned filter is taken into consideration for the purpose of maintaining harmonic voltages compatible with IEEE 519 requirements. In addition to that, a discussion on the filter planning is provided in this work. Given the performance of present day computers and the relatively small size of industrial networks, a simple approach based on trial and error is applied. In the proposed approach all the candidate buses for filter placement are identified first and ideal buses are determined by simulating all possible configurations. In order to reduce the number of filters, the proposed methodology has an objective of minimizing the total investment cost of the designed filters.

The major objectives of this study are (1) to summarize harmonic models for network components for unbalanced conditions, (2) to promulgate the MANA formulation to determine the harmonic current - voltage distortions, (3) to discuss practical solution strategies in order to improve reactive compensation of industrial power systems while reducing resonance problems and limiting harmonic problems.

Models and algorithms are tested with different distribution and industrial systems, and the results show that the methods are effective and suitable for harmonic analysis and planning of passive filters in power systems.

TABLE OF CONTENTS

LIST OF TABLES

LIST OF FIGURES

LIST OF SYMBOLS AND ABBERVIATIONS

(1.1)	Equation 1.1
[1]	Reference 1
$\mathbb{C}$	Complex number
$\boldsymbol{D_c}$	MANA Dependency functions matrix
V_{N-LL}	Nominal line-to-line voltage
$\boldsymbol{I_d}$	MANA Unknown currents in dependent voltage source vector
$\boldsymbol{I_n}$	MANA Nodal currents injection vector
$\boldsymbol{I_s}$	MANA Unknown currents in zero impedance element vector
$\boldsymbol{I_v}$	MANA Unknown source current vector
$\boldsymbol{S_C}$	MANA Adjacency matrix of zero impedance type devices
$S_{cc-1\emptyset}$	Single-phase short-circuit power
$S_{cc-3\emptyset}$	Three-phase short-circuit power
$\boldsymbol{S_D}$	MANA Adjacency matrix of infinite impedance type devices
$\boldsymbol{V_{ibe}}$	MANA Voltage sources vector
$\boldsymbol{V_{ic}}$	MANA Voltage sources adjacency matrix
$\boldsymbol{V_n}$	MANA Unknown node voltages vector
$\boldsymbol{Y_n}$	MANA Linear network admittance matrix
Z_0	Complex zero sequence impedance
Z_1	Complex positive sequence impedance
Z_2	Complex negative sequence impedance
Z_{012}	Complex sequence impedance
Delta	Ungrounded delta connection or system
Y	Wye ungrounded connection or system
Yg	Wye grounded connection or system
GMR	Geometrical Mean Radius
THD	Total Harmonic Distortion
IHD	Individual Harmonic Distortion
IEEE	Institute of Electrical and Electronic Engineers

MANA	Modified-Augmented-Nodal Analysis
p.u.	Per-Unit
X/R	Inductive per resistive ratio
PCC	Point of Common Coupling
PF	Power Factor
IHA	Iterative Harmonic Analysis

LIST OF APPENDICES

CHAPTER 1 INTRODUCTION

1.1 Overview

Immediately upon, the electrical devices with nonlinear current-voltage characteristics such as power converters came into use in the 1970s; the ability of power system to control harmonic propagations has gained attention. However, concerns regarding the harmonic distortions were overlooked around that time, such that the harmonics in distribution systems could cause problems in the performance of network elements. Generally, the harmonics produced by nonlinear devices can reduce efficiency of the power system and in some cases it can even trip circuit breakers. In distribution networks, the end-user suffers from harmonic problems more than the utility sector does [1]. In industrial systems, since the adjustable speed drives, and the arc furnaces are close to each other, the problems caused by harmonic distortions are very likely to occur. Due to these facts, the harmonic propagations in distribution and power systems, particularly for industrial zones, should be precisely analyzed.

Since the power quality is significantly affected by propagation of harmonic distortions in power systems, harmonic control has become a critical issue. One of the most common methods to achieve harmonic distortion reduction is the use of harmonic filters. It should be noted that this reduction greatly depends on the filtering system placement. There are two types of harmonic filters commonly found in industrial systems (i) passive filters and (ii) active filters. The main difference of these filters stand on whether they cancel harmonic distortions within specific frequencies.

1.2 Objective

The main objective of this research project is to develop an algorithm for calculating harmonic voltages and currents in unbalanced networks so that the result can be used for resonance measurements and harmonic filter design. Although the proposed method is suitable for transmission systems or other highly meshed systems, the main focus of this work is on unbalanced distribution systems. The sub objective of this research project is to design and place suitable harmonic filters and accordingly reduce the propagation of harmonic distortions in industrial networks.

1.3 Methodology

According to the specific objective of this project, the present study includes using a mathematical method for determining the harmonic distortions. This method involves the modified augmented nodal analysis and is applied to steady state computations. Once all the system elements are modified into their harmonic models respectively, the developed MANA algorithm is employed for harmonic analysis. It should, nonetheless, be noted that the harmonic models of system elements due to their frequency-dependent nature can be very complex and demanding to obtain when high precision levels are targeted. Generally accepted, steady state models are considered in this work for the harmonic modeling of components. Regarding the metrics on the quality of power, the IEEE standard 519 is considered here as the main reference. The purpose of IEEE 519 standard is to make sure that the utility maintains a certain quality of power at the load terminals and that load is not subjected to high levels of harmonics [2]. Finally, the harmonic analysis is validated by using the IEEE 34 bus distribution test system. The validation test case demonstrates that the proposed algorithm yields precise results.

The secondary objective is related to the optimization of filter design and involves the use of two algorithms. The first algorithm is used to determine the parameters of the passive harmonic filters while respecting the limits set by IEEE 519 and IEEE 18. In this algorithm a systematic procedure to design the harmonic filters is used considering the use of all the passive filters available. It has to be mentioned that the application of passive harmonic filters is a common practice for suppressing harmonic propagations in industrial power systems because they can provide harmonic control and power factor correction simultaneously and also they are much cheaper than active filters. The second algorithm presents a simple strategy to find efficient locations of harmonic filters. A successful filter placement strategy should utilize the minimum number of filters to achieve the greatest positive impact on power quality of the system [3]. Since the number of buses allowing a filter installation in industrial systems is usually not exhaustive, it is possible to determine the optimum filter location by simulating all possible configurations. Although this is a brute force approach, given the performance of present day computers and the size of the industrial networks, it is not demanding in terms of CPU time and it provides guaranteed solution. The effectiveness of the algorithm, on the other hand, is demonstrated on a test case described in chapter 4.

1.4 Report outline

The present thesis is organized into five chapters.

Chapter 1 provides an overview of the research project and information on the objectives and the methodology used.

Chapter 2 presents an algorithm based on MANA for performing harmonic analysis; it also describes and gives insight on the parameters and advanced equivalent circuit models of all power system elements that can be encountered in typical harmonic studies.

Chapter 3 proposes an approach to design and place harmonic filters in the industrial networks.

Chapter 4 presents validation test cases used for testing the presented solution methods.

Chapter 5 is the conclusions of this work. Based on the results, some recommendations and suggestions for future research work are presented.

1.5 Research Contributions

The major contributions of this thesis are listed as follows:

- The harmonic distortions in balanced and unbalanced networks are calculated using the state of the art MANA technique in phasor domain. The MANA approach is already demonstrated to perform for short circuit, power flow, state estimation and fault flow studies. Demonstrating that it can also be used for harmonic studies unifies the solver platform for all the steady state analysis in distribution systems.
- The multiphase harmonic models are presented all together so that they can be of use for harmonic studies.
- The phasor domain harmonic solutions are compared to EMTP-RV (Electromagnetic Transient Program) simulations.
- A systematic study to determine the size and type of harmonic filters in order to suppress harmonic distortions in industrial systems is presented.
- A systematic study to find efficient locations for harmonic filters in industrial power systems is demonstrated by taking into account the standards in effect.

CHAPTER 2 HARMONIC ANALYSIS IN UNBALANCED NETWORKS

The algorithm presented in this section is based on MANA; the same formulation is also applied to the study of resonant conditions. MANA was already used for unbalanced distribution systems and proved to be efficient [4]. In this section, the harmonic models of system components are also presented with their impedance scan with respect to frequency.

2.1 Literature review

The frequency-dependent behavior of system components plays a significant role in harmonic analysis. A concise review on the modeling and analysis of harmonic propagation in ac networks considering the frequency dependent behavior and along with practical considerations is presented in [5]. It should, however, be noted that synchronous machine is modeled using single phase units. Due to this fact, in three phase system, three single phase machines are connected; therefore, the mutual effects are neglected. Several harmonic models and harmonic analysis are described in [6] and [7]. The harmonic model of induction machine under balanced and unbalanced conditions is shown in [8]. The proposed model obtains the harmonic impedance for induction machine of all three sequences (zero, positive, and negative). The appropriate models of synchronous generators for harmonic studies are presented in [9]. These models are developed using detailed "dq0" representations of the synchronous machine. In [10] a synchronous machine model is developed for three-phase harmonic load flow analysis and for initialization of the EMTP-RV. This model can represent both the frequency conversion and the saturation effects under various machine load flow constraints. The model is in the form of a frequency-dependent three-phase circuit. It can therefore easily be incorporated into existing harmonic programs for system-wide harmonic analysis. In [11], a survey on a number of models for linear loads is demonstrated along with their impact on the harmonic impedance of the system.

In distribution systems the state of the art is to develop generic methods that can handle unbalanced networks. In [4], an algorithm based on MANA to calculate multiphase load flow in unbalanced distribution systems is presented. A bibliographical review of the harmonic load flow formulation under balanced condition is provided in [12] which consist of four methods, (i) Harmonic Penetration, which assumes no harmonic interaction between network and harmonic sources, (ii) Iterative Harmonic Penetration (IHP), which considers harmonic influence on

harmonic sources, however, the fixed-point iteration technique, Gauss-Seidel (GS), used in the IHP could present convergence problems, (iii) Simplified Harmonic Load Flow, in this method, A fixed-point iteration of two Newton–Raphson procedures is used: one for load flow and the other for harmonic analysis, (iv) Complete Harmonic Load Flow, this formulation is a natural modification of the load flow where the harmonic sources' treatment and the harmonic voltage calculation have been included. It is based on the simultaneous resolution of power constraints, harmonic current balance, and harmonic source equations. In [13] a multiphase harmonic load flow technique is provided which solves the network at fundamental and harmonic frequencies. The procedure uses an iterative analysis. In [14] and [15] as well, iterative harmonic analysis techniques in frequency domain are presented. The use of Norton equivalent in harmonic analysis is detailed in [16]. A time domain technique is presented in [17]. Different methods for harmonic analysis in frequency domain and time domain are currently detailed in the literature. In [18] a concise yet detailed revision of theoretical fundamentals and principles of classical methods for harmonic analysis in time domain and frequency domain calculations are presented. In this paper, frequency and time domain methods have been developed with the purpose of combining the individual advantages of the frequency and time domain methods.

2.2 Harmonic

Harmonic is defined as a sinusoidal voltage or current that is an integer multiple of the fundamental frequency (60 or 50 Hz). For example, a 180 Hz sine-wave signal, superposed onto the fundamental 60 Hz mains frequency, is defined as the 3rd harmonic (3 x 60 Hz).

2.3 Inter-harmonic

Any signal component between each harmonic order is named as inter-harmonic. In some cases, inter harmonic may play significant role in the total harmonic distortion of a system; however in this work, inter harmonics are not taken into account.

2.4 Characteristics of harmonic

In general, the harmonic voltage at the terminals of an element is given by:

$$V(t) = \sum_{h=1}^{n} |V_h| \cos(h\omega t + \varphi_n) = V_1 \sin(\omega t + \varphi_1) + V_2 \sin(2\omega t + \varphi_2) + V_3 \sin(3\omega t + \varphi_3) + \ldots \qquad (2.1)$$

Where

$V(t)$: Voltage at terminal

V_h : Harmonic voltage at h harmonic order

h : Harmonic order

ω : Angular frequency measured in radians per second

φ_n : Phase shift

In a balanced three phase system, the phase shift between each phase is exactly 120 degrees. Thus, the waveform of V_b and V_c are 120 degrees and 240 degrees shifted from V_a respectively. The voltage at fundamental frequency is given by:

$$V_a = V_1 \cos(\omega_0 t) \tag{2.2}$$

$$V_b = V_1 \cos(\omega_0 t - 120) \tag{2.3}$$

$$V_c = V_1 \cos(\omega_0 t + 120) \tag{2.4}$$

Where:

V_1 : Voltage at fundamental frequency

V_a : Voltage in phase a

V_b : Voltage in phase b

V_c : Voltage in phase c

Due to the symmetry, the harmonic voltage at fundamental frequency has only positive sequence (in balanced networks).

It should be noted that if the waveform is shifted by φ_n, its harmonics are shifted by $h \times \varphi_n$ (h is harmonic order). Therefore, the second harmonic components of the three phase waveform are given by:

$$V_a = V_2 \cos(2\omega_0 t + 2 \times 0) \tag{2.5}$$

$$V_b = V_2 \cos(2\omega_0 t - 2\times 120) = V_2 \cos(2\omega_0 t + 120) \quad (2.6)$$

$$V_c = V_2 \cos(2\omega_0 t + 2\times 120) = V_2 \cos(2\omega_0 t + 240) \quad (2.7)$$

Due to the phase shifts, the harmonic voltage at second harmonic order has only negative sequence.

Third harmonic components are given by:

$$V_a = V_3 \cos(3\omega_0 t + 3\times 0) \quad (2.8)$$

$$V_b = V_3 \cos(3\omega_0 t - 3\times 120) = V_3 \cos(3\omega_0 t + 0) \quad (2.9)$$

$$V_c = V_3 \cos(3\omega_0 t + 3\times 120) = V_3 \cos(3\omega_0 t + 0) \quad (2.10)$$

If we consider the third harmonic components, we can see that the phase shifts in all three phases are equal to zero degree. Therefore, all three terminals are equal in potential. And, accordingly voltage at third harmonic order has only zero sequence.

Eventually, the above reveals that fundamental, fourth, seventh and … harmonics have positive sequence, and they are named positive sequence harmonics. The second, fifth, eighth and … harmonics have negative sequence and they are named negative sequence harmonic. The triplen harmonics have zero sequence and they are named zero sequence harmonic.

2.5 MANA formulation

The MANA formulation is utilized for multiphase harmonic analysis and frequency scan. The generic formulation of MANA is given by:

$$\mathbf{A} \cdot \mathbf{x} = \mathbf{b} \quad (2.11)$$

Where:

A : System of equation

b : Known Variable of system

x : Unknown Variable of system

The detailed format is given by:

$$\begin{bmatrix} \boldsymbol{Y_n^h} & \boldsymbol{V_c} & \boldsymbol{D_c} & \boldsymbol{S_c} \\ \boldsymbol{V_C^t} & \boldsymbol{0} & \boldsymbol{0} & \boldsymbol{0} \\ \boldsymbol{D_C^t} & \boldsymbol{0} & \boldsymbol{0} & \boldsymbol{0} \\ \boldsymbol{S_C^t} & \boldsymbol{0} & \boldsymbol{0} & \boldsymbol{S_d} \end{bmatrix} \cdot \begin{bmatrix} \boldsymbol{V_n^h} \\ \boldsymbol{I_V^h} \\ \boldsymbol{I_D^h} \\ \boldsymbol{I_S^h} \end{bmatrix} = \begin{bmatrix} \boldsymbol{I_n} \\ \boldsymbol{V_b} \\ \boldsymbol{0} \\ \boldsymbol{0} \end{bmatrix} \tag{2.12}$$

Where:

$\boldsymbol{Y_n}$: Linear network admittance matrix

$\boldsymbol{V_c}$: Voltage sources adjacency matrix

$\boldsymbol{D_c}$: Dependency functions matrix

$\boldsymbol{S_c}$: Adjacency matrix of zero impedance type devices

$\boldsymbol{S_d}$: Adjacency matrix of infinite impedance type devices

$\boldsymbol{V_n}$: Vector of unknown nodal

$\boldsymbol{I_v}$: Vector of unknown voltage source currents

$\boldsymbol{I_d}$: Vector of unknown currents in dependent branch functions

$\boldsymbol{I_s}$: Vector of unknown currents in zero impedance element vector

$\boldsymbol{I_n}$: Vector of nodal current injections

$\boldsymbol{V_b}$: Vector of known source voltages

2.6 Impedance scan (Frequency scan)

An impedance scan, also known as frequency scan is used to identify the resonance conditions in the system. In this approach, unit current is injected to the network then the calculated voltage gives the driving point impedance. A plot of magnitude of driving point impedance versus frequency provides an indication of the resonance condition. A sharp rise in the impedance implies parallel resonance which gives the maximum impedance; on the other hand, the lowest point of the impedance scan identifies series resonance.

2.7 Harmonic analysis

The harmonic analysis is the procedure used for obtaining the harmonic voltages in electric power systems at harmonic frequencies. This procedure can be either performed using time domain tools or frequency domain tools. The time domain tools provide higher levels of sophistication with circuit based modeling options and higher precision [19]. However, less computation time is required in frequency domain tools, and reasonable accuracy for practical applications is usually achievable. Therefore frequency domain solution is widely adopted for harmonic studies. In this work only the frequency domain solution is considered. As the objective is to study unbalanced networks using a general and flexible approach, the MANA method is selected to obtain the system of equations for harmonic analysis. In balanced three phase systems, under balanced operating conditions, harmonics on each phase are related to other phases with specific equations (refer to the characteristics of harmonics). As mentioned before, the triple harmonics appear as zero sequence components. As such, in grounded wye configurations, these harmonics flow in the lines and neutral/grounding circuits, while in delta or ungrounded systems they cannot exist. Similar analysis shows that the fifth harmonic appears as negative sequence, seventh as positive sequence, etc. therefore, the impedances and the connection types of rotating machines, transmission lines, and transformers should be accounted for [5]. Under unbalanced conditions, the three phase voltages at the terminals of the loads are not symmetrical; consequently, propagation of harmonics is more complex and a general multiphase solution technique such as MANA is required.

Generally, harmonic studies in frequency domain consist of two steps:

1- Fundamental frequency load flow

2- Harmonic frequency steady state computation in which the loads are considered as constant impedances.

In this work both steps are performed using the MANA formulation. The MANA load flow formulation is used in the first step and it aims to determine the voltages and currents at fundamental frequency. The steady state MANA formulation is used in the second step and the objective is to obtain the harmonic voltages and currents at each bus at each harmonic frequency.

Another method used in harmonic studies is the Iterative Harmonic Analysis (IHA). In this method, loads are not modeled as constant impedance and, fixed point technique is performed to determine the proper value of load impedances at each harmonic frequency. In some cases, IHA may present convergence problem. Due to this fact, the steady state computation is recommended.

2.7.1 Algorithm of harmonic analysis

The algorithm of harmonic analysis is as follows:

Step 1 - Initialization

- Determine voltage and current at fundamental frequency using MANA load flow formulation [4].

Step 2 – Build MANA matrix for steady state computation of network

- Identify the harmonic order
- Short circuit the voltage sources, and modify into the equivalent impedance
- Modify nonlinear loads into the Norton equivalent load models at harmonic frequency (refer to modeling of network component) (Figure 2.2)
- Modify network elements into harmonic models at harmonic frequency (refer to modeling of network component) (Figure 2.1)
- Construct and solve the following equation (MANA steady state computation)

$$\begin{bmatrix} \boldsymbol{Y}_n^h & \boldsymbol{D}_c & \boldsymbol{S}_c \\ \boldsymbol{D}_c^t & \mathbf{0} & \mathbf{0} \\ \boldsymbol{S}_c^t & \mathbf{0} & \boldsymbol{S}_d \end{bmatrix} \begin{bmatrix} \boldsymbol{V}_n^h \\ \boldsymbol{I}_d^h \\ \boldsymbol{I}_s^h \end{bmatrix} = \begin{bmatrix} \boldsymbol{I}_n^h \\ \mathbf{0} \\ \mathbf{0} \end{bmatrix} \tag{2.13}$$

Where:

$\boldsymbol{I}_n^h$: Harmonic current (harmonic source)

Step 3 – Repeat step 2 for all harmonic frequencies

Result: harmonic voltages at each bus, harmonic currents at transformers and harmonic current through switches.

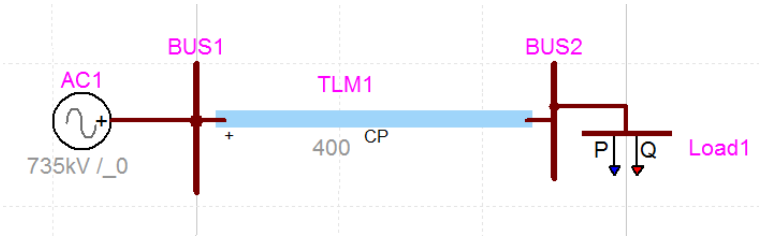

Figure 2-1Circuit in fundamental frequency

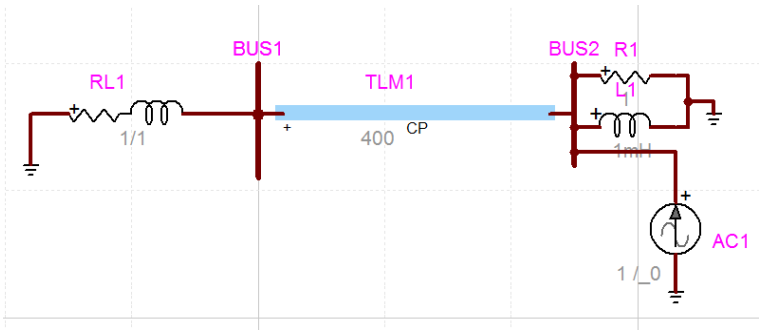

Figure 2-2 Nonlinear devices is modelled using Norton equivalent at harmonic frequencies

2.7.2 Flowchart of harmonic analysis

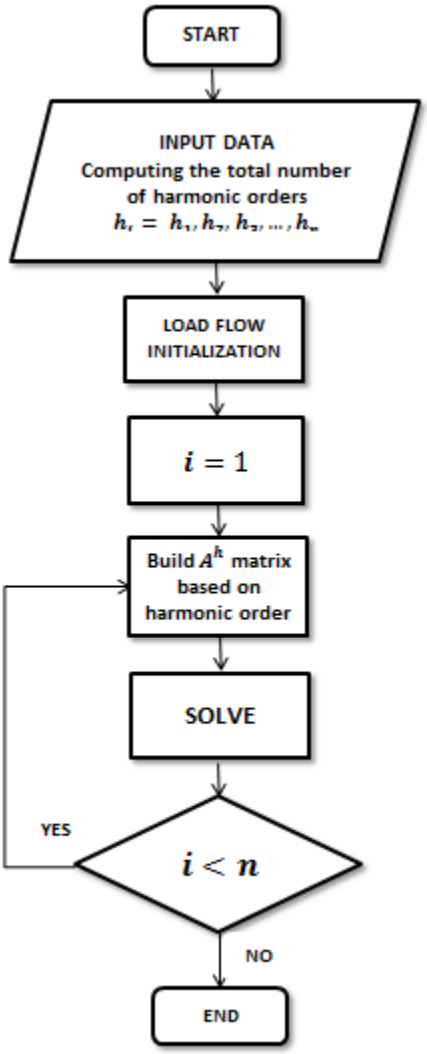

Figure 2-3 Flowchart of harmonic analysis

2.8 Iterative harmonic analysis (IHA)

There are various approaches to determine the harmonic distortions based on iterative calculations. The simplest one uses the concepts of fixed point or Gauss. In this method, harmonic influence on behavior of nonlinear devices is taken into account.

The algorithm of Iterative Harmonic Analysis (IHA) is very similar to the algorithm of harmonic analysis (direct analysis based on MANA), however, the steady state computation of harmonic analysis is complemented by iterative analysis.

Once the calculation of the voltages at fundamental frequency based on the load flow is reached, the linear devices of the network is modified into their harmonic models and the system is reduced to the nonlinear loads. Then afterward, at each iteration, the latest values of distorted terminal voltages are employed to determine the harmonic current injection by solving the linear system with Gauss – Seidel algorithm [6]. Eventually, the direct analysis (steady state computation) is used to calculate the harmonic voltages. It should be mentioned that this method can present the convergence problem [12]. The algorithm of IHA is presented in Figure 2-4.

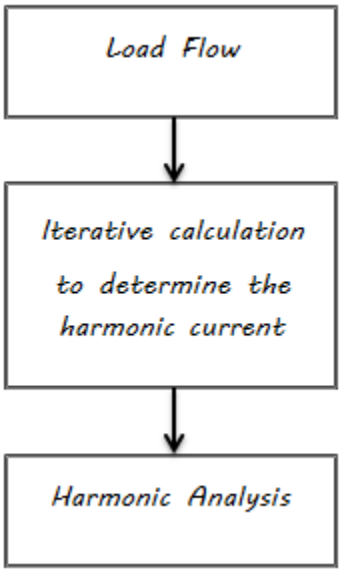

Figure 2-4 Iterative Harmonic Analysis algorithm

2.9 Harmonic modeling of the network elements

The harmonic models of the system elements are given in this section.

2.9.1 Overhead line

There are many approaches to determine the impedance matrices of the distribution and transmission line due to the earth return model and the frequency interest. The first approach to model overhead line that included the effect of earth return was published in 1926 [20]. This line model is known as full Carson line model. However, over the years, the calculation procedures of the Carson model have been simplified. Both the simplified Carson model and full Carson model are detailed in Kersting's book [21].

Carson line model

The calculation procedure for two conductors is presented in Figure 2-5. The self and mutual impedance of each conductor is calculated from the conductor *i* and *k*, and their images *i'* and *k'*.

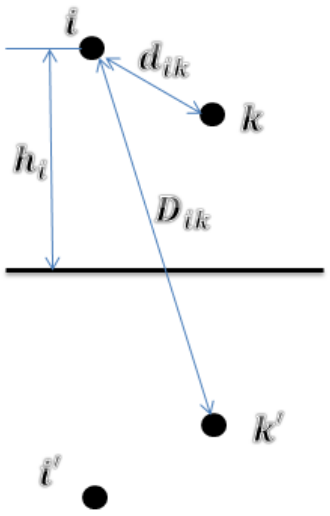

Figure 2-5 Phase conductors and images

Due to effect of earth return, correction factor should be applied to the computation of self and mutual impedances. This correction factor can be calculated as:

$$P=\frac{\pi}{8}-\frac{1}{3\sqrt{2}}k\cos\theta+\frac{k^2}{16}\cos 2\theta+\frac{k^2}{16}\cos 2\theta\left(0.6728+\ln\frac{2}{k}\right)+\frac{k^2}{16}\theta\sin 2\theta+\frac{k^3\cos 3\theta}{45\sqrt{2}}-\frac{\pi k^4\cos 4\theta}{1536} \quad (2.14)$$

Where k and θ are defined as:

$$k=1.713\times10^{-3}h_i\sqrt{\frac{f}{\rho}} \quad (2.15)$$

$$\theta=0 \quad (2.16)$$

$$Q=-0.0386+\frac{1}{2}\ln\frac{2}{k}+\frac{1}{3\sqrt{2}}k\cos\theta-\frac{\pi k^2\cos 2\theta}{64}+\frac{k^3\cos 3\theta}{45\sqrt{2}}-\frac{k^4\theta\sin 4\theta}{384}\left(\ln\frac{2}{k}+1.0895\right) \quad (2.17)$$

Where k and θ are defined as:

$$k=0.8565\times10^{-3}D_{ik}\sqrt{\frac{f}{\rho}} \quad (2.18)$$

$$\theta = \cos^{-1}\left(\frac{h_i + h_k}{D_{ik}}\right) \tag{2.19}$$

The simplified model is provided as follows:

$$P = \frac{\pi}{8} \tag{2.20}$$

$$Q = -0.0386 + \frac{1}{2}\ln\frac{2}{k} \tag{2.21}$$

As can be seen, in simplified method, the function of variable θ is ignored.

The self-resistance and self-inductive reactance of each conductor can be determined as:

$$R_{ii} = R_c + 4\omega PG \tag{2.22}$$

$$X_{ii} = X_{int} + 2\omega G\ln\left(\frac{2h_i}{r_i}\right) + 4\omega QG \tag{2.23}$$

where

$$X_{int} = 2\omega G\ln\left(\frac{r_i}{GMR_i}\right) \tag{2.24}$$

The self and mutual impedance of the transmission line based upon Carson line model are obtained from following equations:

$$Z_{ii}(f) = R_c + 0.00158836 \times f + 0.00202237 \times f \times 1j \times \left(\ln\frac{1}{GMR_i} + 7.6786 + \left(\frac{1}{2}\right) \times \ln\left(\frac{\rho}{f}\right)\right) \tag{2.25}$$

$$Z_{ik}(f) = 0.00158836 \times f + 0.00202237 \times f \times 1j \times \left(\ln\frac{1}{D_{ik}} + 7.6786 + \left(\frac{1}{2}\right) \times \ln\left(\frac{\rho}{f}\right)\right) \tag{2.26}$$

$$D_{ij} = \sqrt{\left(x_i^2 - x_k^2\right) + \left(y_i^2 - y_k^2\right)} \tag{2.27}$$

where:

Z_{ii} : Self-impedance of conductor i in Ω / mile

Z_{ik} : Mutual-impedance of conductor *i* in Ω / mile

Ri : Resistance of conductor i in Ω / mile

f : System frequency in Hz

GMR_i : Geometric Mean Radius of conductor i in ft.

D_{ik} : Distance between conductors i and j in ft.

ρ : Resistivity of earth in Ω / meters (assume 100 Ω / meters)

R_c : DC resistance at 25 C in Ω

x_i : Horizontal distance between conductors in ft

y_i : Veridical distance between conductors in ft

G : Multiplying factor (0.1609347 x 10^{-3} ohm/mile)

R_{ii} : Self-resistance of the conductors

X_{ii} : Self-inductive reactance

Deri line model

Deri equations for self and mutual impedance of a distribution or transmission line are obtained from the simplification to the full Carson line model. It should be taken into account, the simplified Carson has some convenient approximations for limited range of frequencies and medium frequencies are not covered. On the other hand, Deri approach results in simple formulas which are valid throughout, from very low frequencies up to several MHz [22]. Thus, Deri line models are employed in the harmonic studies of the lines. Deri line model is provided by using:

$$p = \frac{1}{\sqrt{j\omega\mu_0\sigma}} \quad (\sigma = \frac{1}{\rho}) \tag{2.28}$$

$$\sigma_c = \frac{1}{\pi\left(r_e^2 - r_i^2\right) R_i} \tag{2.29}$$

$$p_c = \frac{1}{\sqrt{j\ \omega\ \mu_0 \sigma_c}} \tag{2.30}$$

$$Z = \frac{1}{2\pi\ \sigma_c\ r_e\ p_c} \tag{2.31}$$

$$Z_c = (R^n + Z^n)^{\frac{1}{n}} \quad (n = 2) \tag{2.32}$$

$$Z_{ii} = j\omega \frac{\mu_0}{2\pi} \ln \frac{2(h_i + p)}{r_e} + Z_c \tag{2.33}$$

$$Z_{ij} = j\omega \frac{\mu_0}{2\pi} \ln \frac{\sqrt{(h_i + h_k + 2p)^2 + d_{ik}^2}}{\sqrt{(h_i - h_k)^2 + d_{ik}^2}} \tag{2.34}$$

Where:

Z_{ii} : Self-impedance of conductor *i* in Ω / km

Z_{ij} : Mutual-impedance of conductor *i* in Ω / km

Ri : Resistance of conductor *i* in Ω / km

ω : $2\pi \times f$

h_i : Heights of the conductors *i* above the ground in meter

h_k : Heights of the conductors' *k* above the ground in meter

μ_0 : $4\pi \times 1e-7$

f : System frequency in Hz

d_{ik} : Horizontal separation in meter

r_e : External radius in meter

r_i : Internal radius in meter

R_i : DC resistance at 25 Hz in Ω

The most difference in the line impedance matrices of the simplified Carson, full Carson and Deri approaches is coming from difference assumptions for internal impedance of the conductors and handling of the conductor GMR [23].

The equivalent impedance matrix of the line calculated by Carson or Deri formula is given by:

$$\boldsymbol{Z_{abcn}(f)} = \begin{bmatrix} Z_{aa}(f) & Z_{ab}(f) & Z_{ac}(f) & Z_{an}(f) \\ Z_{ba}(f) & Z_{bb}(f) & Z_{bc}(f) & Z_{bn}(f) \\ Z_{ca}(f) & Z_{cb}(f) & Z_{cc}(f) & Z_{cn}(f) \\ Z_{na}(f) & Z_{nb}(f) & Z_{nc}(f) & Z_{nn}(f) \end{bmatrix} \tag{2.35}$$

$$\begin{bmatrix} [V_{abc}] \\ [V_{ng}] \end{bmatrix} = \begin{bmatrix} [V'_{abc}] \\ [V'_{ng}] \end{bmatrix} + \begin{bmatrix} [Z_{ij}] & [Z_{in}] \\ [Z_{nj}] & [Z_{nn}] \end{bmatrix} \times \begin{bmatrix} [I_{abc}] \\ [I_n] \end{bmatrix} \tag{2.36}$$

After Kron's reduction, the equation is given by:

$$[Z_{abc}] = [Z_{ij}] - [Z_{in}] \times [Z_{nn}]^{-1} \times [Z_{nj}] \tag{2.37}$$

$$Z_{abc}(f)=\begin{bmatrix} Zs_{aa}(f) & Zs_{ab}(f) & Zs_{ac}(f) \\ Zs_{ba}(f) & Zs_{bb}(f) & Zs_{bc}(f) \\ Zs_{ca}(f) & Zs_{cb}(f) & Zs_{cc}(f) \end{bmatrix} \quad (2.38)$$

$$Z_{series}(f)=Z_{abc}(f) \quad (2.39)$$

Several effects which are normally ignored at power frequencies have to be included at harmonic frequencies, for instance [24]:

- Frequency dependence
- Long line effects
- Line impedances
- Line transpositions
- VAR compensation plant

In this section frequency dependence, long line effects and line impedances are explained. Line transpositions and VAR compensation plant are detailed in [24]. For calculation of transmission line parameters in harmonic frequencies, following theories should be covered:

- Evaluation of lumped parameters or PI model
- Evaluation of distributed parameters or distributed model
- Evaluation of Skin effect in transmission lines

1- PI (lumped parameters)

Figure 2-6 presents the equivalent circuit of PI. This model consists of series impedance and shunt capacitance which is divided into two equal parts and placed at the two ends of the line. The shunt capacitance of the line is computed as follows:

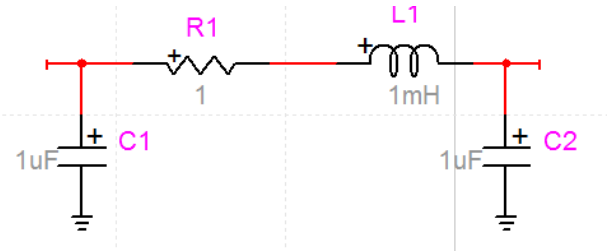

Figure 2-6 PI model

$$\hat{P}_{ii} = \frac{\mathbf{1}}{\mathbf{2}\pi\varepsilon} \times \mathbf{ln} \frac{S_{ii}}{RD_i} \quad (\frac{mile}{\mu F}) \tag{2.40}$$

$$\hat{P}_{ij} = \frac{\mathbf{1}}{\mathbf{2}\pi\varepsilon} \times \mathbf{ln} \frac{S_{ij}}{D_{ij}} \quad (\frac{mile}{\mu F}) \tag{2.41}$$

$$S_{ii} = \mathbf{2} \times y_{\mathrm{i}} \tag{2.42}$$

$$S_{ij} = \sqrt{((D_{ij})^2 + (S_{ii})^2)} \tag{2.43}$$

$$S_{in} = \sqrt{((x_{\mathrm{n}} - x_i)^2 + (-y_{\mathrm{n}} - y_i)^2)} \tag{2.44}$$

where

P_{ii} : Self-impedance of conductor i in Ω / mile

P_{ij} : Mutual-potential coefficients of conductor

S_{ii} : Distance from Conductor i to its image. (*ft.*)

S_{ii} : Distance from Conductor i to the image of Conductor j *(ft.)*

S_{in} : Distance from Conductor i to the image of Neutral *(ft.)*

RD_i : Radius of Conductor *i* in *ft*.

D_{ij} : Distance from Conductor i to Conductor *j* (*ft.*)

ε : Permittivity of air (Assume 1.4240×10^{-2} $(\frac{\mu F}{mile})$)

$$\left[\hat{\boldsymbol{P}}_{\boldsymbol{primitive}}\right] = \begin{bmatrix} \hat{P}_{aa} & \hat{P}_{ab} & \hat{P}_{ac} & \hat{P}_{an} \\ \hat{P}_{ba} & \hat{P}_{bb} & \hat{P}_{bc} & \hat{P}_{bn} \\ \hat{P}_{ca} & \hat{P}_{cb} & Z_{cc} & \hat{P}_{cn} \\ \hat{P}_{na} & \hat{P}_{nb} & \hat{P}_{nc} & \hat{P}_{nn} \end{bmatrix} \tag{2.45}$$

$$\left[\hat{\boldsymbol{P}}_{\boldsymbol{primitive}}\right] = \begin{bmatrix} \left[\hat{\boldsymbol{P}}_{\boldsymbol{ij}}\right] & \left[\hat{\mathbf{P}}_{\mathbf{in}}\right] \\ \left[\hat{\boldsymbol{P}}_{\boldsymbol{nj}}\right] & \left[\hat{\boldsymbol{P}}_{\boldsymbol{nn}}\right] \end{bmatrix} \tag{2.46}$$

Kron's reduction is applied to obtain:

$$\left[\boldsymbol{P}_{\boldsymbol{abc}}\right] = \left[\boldsymbol{P}_{\boldsymbol{ij}}\right] - \left[\boldsymbol{P}_{\boldsymbol{in}}\right] \times \left[\boldsymbol{P}_{\boldsymbol{nn}}\right]^{-1} \times \left[\boldsymbol{P}_{\boldsymbol{nj}}\right] \tag{2.47}$$

$$\left[\boldsymbol{C}_{\boldsymbol{abc}}\right] = \left[\boldsymbol{P}_{\boldsymbol{abc}}\right]^{-1} \tag{2.48}$$

$$\left[\boldsymbol{Y}_{abc}\right]=\mathbf{1}j\times\mathbf{2}\pi f\times\left[\boldsymbol{C}_{abc}\right]\times\mathbf{1.609344}\times l \quad (\mu S) \tag{2.49}$$

where

f : Frequency in *Hz*

l : Length in *km*

2- Equivalent PI (distributed parameters)

Due to standing wave effect on voltage and current in long line, a number of PI models (lumped parameters) are connected in series to improve accuracy of voltage and current. According to the power system harmonic book written by Arrilaga, three phase PI model can provide accuracy to 1.2% for quarter wavelength line (a quarter wavelength corresponds with 1500 and 1250 km at 50 and 60 Hz respectively). As frequency increase the number of nominal PI section to maintain a particular accuracy increases proportionally. For instance, a 300 km line requires 30 nominal PI section to maintain the 1.2% accuracy [6]. Therefore, the long line effect should be included. And, the line parameters are distributed along the length of the line in a way to avoid lumping them in one place. In distributed model, the equivalent PI model (distributed parameters) is calculated from the PI model (lumped parameters) by multiplying the correction factors to the series impedance and shunt admittance. For the single phase the correction factor is given by:

For series impedance:

$$\frac{\mathbf{sinh}(x\sqrt{Z`Y`})}{x\sqrt{Z`Y`}} \tag{2.50}$$

For shunt admittance

$$\frac{\mathbf{tanh}(\frac{x\sqrt{Z`Y`}}{\mathbf{2}})}{x\frac{\sqrt{Z`Y`}}{\mathbf{2}}} \tag{2.51}$$

where

x : Length of the line

$Z`$: Series impedance calculated in PI nominal in Ω/km

$Y`$: Shunt admittance which is calculated in PI nominal in Ω^{-1}/km

Since there is no direct way of computing *sinh* or *tanh* of a matrix, eigenvalues and eigenvectors are employed for three phase line models.

$$T_v = eig\left\{\boldsymbol{Z}_{abc} \times \boldsymbol{Y}_{abc}\right\} \tag{2.52}$$

$$T_i = eig\left\{\boldsymbol{Y}_{abc} \times \boldsymbol{Z}_{abc}\right\} \tag{2.53}$$

$$\boldsymbol{Z}_m = T_v^{-1} \times \boldsymbol{Z}_{abc} \times T_i \tag{2.54}$$

$$\boldsymbol{Y}_m = T_i^{-1} \times \boldsymbol{Y}_{abc} \times T_v \tag{2.55}$$

$$\boldsymbol{\Gamma}_m = \sqrt{diag\left\{\boldsymbol{Z}_m \times \boldsymbol{Y}_m\right\}} \tag{2.56}$$

$$T_i^T = T_v^T \tag{2.57}$$

$$\boldsymbol{Z}_{series}(f) = \boldsymbol{Z}_{abc}(f) \times T_i \, \boldsymbol{\Gamma}_m^{-1} \sinh(diag\left(\boldsymbol{\Gamma}_m\right) l) T_i^{-1} \tag{2.58}$$

$$\boldsymbol{Y}_{shunt}(f) = 2 \times T_i \, \boldsymbol{\Gamma}_m^{-1} \tanh(diag\left(\boldsymbol{\Gamma}_m\right) \frac{l}{2}) T_i^{-1} \times \boldsymbol{Y}_{abc}(f) \tag{2.59}$$

where

f : Frequency in *Hz1*

Z_{abc} : Series impedance calculated in PI nominal in Ω/km

Y_{abc} : Shunt admittance which is calculated in PI nominal in Ω^{-1}/km

Z_{series} : Series distributed impedance in Ω

Y_{shunt} : Shunt distributed impedance in Ω

The use of PI model (lumped parameters) at fundamental frequency can offer several advantages:

- It requires lowest calculations and is easy to be implemented.
- It can be used in any configuration or number of parallel circuits.
- It can be used in the simulation related to transient or dynamic processes.

Moreover, PI model (lumped parameters) has some disadvantages:

- There are considerable errors in the use of lumped parameter when the transmission length is greater than 150 km at fundamental frequency (50 or 60 Hz) and 15 km at 600 Hz. Therefore, transmission lines cannot be represented with PI (lumped parameters) at harmonic frequencies.

- PI model does not represent frequency dependence on R and L in the case of studies related to the frequency response or harmonics [25].

Equivalent PI (distributed parameters) must be used in any study where the frequency changes are relevant to the results such as harmonic analysis [25].

3- Skin Effect

In transmission lines, the current flowing tends to flow on the surface of the conductor. Due to this fact, there is an increase in the resistance and decrease in internal inductance. This effect increases as frequency increases and it is termed the skin effect [6].

The skin effect in transmission lines is explained in [6] and [24]. The equation of skin effect is provided as follows:

$$Z_{skin\ ll} = \sqrt{R_0^2 + Z_\infty} \tag{2.60}$$

$$R_0 = \frac{1}{\pi(r_{ext,l}^2 - r_{int,l}^2)\delta_c} \tag{2.61}$$

$$R_0 = \frac{1}{\pi(r_{ext,l}^2 - r_{int,l}^2)\delta_c} \tag{2.62}$$

$$Z_\infty = \frac{1}{2\pi r_{ext,l}\delta_c\rho_C} \tag{2.63}$$

$$\rho_C = \frac{1}{\sqrt{j\omega\mu_0\delta_c}} \tag{2.64}$$

where

$r_{int,l}$: Internal radius of the conductor l in *m*

$r_{int,l}$: External radius of the conductor l in *m*

δ_c : Conductivity of the conductor in *S/m*

The impedance scan of a transmission line with different harmonic models are presented in Figures 2.7 to 2.12; the line length is 300 km and Deri equation is used to calculate the series impedance of the line. Table 2-1 shows the line parameters data at fundamental frequency.

Table 2-1 Line parameters data (in 60 Hz)

	R(ohm/km)	**X(ohm/km)**	**G(µS/km)**	**B (µS/km)**
Phase A	0.2013	0.7582	0.0	2.6759
Phase B	0.2022	0.7464	0.0	2.7844
Phase C	0.2028	0.7397	0.0	2.7094
Phase AB	0.0481	0.2455	0.0	-0.5038
Phase AC	0.0481	0.2455	0.0	-0.5038
Phase BC	0.0481	0.2455	0.0	-0.5038

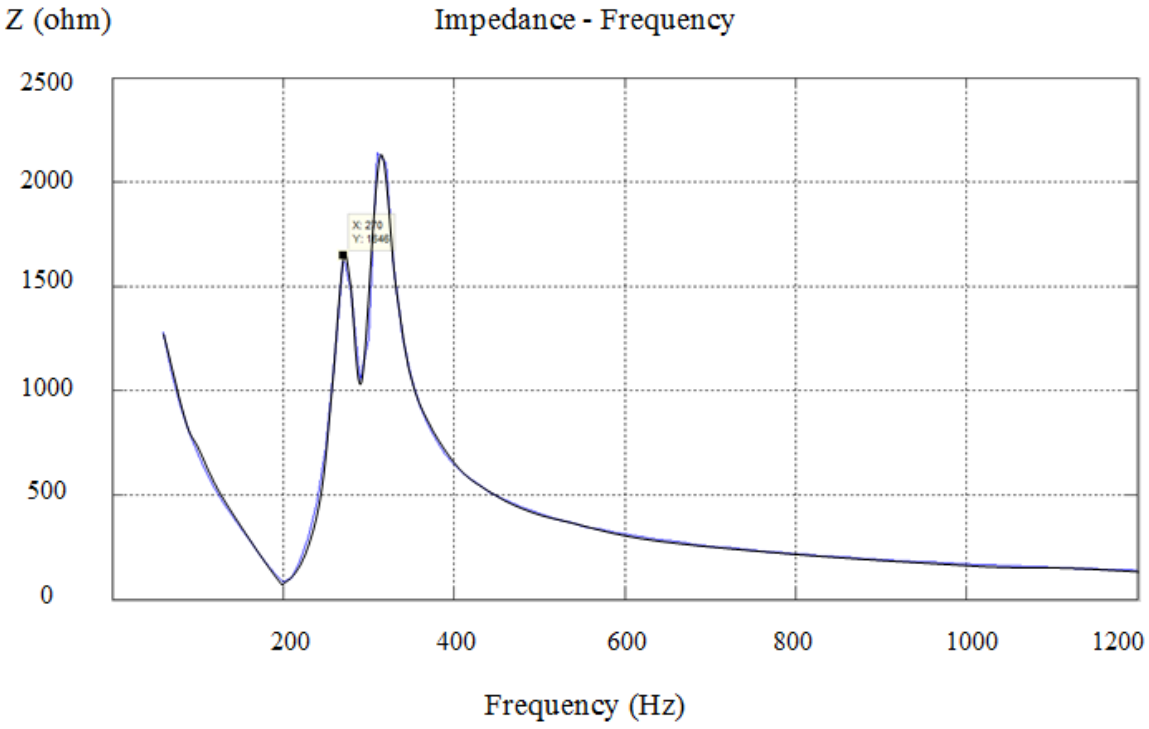

Figure 2-7 Impedance characteristic of a PI nominal line (60Hz <f<1200 Hz)

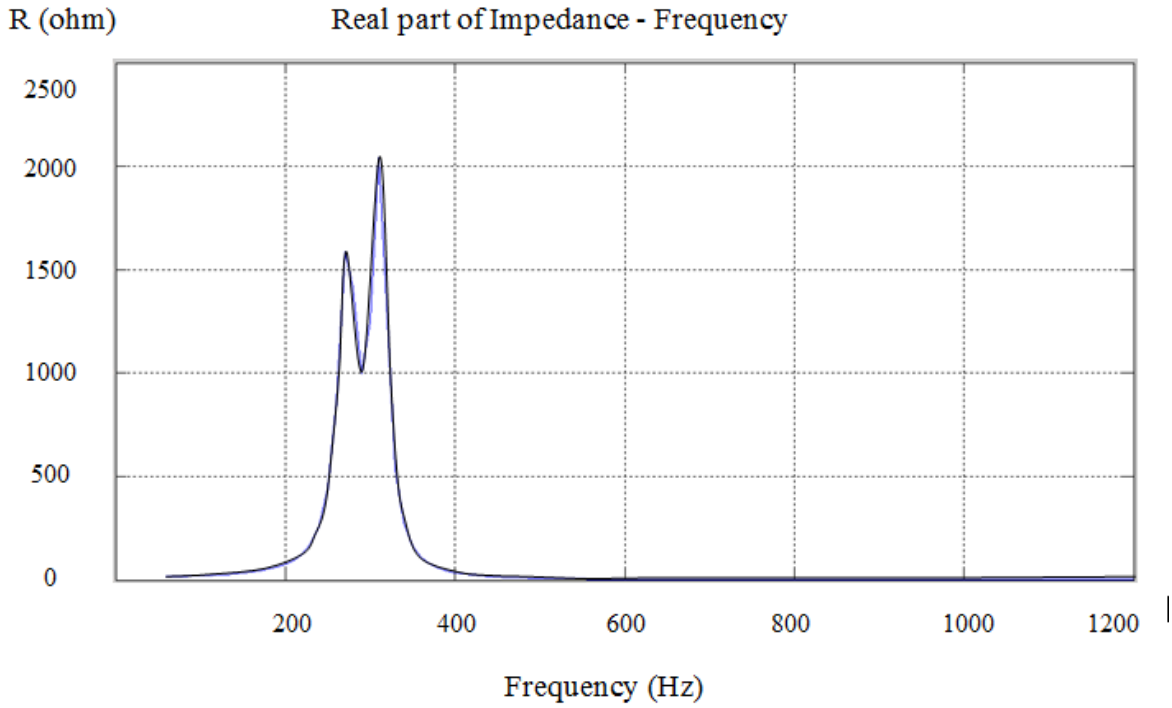

Figure 2-8 Real part of a PI nominal line (60Hz <f<1200 Hz)

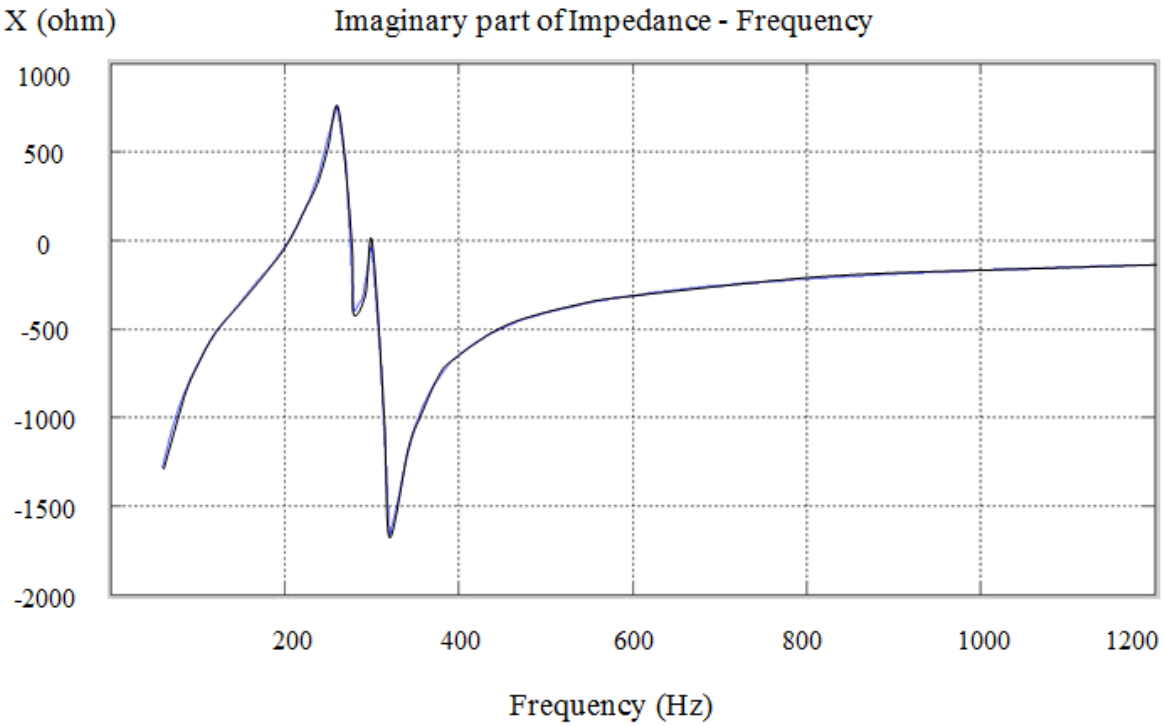

Figure 2-9 Imaginary part of a PI nominal line (60Hz <f<1200 Hz)

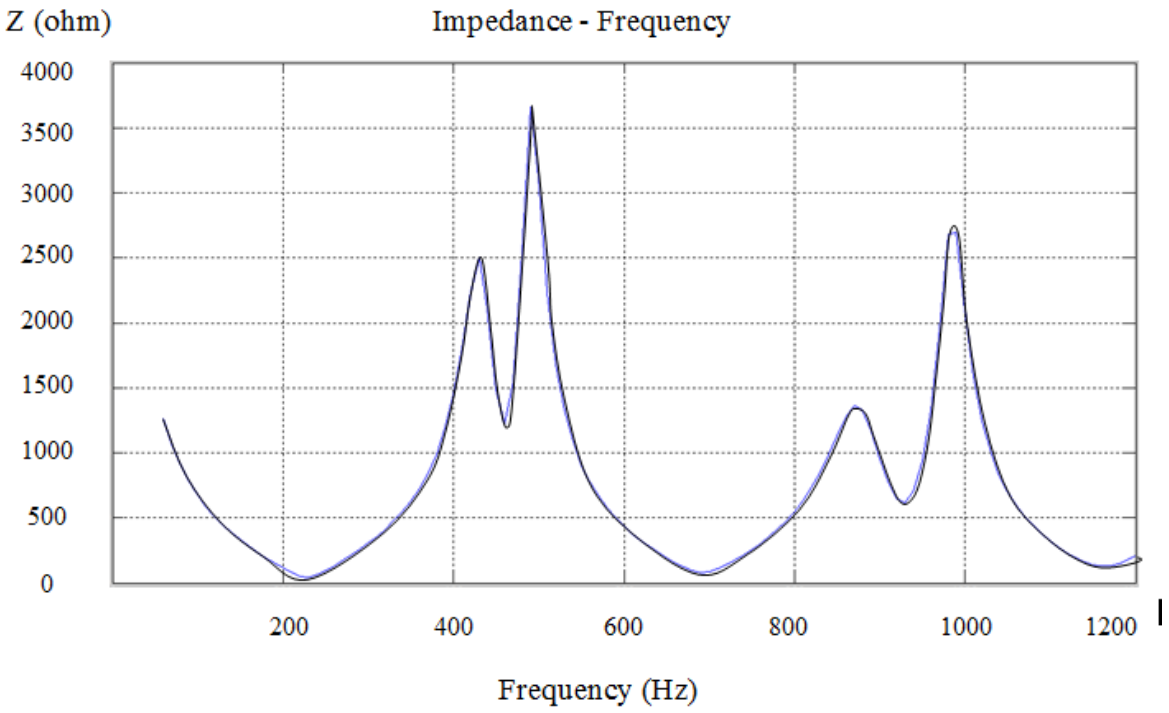

Figure 2-10 Impedance characteristic of a distributed line (equivalent PI) (60Hz <f<1200 Hz)

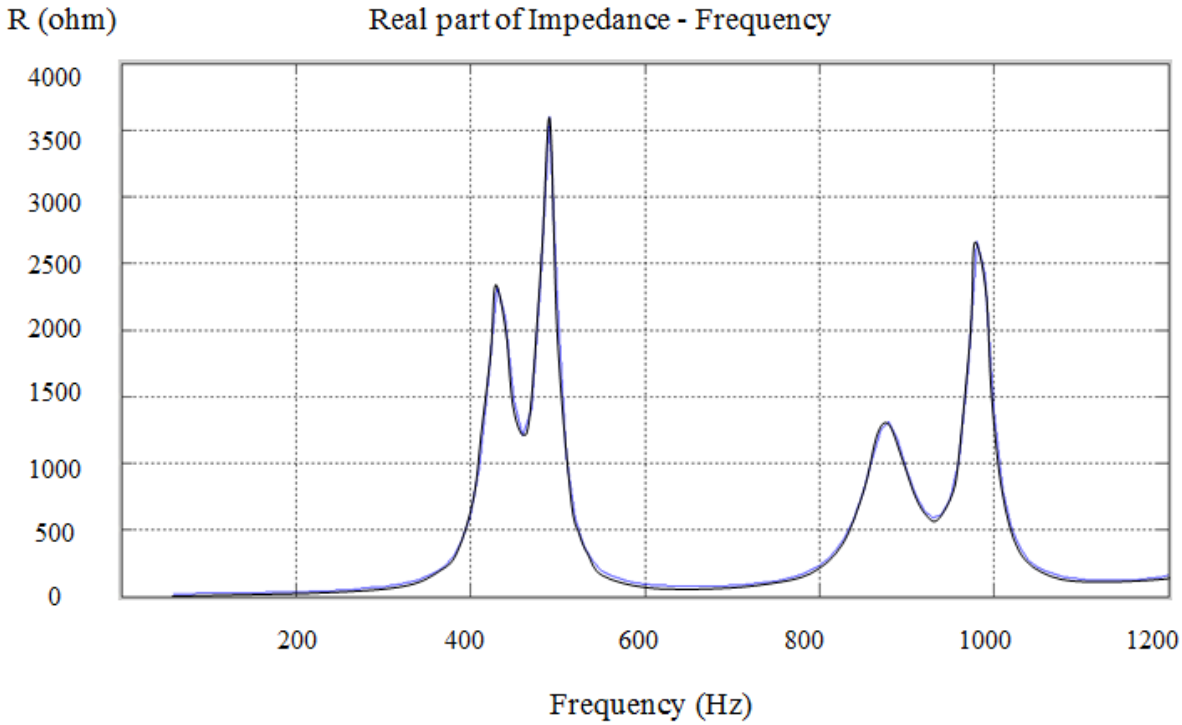

Figure 2-11 Real part of a distributed line (equivalent PI) (60Hz <f<1200 Hz)

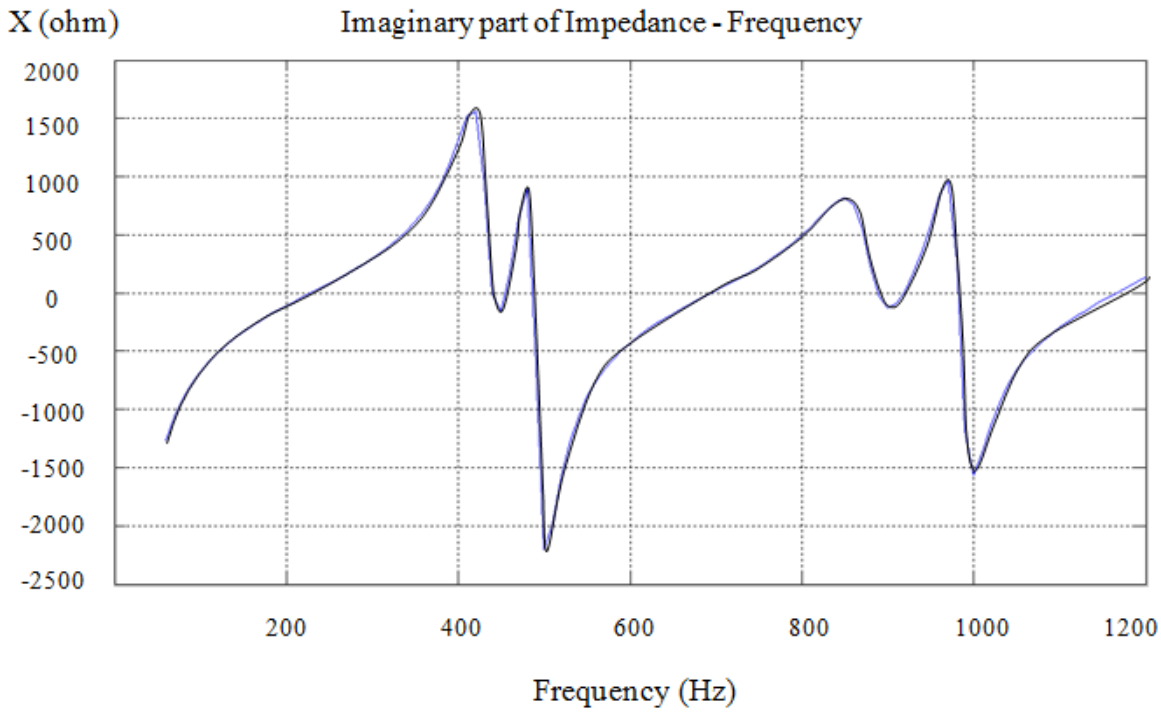

Figure 2-12 Imaginary part of a distributed line (equivalent PI) (60Hz <f<1200 Hz)

2.9.2 Cable

The harmonic model of cables is very similar to overhead lines. However, cables have higher shunt capacitance than overhead lines [5]. Therefore, the equivalent PI model (distributed parameters) can be applied for cables.

2.9.3 Voltage sources

At harmonic frequencies, the sources are grounded and represented by lumped impedance; the equivalent admittance matrix of the source is constructed by:

$$\boldsymbol{Z}_a^h = R + jX \times h \tag{2.65}$$

$$\boldsymbol{Y}_{source}^h = [\boldsymbol{Z}_{abc}^h]^{-1} = \begin{bmatrix} Y_x^h & Y_y^h & Y_z^h \\ Y_z^h & Y_x^h & Y_y^h \\ Y_y^h & Y_z^h & Y_x^h \end{bmatrix} \tag{2.66}$$

Where

R : Resistance of source

X : Reactance of source

$Z(h)$: Harmonic impedance of the source in *ohm*

h : Harmonic order

$\boldsymbol{Y_n}$ is a 2n x 2n matrix for n phase line:

$$\boldsymbol{Y_n} = \boldsymbol{Y_{source}^h} = \begin{bmatrix} Y_x^h & Y_y^h & Y_z^h \\ Y_z^h & Y_x^h & Y_y^h \\ Y_y^h & Y_z^h & Y_x^h \end{bmatrix} \tag{2.67}$$

2.9.4 Transformers

The transformers at harmonic frequencies are represented with constant RL branches. The equivalent circuit is shown in Figure 2-13. The frequency dependence is usually ignored as the harmonic frequencies cover a small range frequency band. The nonlinear characteristics of the magnetizing branch and winding stray capacitance tend to produce harmonic distortions (mainly 3rd). Consequently, a harmonic source can be used to represent these distortions, although the effect is often negligible.

The harmonic impedance of transformers is modified with following equation:

$$Z(h) = R + jX \times h \tag{2.68}$$

Where

R : Resistance of transformer

X : Reactance of transformer

The admittance matrix of the transformer in general format can be computed using:

$$\boldsymbol{Y} = \begin{bmatrix} Z & \mathbf{0} & \mathbf{0} \\ \mathbf{0} & Z & \mathbf{0} \\ \mathbf{0} & \mathbf{0} & Z \end{bmatrix}^{-1} \tag{2.69}$$

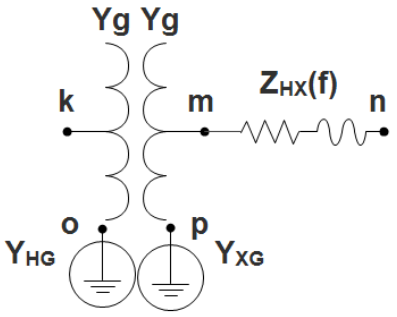

Figure 2-13 Yg yg transformer

The equivalent admittance of Ygyg transformer shown in figure 2.13 is given by:

$$\mathbf{Y_n} = \begin{bmatrix} & k_a & k_b & k_c & m_a & m_b & m_c & n_a & n_b & n_c & o & p \\ k_a & 0 & 0 & 0 & 0 & 0 & 0 & 0 & 0 & 0 & 0 & 0 \\ k_b & 0 & 0 & 0 & 0 & 0 & 0 & 0 & 0 & 0 & 0 & 0 \\ k_c & 0 & 0 & 0 & 0 & 0 & 0 & 0 & 0 & 0 & 0 & 0 \\ m_a & 0 & 0 & 0 & Y_{sHX\_1} & Y_{mHX} & Y_{mHX} & -Y_{sHX\_1} & -Y_{mHX} & -Y_{mHX} & 0 & 0 \\ m_b & 0 & 0 & 0 & Y_{mHX} & Y_{sHX\_2} & Y_{mHX} & -Y_{mHX} & -Y_{sHX\_2} & -Y_{mHX} & 0 & 0 \\ m_c & 0 & 0 & 0 & Y_{mHX} & Y_{mHX} & Y_{sHX\_3} & -Y_{mHX} & -Y_{mHX} & -Y_{sHX\_3} & 0 & 0 \\ n_a & 0 & 0 & 0 & -Y_{sHX\_1} & -Y_{mHX} & -Y_{mHX} & Y_{sHX\_1} & Y_{mHX} & Y_{mHX} & 0 & 0 \\ n_b & 0 & 0 & 0 & -Y_{mHX} & -Y_{sHX\_2} & -Y_{mHX} & Y_{mHX} & Y_{sHX\_2} & Y_{mHX} & 0 & 0 \\ n_c & 0 & 0 & 0 & -Y_{mHX} & -Y_{mHX} & -Y_{sHX\_3} & Y_{mHX} & Y_{mHX} & Y_{sHX\_3} & 0 & 0 \\ o & 0 & 0 & 0 & 0 & 0 & 0 & 0 & 0 & 0 & Y_{Hg} & 0 \\ p & 0 & 0 & 0 & 0 & 0 & 0 & 0 & 0 & 0 & 0 & Y_{Xg} \end{bmatrix} \quad (2.70)$$

Where

Y_{sHX_i} : Self admittance seen on the low side for unit i, i = 1, 2, 3

Y_{Hg} : Grounding admittance for high side

Y_{Xg} : Grounding admittance for low side

Three phase power transformer can also give a phase shift to harmonic voltages and currents. The matrix $\boldsymbol{D_c}$ accounts for it in the MANA formulation

$\boldsymbol{D_c}$ (for Yg yg) is given by:

$$\boldsymbol{D_c} = \begin{bmatrix} & q_1 & q_2 & q_3 \\ k_a & -g_1 & \mathbf{0} & \mathbf{0} \\ k_b & \mathbf{0} & -g_2 & \mathbf{0} \\ k_c & \mathbf{0} & \mathbf{0} & -g_3 \\ m_a & \mathbf{1} & \mathbf{0} & \mathbf{0} \\ m_b & \mathbf{0} & \mathbf{1} & \mathbf{0} \\ m_c & \mathbf{0} & \mathbf{0} & \mathbf{1} \\ o & g_1 & g_2 & g_3 \\ p & \mathbf{-1} & \mathbf{-1} & \mathbf{-1} \end{bmatrix} \quad (2.71)$$

Where

g_i : Turn ratio of the ideal transformer i, i = 1,2,3

2.9.5 Loads

Loads may either significant affect in damping or resonance conditions of the systems, particularly at higher frequencies. Harmonic modeling of linear loads is related to (i) load size (ii) composition and (iii) connection types. A typical composition of ordinary loads is presented in Table 2-2. There are three types of loads: 1- Spot loads (Resistive) 2- Rotating loads (inductive) 3- Nonlinear loads (harmonic sources)

Table 2-2 Typical load composition [9]

Nature	**Type of loads**	**Electrical Characteristics**
Domestic	Incandescent lamps	Spot load (Resistive)
Commercial	Fluorescent lamps	Nonlinear loads (harmonic sources)
Industrial	Motors	Rotating loads (inductive)
	Computers	Nonlinear loads (harmonic sources)
	Home electronics	Nonlinear loads (harmonic sources)
	Resistive heater	Spot loads (Resistive)
	Air conditioning	Rotating loads (inductive)
	ASDs	Nonlinear loads (harmonic sources)
	Pumps	Rotating loads (inductive)
	Arc Furnace	Nonlinear

1- Spot loads

Four types of harmonic models are available for spot loads: (i) RL series (ii) RL parallel (iii) RL parallel with skin effect and (iv) CIGRE/EDF. Loads at fundamental frequency are represented as PQ loads. However, in harmonic frequencies, they are modified into equivalent admittances which are calculated from active and reactive power at fundamental frequency. Three single phase units are used to obtain a three phase model.

(i) RL Series

In harmonic modeling of systems, individual loads are represented with RL series. Following schema shows the harmonic model of RL series loads at harmonic frequencies:

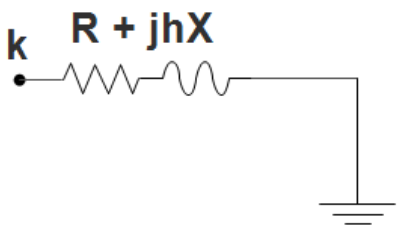

Figure 2-14 Equivalent circuit for RL series load

The equivalent impedance is calculated as follows:

$$R = P.\frac{V^2}{P^2 + Q^2} \tag{2.72}$$

$$X(h) = h.Q.\frac{V^2}{P^2 + Q^2} \tag{2.73}$$

$$Z_i(h) = R_i + j.X_i(h) \tag{2.74}$$

Where

V : Nominal voltage in volts

P : Active power for each phase in W

Q : Reactive power for each phase in VAR

(ii) RL Parallel

Figure 2-15 shows a RL parallel load. In harmonic modeling of systems, lumped loads are represented with RL parallel.

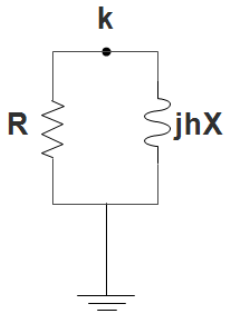

Figure 2-15 Equivalent circuit of RL parallel

Equivalent impedance is calculated as follows:

$$R = \frac{V^2}{P} \tag{2.75}$$

$$X(h) = h.\frac{V^2}{Q} \tag{2.76}$$

$$Z_i(h) = R_i \,||\, j.X_i(h) \tag{2.77}$$

(iii) RL parallel with skin effect

Figure 2-16 shows the scheme of RL parallel with skin effect. This harmonic model is best used to represent lumped loads in the systems. In addition, it can provide frequency dependent parameters.

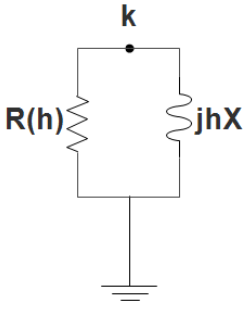

Figure 2-16 RL equivalent circuit of RL parallel with skin effect

Equivalent impedance is calculated as follows:

$$R(h) = \frac{V^2}{m(h).P} \tag{2.78}$$

$$X(h) = h.\frac{V^2}{m(h).Q} \tag{2.79}$$

$$m(h) = \mathbf{0.1}.h + \mathbf{0.9} \tag{2.80}$$

$$Z_i(h) = R_i \,||\, j.X_i(h) \tag{2.81}$$

Note that, whether the induction motor demand over the total demand is less than 0.1 or the linear loads behave as constant impedance, the model (i), (ii) and (iii) can provide a good approximation [11].

(iv) CIGRE/EDF

The CIGRE type C is best used to represents bulk loads as series and parallel RL circuit. In this model, the resistive part of the load is calculated for the distribution transformers including a series reactance. The inclusion of the distribution transformer reactance tends to reduce damping at higher frequencies [11]. It should however be noticed that this approximation is not valid for $h < 5$. Figure 2-17 shows the equivalent impedance of a CIGRE type C. This harmonic model is suggested by IEEE Power Eng. Soc. T&D Committee.

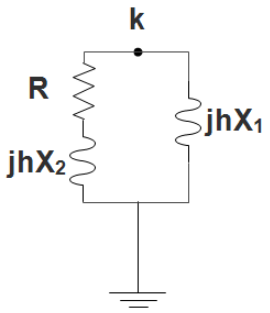

Figure 2-17 Equivalent circuit of a CIGRE type C

Equivalent impedance is calculated by:

$$R = \frac{V^2}{P} \tag{2.82}$$

$$X_1 = \frac{h.R}{\left(\mathbf{6.7} \times \frac{Q}{P}\right) - \mathbf{0.74}} \tag{2.83}$$

$$X_2 = \mathbf{0.073.}\ h.\ R \tag{2.84}$$

$$Z_i(h) = (R + jX_1) \| (j.X_2(h)) \tag{2.85}$$

Y connection of spot load is presented in figure 2.18

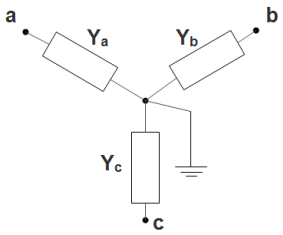

Figure 2-18 Y connection of spot load

For Y connection the impedance is given by:

$$\boldsymbol{Y_{kk}} = \left[\boldsymbol{Z_i(h)}\right]^{-1} = \begin{bmatrix} Z_a(h) & \mathbf{0} & \mathbf{0} \\ \mathbf{0} & Z_b(h) & \mathbf{0} \\ \mathbf{0} & \mathbf{0} & Z_c(h) \end{bmatrix}^{-1} \tag{2.86}$$

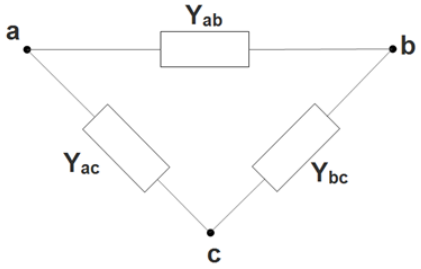

Figure 2-19 Delta connection of spot load

Figure 2-19 illustrates delta connection of spot loads. Equivalent impedance is given by:

$$Y_{ij}(h) = (Z_{ij}(h))^{-1} \tag{2.87}$$

$$Y_{ii}(h) = (Z_{ii}(h))^{-1} \tag{2.88}$$

$$\boldsymbol{Y_{kk}} = \begin{bmatrix} Y_{ab}(h) + Y_{ac}(h) & -Y_{ab}(h) & -Y_{ac}(h) \\ -Y_{ab}(h) & Y_{ab}(h) + Y_{bc}(h) & -Y_{bc}(h) \\ -Y_{ac}(h) & -Y_{bc}(h) & Y_{cb}(h) + Y_{ac}(h) \end{bmatrix} \tag{2.89}$$

Where

Z_{ij} : Equivalent impedance of each load (each phase) for delta connection

Eventually:

$$\boldsymbol{Y_{kk}} = \begin{bmatrix} Y_x^h & Y_y^h & Y_z^h \\ Y_z^h & Y_x^h & Y_y^h \\ Y_y^h & Y_z^h & Y_x^h \end{bmatrix} \tag{2.90}$$

$$\boldsymbol{Y_n} = \begin{bmatrix} & k_a & k_b & k_c \\ k_a & Y_x^h & Y_y^h & Y_z^h \\ k_b & Y_z^h & Y_x^h & Y_y^h \\ k_c & Y_y^h & Y_z^h & Y_x^h \end{bmatrix} \tag{2.91}$$

For a load has P = 1500 kW and Q = 500 kVAR, the impedance scan of all types of harmonic models are presented in Figures 2-20 to 2-27.

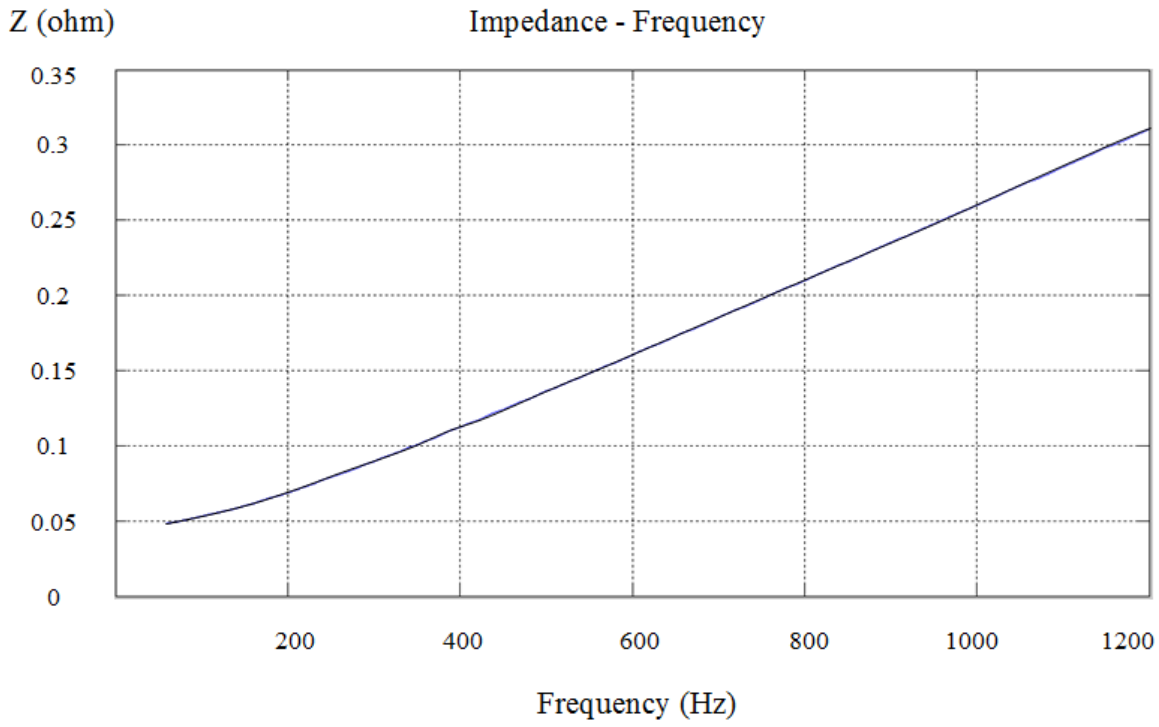

Figure 2-20 Impedance scan of RL series load (60 Hz < f < 1200 Hz)

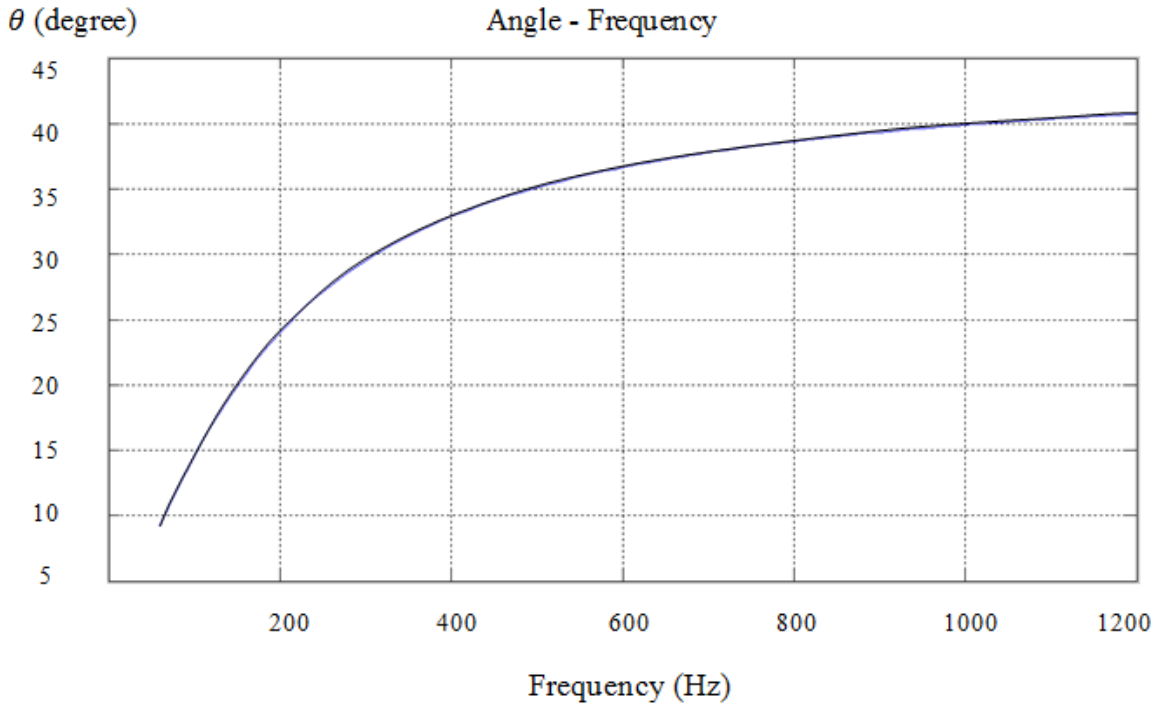

Figure 2-21 Impedance phase of RL series load (60 Hz < f < 1200 Hz)

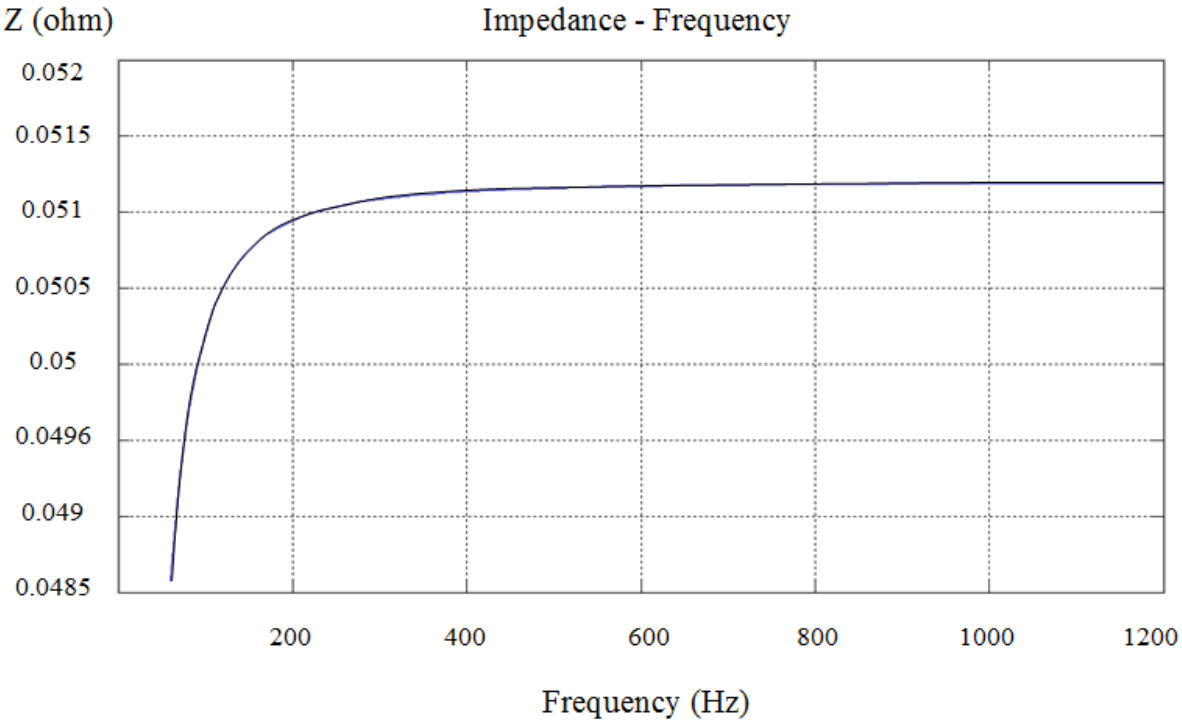

Figure 2-22 Impedance scan of RL parallel load (60 Hz < f < 1200 Hz)

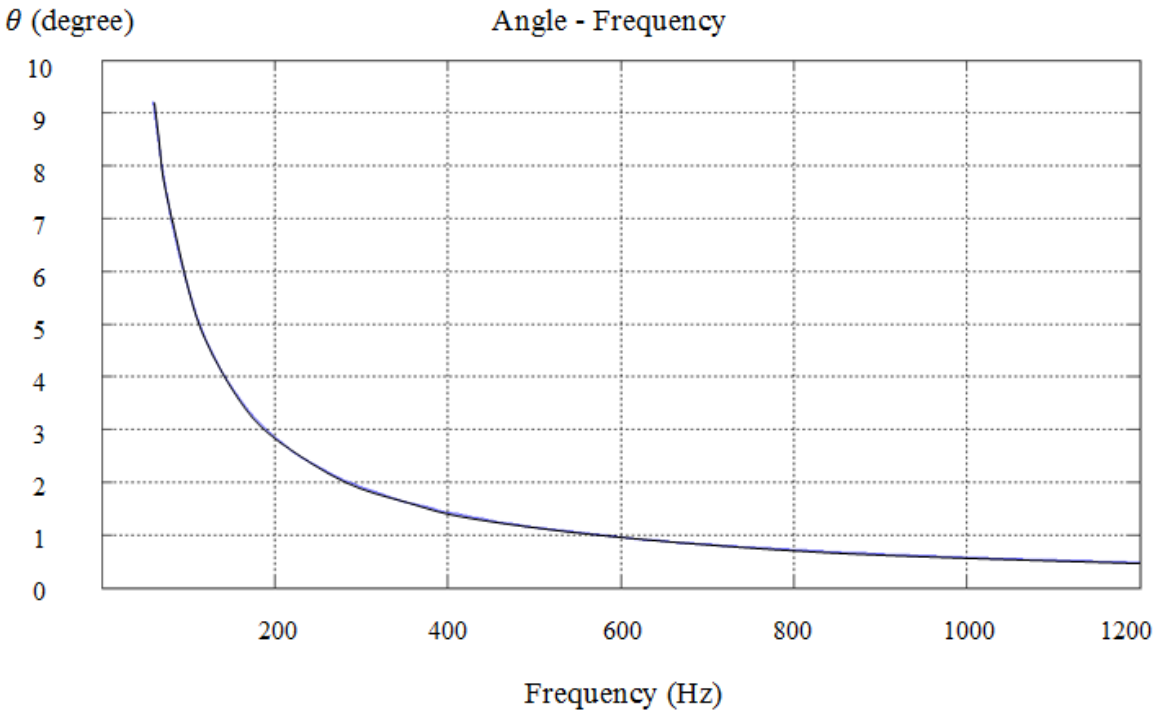

Figure 2-23 Impedance phase of RL parallel load (60 Hz < f < 1200 Hz)

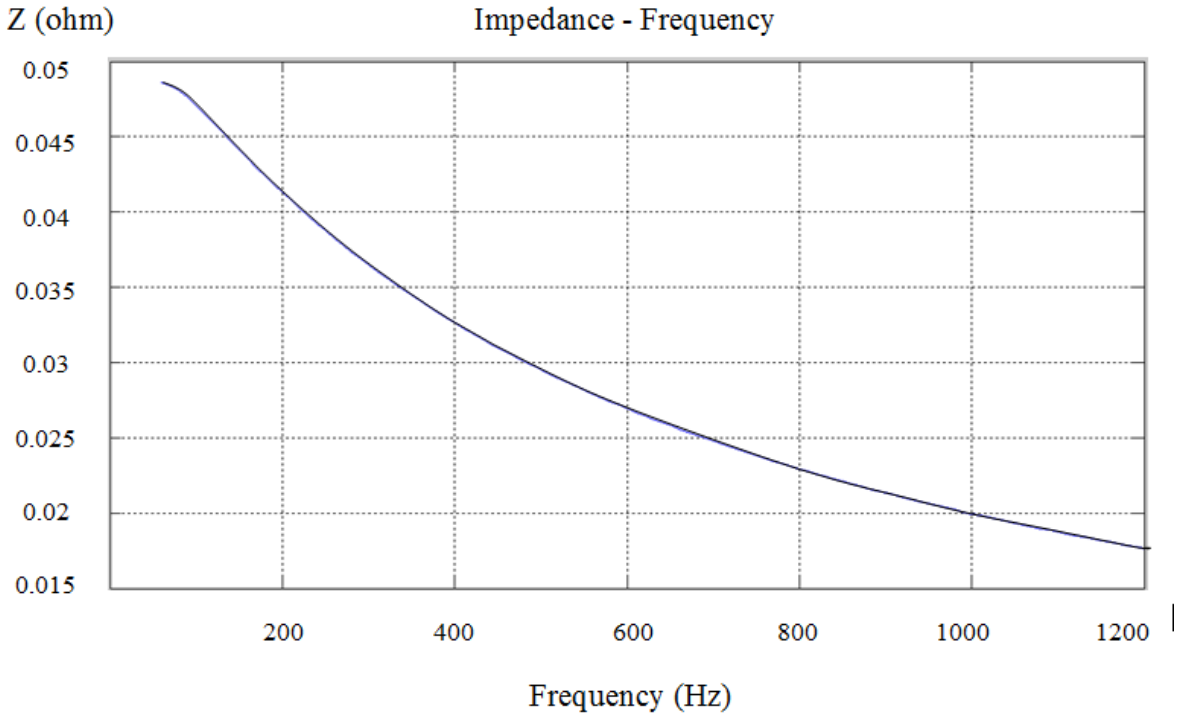

Figure 2-24 Impedance scan of RL parallel load with skin effect (60 Hz < f < 1200 Hz)

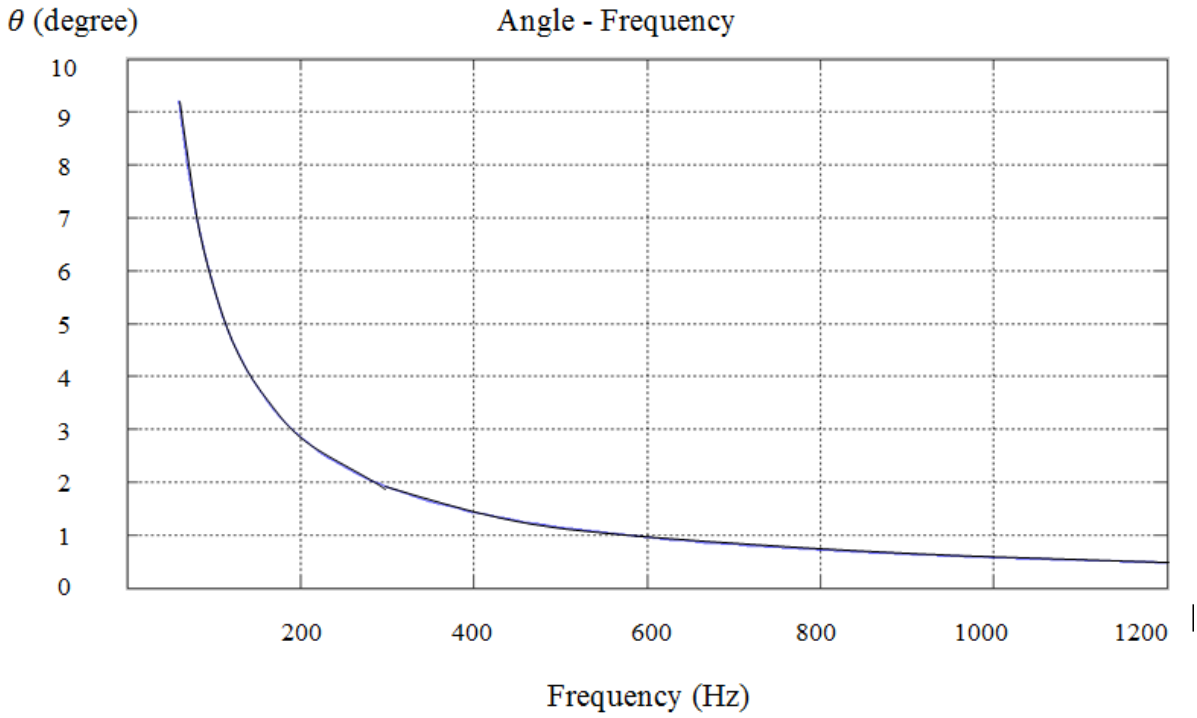

Figure 2-25 Impedance phase of RL parallel load with skin effect (60 Hz < f < 1200 Hz)

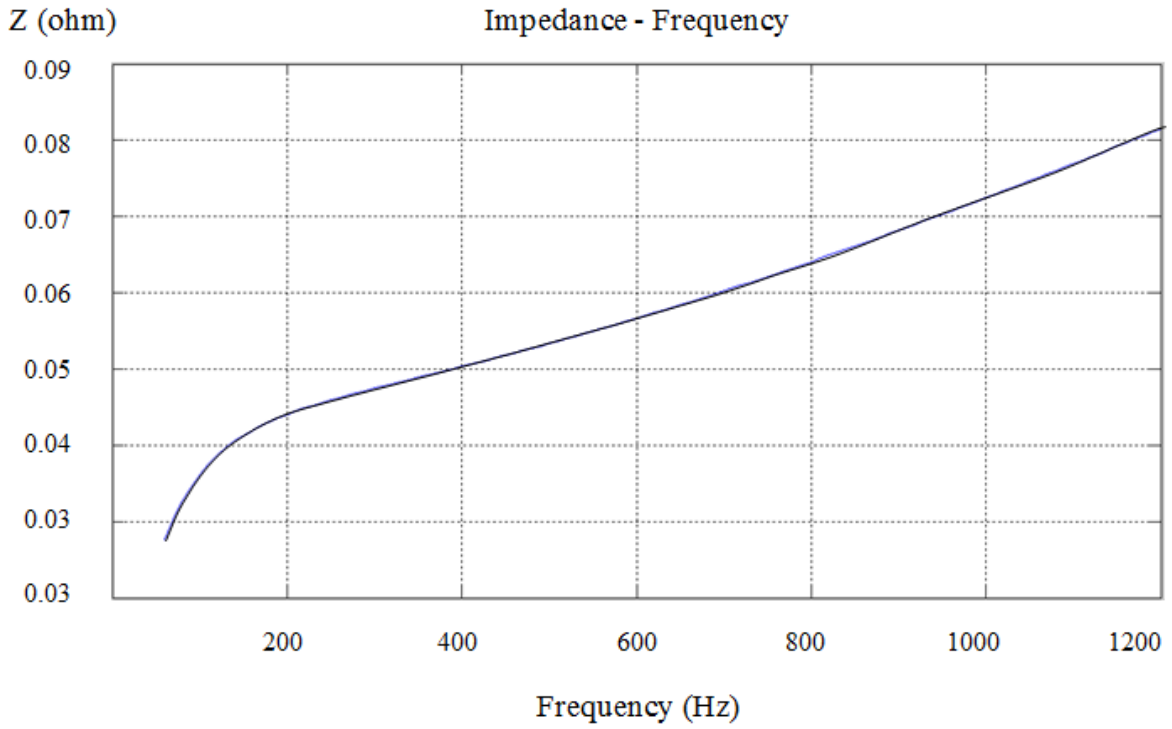

Figure 2-26 Impedance scan of CIGRE type C (60 Hz < f < 1200 Hz)

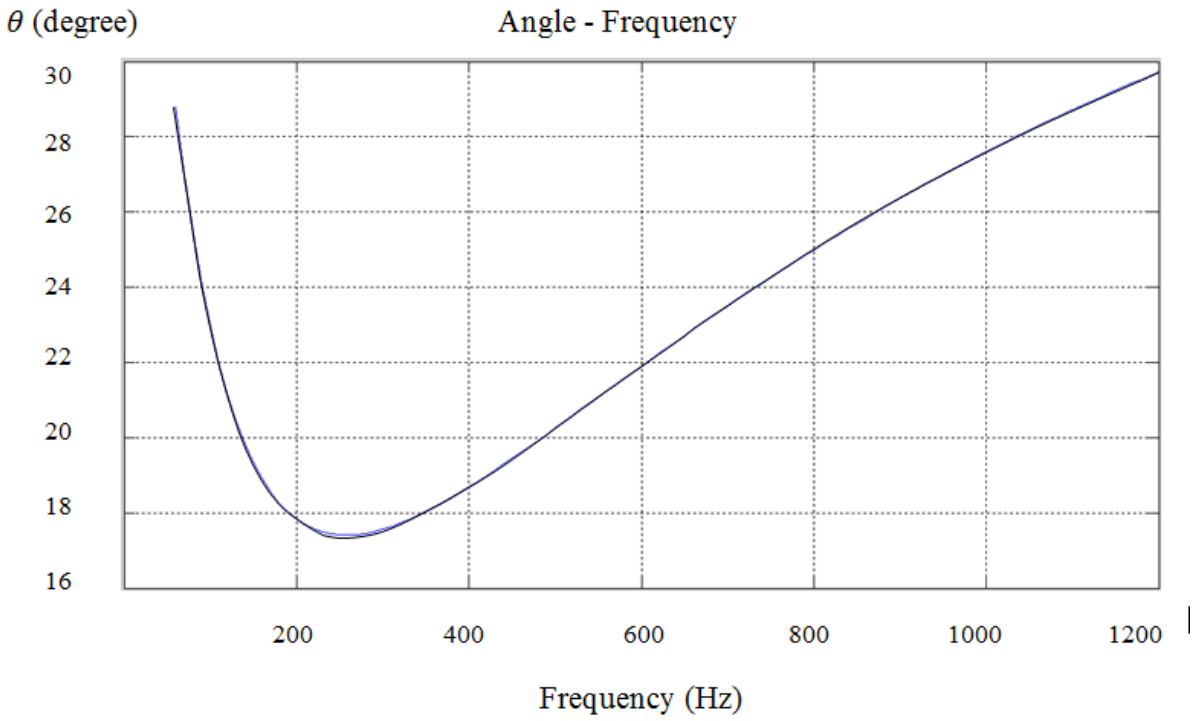

Figure 2-27 Impedance phase of CIGRE type C (60 Hz < f < 1200 Hz)

2- Rotating load

Two types of harmonic models are available for rotating loads: (i) Induction Motor (ii) Synchronous Motor

The harmonic models present in this work are based on sequence impedance. Under unbalance conditions or for inter-harmonic studies, it is necessary to obtain the harmonic impedance for machines of all three sequences (zero, positive, and negative).

(i) Induction Motor

Induction machine is represented with the sequence impedances. The positive and negative impedance of the induction machine is presented in equation 2.84 to 2.86. Figure 2.28 presents the equivalent circuit of induction motor which is composed of stator impedance, a magnetization branch with a core loss resistance, and slip-dependent rotor impedance. Since the type of connection of induction machine is Delta or Y ungrounded, there is no path for zero sequence current in a circuit; the zero sequence impedance is infinite consequently.

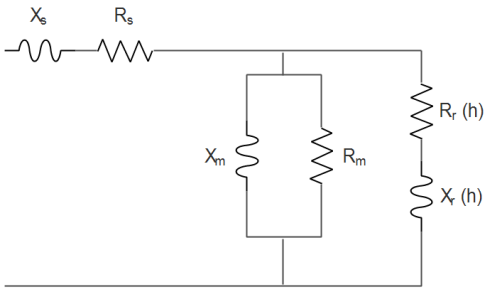

Figure 2-28 Equivalent circuit of induction motor

The harmonic slips of induction for positive sequence harmonics and negative sequence harmonics are deference. The harmonic slips of the induction motor for each harmonic sequence are given by:

$$S_h = \frac{\omega_h - \omega_r}{\omega_h} = \frac{h+s-1}{h} \cong \frac{h-1}{h} \left(\text{for } h \neq 1 \right) \quad \textit{for Positive harmonic sequence} \tag{2.92}$$

$$S_h = \frac{h+1}{h} \left(\text{for } h \neq 1 \right) \quad \textit{for Negative harmonic sequence} \tag{2.93}$$

where

ω_h : Synchronous frequency

ω_r : Rotor angular frequency

s : Conventional slip at fundamental frequency

In the case of deep bar, a double – cage motor, the rotor resistance (R_r) increases significantly at slip frequencies due to skin effect, which concentrate the rotor current in the outer edge of the rotor bar. The rotor reactance (X_r) decreases slightly as the slip frequency decreases [5]. Therefore, the equation of rotor resistance and reactance due to skin effect are modified with following equations:

$$R_r(h) = \frac{R_r}{S_h} \times \left(1 + CFR \times S_h \right) \tag{2.94}$$

$$X_r(h) = X_r \times \left(1 + CFX \times S_h \right) \tag{2.95}$$

where

$R_r(h)$: Frequency dependent rotor resistance

$L_r(h)$: Frequency dependent rotor inductance

R_r : Dc rotor resistance

X_r : Dc rotor reactance

CFR : Rotor cage factors for rotor resistance

CFX : Rotor cage factors for rotor inductance

S_h : is the slip at the harmonic frequency

Stator impedance:

$$Z_s(h) = R_s + h \times jX_s \tag{2.96}$$

where

R_s : Stator resistance.

X_s : Stator reactance.

Magnetization:

$$R_m(h) = R_m \times \frac{3}{4 \times h} + \left(\frac{1}{4 \times h^2}\right) \tag{2.97}$$

$$X_m(h) = h \times X_m \tag{2.98}$$

$$Z_m(h) = \frac{(R_m(h) \times jX_m(h))}{(R_m(h) + jX_m(h))} \tag{2.99}$$

where

R_m : Magnetization resistance.

X_m : Magnetization reactance.

In unbalanced three phase system, the equivalent admittance matrix of induction machine is calculated from the sequence admittance matrix by means of Fortescue transformation.

$$Z_p(h) = Z_s(h) + (Z_m(h) \| Z_{pr}(h)) \tag{2.100}$$

$$Z_n(h) = Z_s(h) + (Z_m(h) \| Z_{nr}(h)) \tag{2.101}$$

$$\boldsymbol{Z}_{induction} = \begin{bmatrix} \infty & \mathbf{0} & \mathbf{0} \\ \mathbf{0} & Z_p & \mathbf{0} \\ \mathbf{0} & \mathbf{0} & Z_n \end{bmatrix} \tag{2.102}$$

$$\boldsymbol{Z}_{abc} = \boldsymbol{A} \times \boldsymbol{Z}_{induction} \times \boldsymbol{A}^{-1} \tag{2.103}$$

$$\boldsymbol{Y}^{h}_{induction} = \boldsymbol{Z}^{-1}_{induction} \tag{2.104}$$

where

$Z_n\,(h)$: Negative sequence rotor impedance.

$Z_p(h)$: Positive sequence rotor impedance.

$\boldsymbol{Y_n}$ of induction machine is given by:

$$\boldsymbol{Y}_{kk} = \boldsymbol{Y}^{h}_{induction} \tag{2.105}$$

$$\boldsymbol{Y}_{n} = \left[\boldsymbol{Y}_{kk}\right] \tag{2.106}$$

$$\boldsymbol{Y}_{n} = \begin{bmatrix} & k_a & k_b & k_c \\ k_a & Y^h_x & Y^h_y & Y^h_z \\ k_b & Y^h_z & Y^h_x & Y^h_y \\ k_c & Y^h_y & Y^h_z & Y^h_x \end{bmatrix} \tag{2.107}$$

The impedance characteristic of an induction machine is shown in figures 2.28 to 2.29 for the following induction machine parameters:

Rs = 5.0288 ohm, Xs = 20.1153 ohm, Rm = 6275.97 ohm, Xm = 704.04 ohm, Rr = 5.3479 ohm, Xr = 20.1153 ohm, CFr = 0.0, CFx = 0.0

Note that all parameters are determined at fundamental frequency (60 Hz)

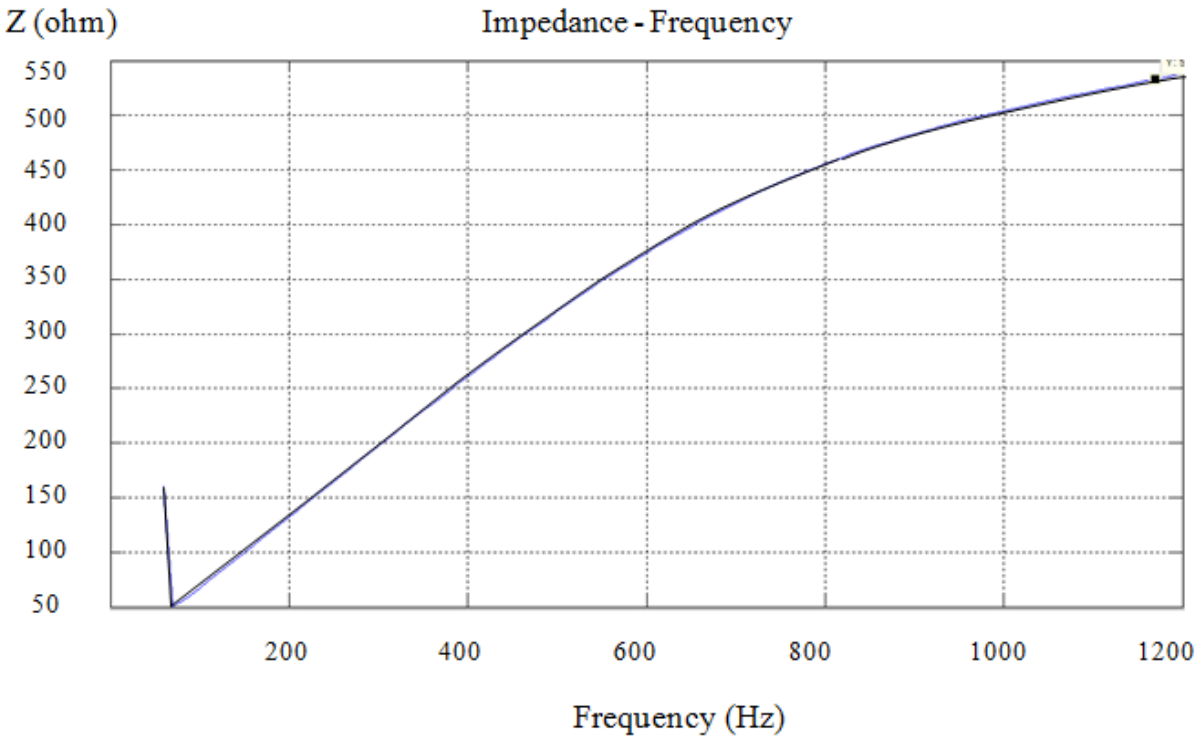

Figure 2-29 Impedance scan of induction motor (60Hz < f< 1200 Hz)

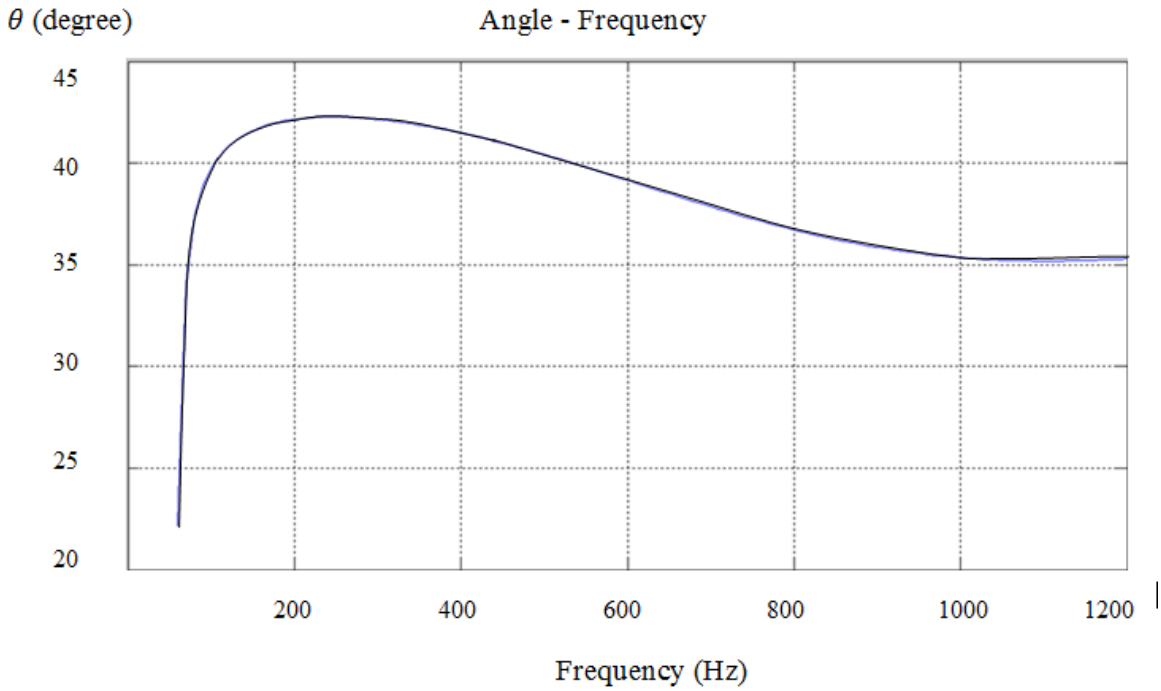

Figure 2-30 Phase impedance of induction motor (60Hz < f< 1200 Hz)

(ii) Synchronous Motor

The harmonic model of synchronous machine is represented with sequence impedance. For the frequencies slightly greater than fundamental frequency, the sub-transient reactance multiplied harmonic order is employed for positive and negative sequence harmonics and the zero sequence reactance multiplied harmonic order is employed for zero sequence harmonics. Hence, the harmonic impedance of the synchronous machine is modified with following equations:

$$X'' = \frac{X_d'' + X_q''}{\mathbf{2}} \tag{2.108}$$

$$X_1(h) = h \times X'' \tag{2.109}$$

$$X_2(h) = h \times X'' \tag{2.110}$$

$$X_0(h) = h \times X_0 \tag{2.111}$$

where

X_d'' : Sub-transient reactance (d axis)

X_q'' : Sub-transient reactance (q axis)

X_0 : Zero sequence reactance

X_1 : Positive sequence reactance

X_2 : Negative sequence reactance

The resistance of the machine should be corrected due to the skin effect. The resistance at high frequencies is modified with following equation:

$$R(h) = R(\mathbf{1.0} + Ah^B) \tag{2.112}$$

where

R : Armature dc resistance

$$\boldsymbol{Z}_{synch}^{h} = \boldsymbol{A} \times \boldsymbol{Z}_{012} \times \boldsymbol{A}^{-1} \tag{2.113}$$

$$\boldsymbol{Y}_{synch}^{h} = [\boldsymbol{Z}_{synch}^{h}]^{-1} = \begin{bmatrix} Y_x^h & Y_y^h & Y_z^h \\ Y_z^h & Y_x^h & Y_y^h \\ Y_y^h & Y_z^h & Y_x^h \end{bmatrix} \tag{2.114}$$

where

$\boldsymbol{Z_{012}}$: Sequence impedance of the synchronous machine

$\boldsymbol{Y_n}$ for Y grounded motor is defined by:

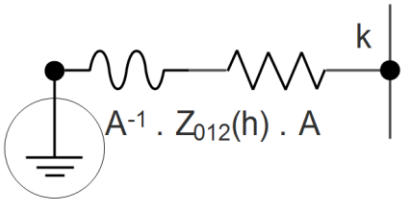

Figure 2-31 Synchronous motor (Yg)

$$\boldsymbol{Y_{kk}} = \boldsymbol{Y_{synch}^{h}} \tag{2.115}$$

$$\boldsymbol{Z_{g}^{h}} = h \times Z_g \tag{2.116}$$

$$\boldsymbol{Y_n} = \begin{bmatrix} Y_g^h & \mathbf{0} \\ \mathbf{0} & \boldsymbol{Y_{kk}} \end{bmatrix} \tag{2.117}$$

$\boldsymbol{Y_n}$ in detail format is given by:

$$\boldsymbol{Y_n} = \begin{bmatrix} & g & k_a & k_b & k_c \\ g & Y_g^h & \mathbf{0} & \mathbf{0} & \mathbf{0} \\ k_a & \mathbf{0} & Y_x^h & Y_y^h & Y_z^h \\ k_b & \mathbf{0} & Y_z^h & Y_x^h & Y_y^h \\ k_c & \mathbf{0} & Y_y^h & Y_z^h & Y_x^h \end{bmatrix} \tag{2.118}$$

$\boldsymbol{Y_n}$ for Delta connection is defined by:

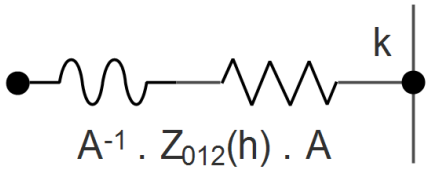

Figure 2-32 Synchronous motor (Delta or Y)

$$\boldsymbol{Y_n} = \left[\boldsymbol{Y_{kk}}\right] \tag{2.119}$$

$$\boldsymbol{Y_n} = \begin{bmatrix} & k_a & k_b & k_c \\ k_a & Y_x^h & Y_y^h & Y_z^h \\ k_b & Y_z^h & Y_x^h & Y_y^h \\ k_c & Y_y^h & Y_z^h & Y_x^h \end{bmatrix} \tag{2.120}$$

Impedance scan of a synchronous machine is shown in Figure 2.31; the parameters of the machine are presented in Table 2-3. As can be seen from Figure 2-32, the phase impedance of synchronous machine is mostly 90 degree.

Table 2-3 Parameters of synchronous machine at fundamental frequency 60 Hz

	R (ohm)	**X (ohm)**
Steady state	17.62344	176.23
Transient	9.09411	115.8898
Sub transient	7.90792	100.7737
Zero sequence	2.60961	33.25
Negative sequence	7.90792	100.7737
Grounding	0.0	0.0

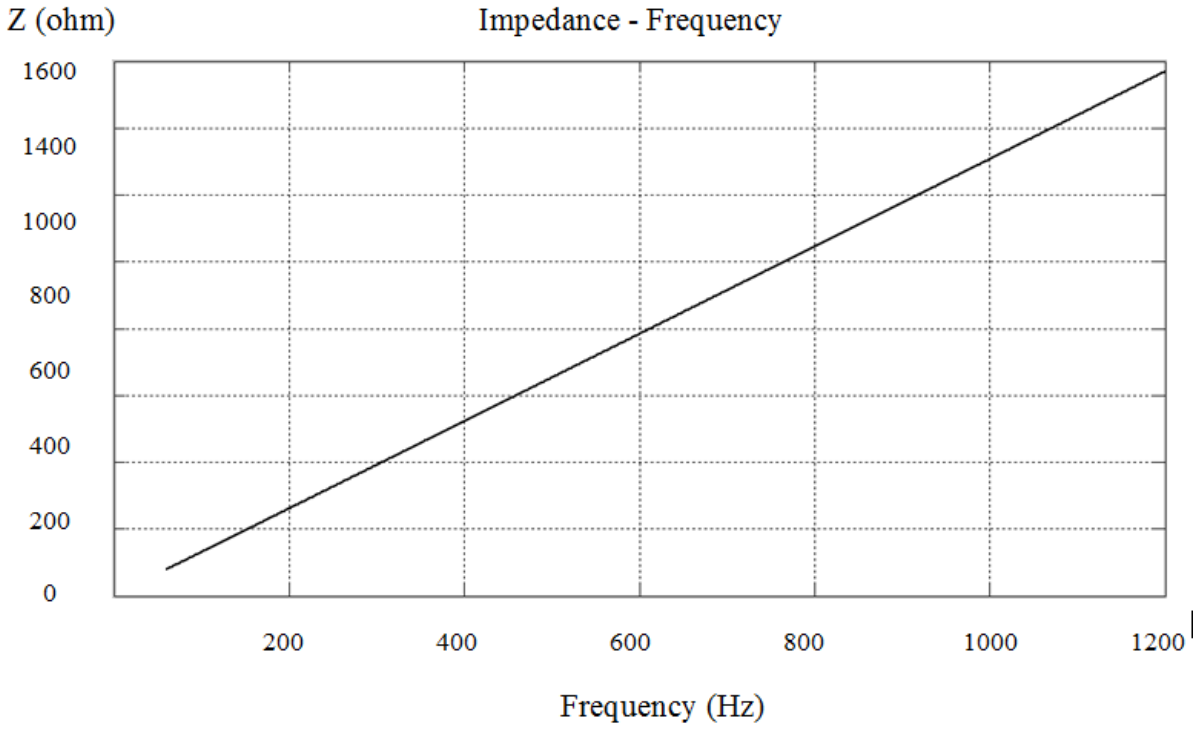

Figure 2-33 Impedance characteristic of synchronous machine (60 Hz < f<1200 Hz)

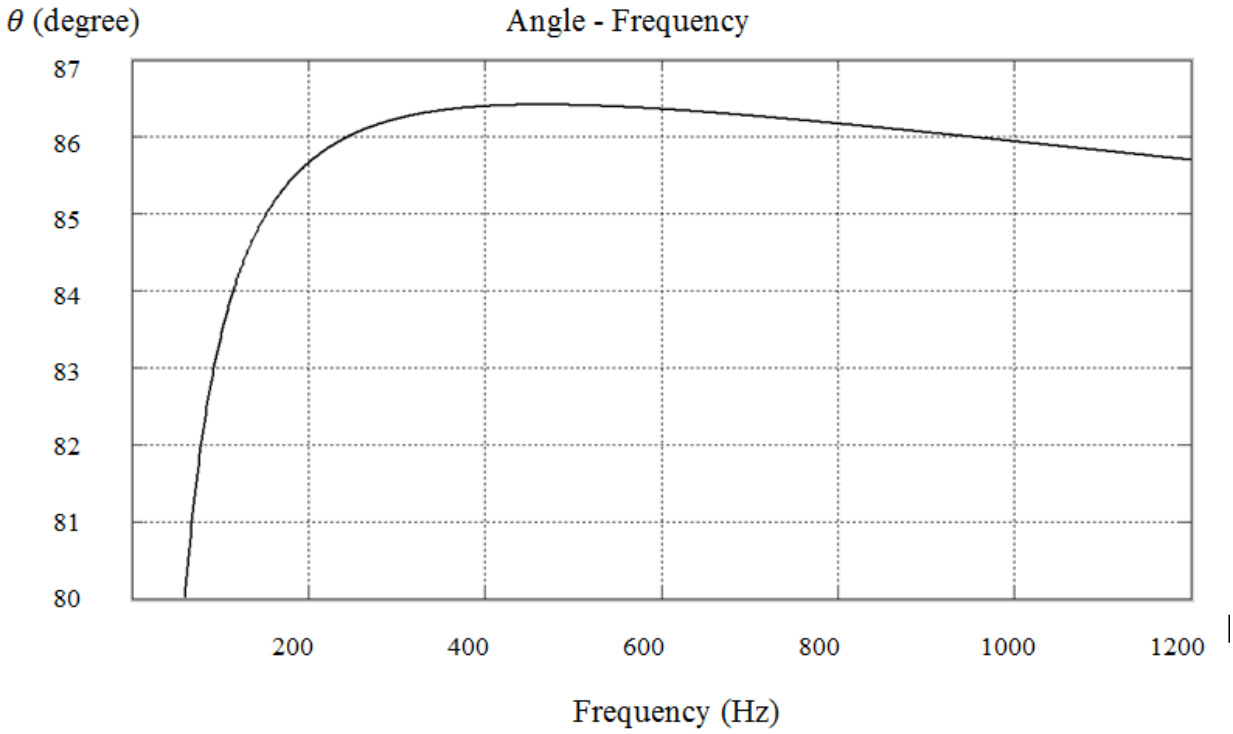

Figure 2-34 Phase impedance of the synchronous machine (60 Hz < f < 1200 Hz)

3- Nonlinear devices

Figure 2-35 shows a nonlinear device. The nonlinear devices do not draw a sinusoidal current when supplied by a sinusoidal voltage source. In frequency domain solution, the harmonic distortions produced by nonlinear devices are decomposed into multiple frequency sinusoidal sources due to distortions generated at several frequencies. Converters, nonlinear impedances with saturation curves such as transformers and electric arc furnaces are common harmonic sources in industrial networks.

The equivalent circuit of a nonlinear device is presented in Figure 2-36. Generally, the harmonic model for a nonlinear device is a Norton equivalent circuit, consisting of a current source at the harmonic frequency in parallel with impedance. In this model, the harmonic distortion is presented with current source and the linear part of the load is represented with parallel RL. The values of harmonic current produced by nonlinear loads at each harmonic frequency are provided by the manufacturer of the device.

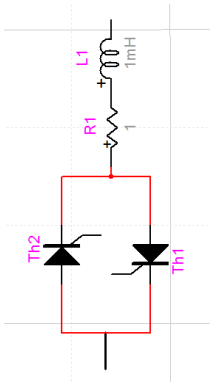

Figure 2-35 Nonlinear load

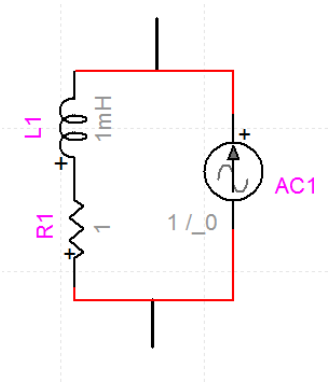

Figure 2-36 Norton equivalent of a nonlinear load

The harmonic current in MANA is given by:

$$\boldsymbol{I}_{\boldsymbol{b}}^{\boldsymbol{h}} = \begin{bmatrix} & \mathbf{1} \\ q_1 & \tilde{I}_{aequ}^{h} \\ q_2 & \tilde{I}_{bequ}^{h} \\ q_3 & \tilde{I}_{cequ}^{h} \end{bmatrix} \tag{2.121}$$

where

$\tilde{I}_{i,equ}^{h}$: Harmonic current at phase i (a,b,c)

CHAPTER 3 PLANNING OF LARGE HARMONIC FILTERS IN INDUSTRIAL NETWORKS

In this chapter, the use of passive harmonic filters to control and limit the harmonic voltages and currents are discussed. Different types of passive filters used to decrease harmonic distortions within IEEE 519 requirements, are detailed.

This chapter also shows a simple methodology to place harmonic filters in a system with multiple harmonic sources. This methodology is based on brute face search while it attempt to reduce possible candidates and accordingly speed up the process.

3.1 Literature review

In [26] two strategies for calculating the parameters of harmonic filters are suggested: 1- fundamental frequency reactive power compensation and 2- calculation of filter parameters using Z-bus method. The methodology used in [27] to size harmonic filters considers: 1- reactive compensation 2- IEEE standards for maximum harmonic distortions 3- power system variations 4- filter detuning. In [7] the filter sizing for high pass filters and single tuned filters are presented. A systematic approach to design single tuned filter is described in [28]. The proposed method considers the detuning effects due to temperature and frequency variations, as well as manufacturing tolerances. In [29] a transfer function approach in the analysis and design of passive harmonic filters is presented. The transfer function approach derives an analytical formulation of a utility system including passive filter with a basis of Laplace transformation. In [30] a particle swarm optimization method with nonlinear time-varying evolution is used in the planning of passive harmonic filters for a system under multiple harmonic sources. The aim of this optimization is to minimize the cost of filters and the filters loss.

Many efforts have been put to find the most efficient location for placing harmonic filters. A chance constrained programming model for optimal planning of harmonic filters is presented in [31]. Considering the randomness of the decision environment as well as the merits and shortcomings of these two kinds of filters, a chance constrained programming model for unified optimal allocation of active and passive filters is proposed in this paper, and a stochastic simulation based genetic algorithm to solve the model is developed. In [32] an approach for determining optimal or near-optimal locations and sizes of single-tuned passive harmonic filters

among existent capacitor busses in a power system is explained. In this paper, the constrained problem is formulated and is solved by a genetic algorithm-based optimizer. Another approach for filter allocation is described in [3]. The proposed strategy requires a limited knowledge of the system impedance; in addition, it is independent of the knowledge of the harmonic current injection locations and parameters. In [33] the harmonic filters are placed at different locations in IEEE 13 bus industrial system and the results are compared. The genetic algorithm and simulated annealing are common methodologies used to harmonic filter allocation. In [34] , [35] and [36], genetic algorithm for harmonic filter allocation is discussed. However, given the small number of nodes in industrial networks and the efficiency of frequency domain solvers, it is possible to address straightforward techniques as will be demonstrated in this work.

3.2 Harmonic filter

The harmonic filters are one of the solutions for control of harmonic distortion. They are three types of harmonic filters:

1- Passive harmonic filters

2- Active harmonic filters

3- Hybrid harmonic filters

3.2.1 Passive harmonic filters

Passive harmonic filters are designed to provide low impedance at tuned frequencies. There are two configurations, use of series reactors or shunt impedances. Although the shunt impedance is more costly than the series reactor, they successfully accomplish two purposes:

1- Control of harmonics

2- Power factor correction

Series reactors provide significant harmonic reduction at high harmonic orders (h>11), however at low harmonic orders, the reduction is not considerable.

3.2.2 Active harmonic filter

Active harmonic filters inject specific current to control harmonic distortions and compensate the reactive power. The performance of active filters depend also on its control algorithm, they can also be used to regulate the terminal voltage simultaneously.

3.2.3 Hybrid harmonic filter

In some industrial applications, the combination of the active filters and passive filters are used and this combination is called hybrid harmonic filter. Due to this combination, the size of active filter is reduced. Hence, the hybrid filter can provide active filter reaction at reasonable costs.

3.3 Passive filter design

The aim in filter design is to size capacitor bank to trap certain harmonics at a certain degree by using a tuning reactor. In some cases, an external resistance can be added for the following reasons

1- Change the sharpness of tuning frequency

2- Control the maximum current allowed through the filter

3- Avoid the overheating of filter

As a result, the harmonic filter design involves four steps:

1- Determine the reactive compensation of the bus.

2- Size the capacitor bank of harmonic filter according to the required reactive power.

3- Tune the reactor at the harmonic frequency.

4- Size the resistance according to the quality factor of the filter.

3.3.1 Single tuned harmonic filter

The single tuned filter is the most common filter in industrial applications. They provide a very small impedance path at the tuned frequency, and absorb the harmonic current consequently. They can result in resonances in the system. Because of that they are not recommended to be

used at high frequencies. The equivalent circuit of a single tuned filter is illustrated in Figure 3-1. And, the impedance is presented in Figure 3-2.

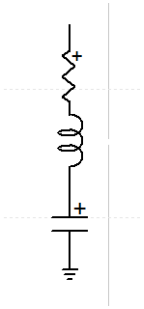

Figure 3-1 Single tuned filter

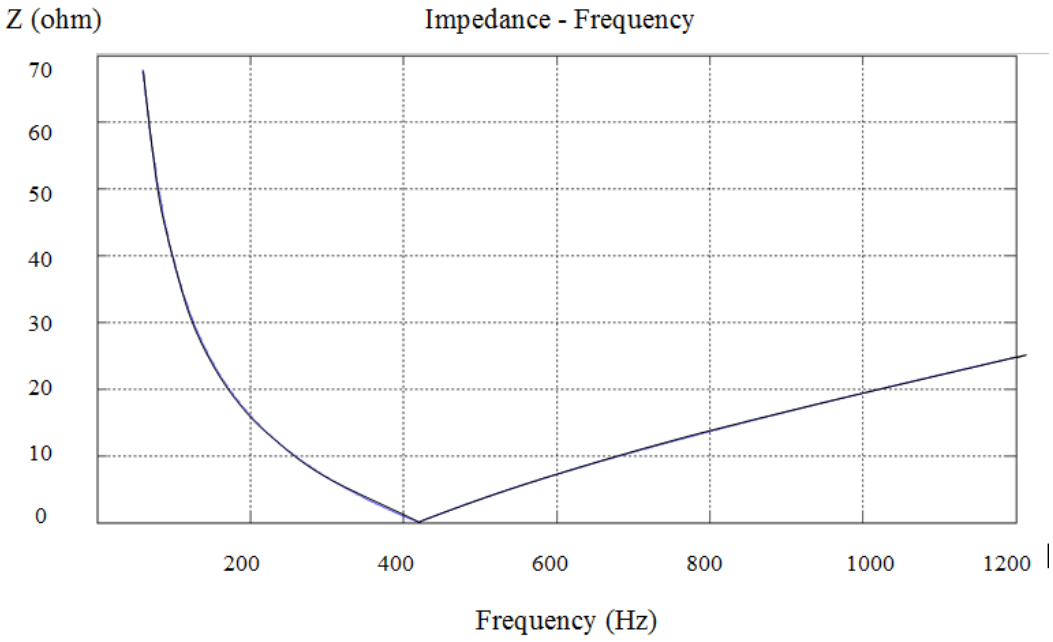

Figure 3-2 Impedance Scan of single tuned harmonic filter (tuned at 420 Hz)

3.3.2 High pass harmonic filter

High pass harmonic filters provide small impedance path at high harmonic orders. This type of harmonic filters can suppress harmonic propagation over a broader range frequency and is not sensitive only to the tuned frequency. The power loss due to the resistor is significant for this type of filter. The equivalent circuit of a high pass harmonic filter is presented in figure 3-3. And, the impedance scan is presented in Figure 3-4.

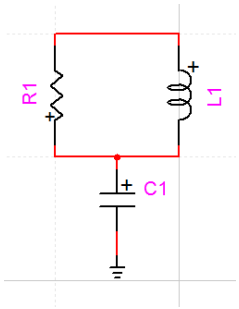

Figure 3-3 High pass harmonic filter

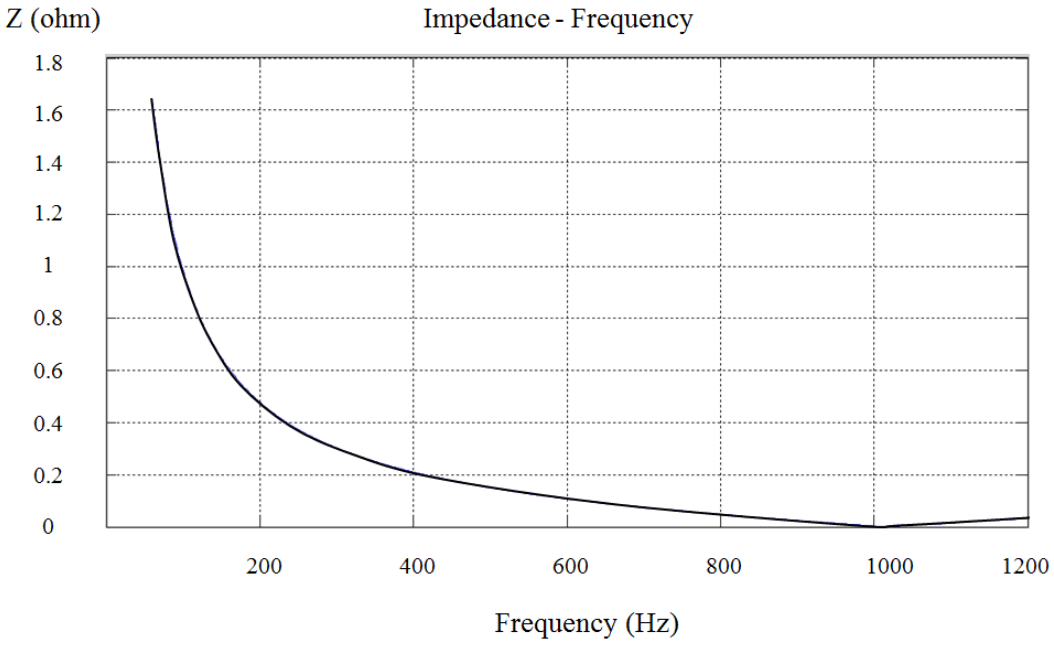

Figure 3-4 Impedance Scan of High pass harmonic filter (tuned at1020 Hz)

3.3.3 C-Type harmonic filter

The C-type filters are created by adding a capacitor (C_2) to L branch of the high pass filters. They are suitable for filtering any frequencies (high or low). Moreover, they are mostly recommended for heavy industrial network (e.g. steel factory) and are also widely used in distribution networks and high voltage transmission systems to filter 3rd harmonics. The equivalent circuit of a C-type harmonic filter is show in Figure 3-5.

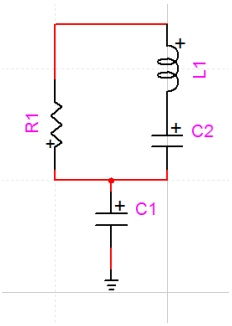

Figure 3-5 C-Type harmonic filter

3.3.4 Multiple filter banks

When it is necessary to control harmonic distortions composed of several dominant harmonic components, the harmonic filter should consist of several branches such that each branch attenuates the distortion due to a specific harmonic component. One can consider a filter with several single tuned, high pass and C- Type filters.

It is not required to tune harmonic filters for each harmonic order. Most of the time, one harmonic filter tuned for the specific frequency can suppresses the distortions of rang of frequencies. Figure 3.6 shows a multiple filters bank at the point of network connection.

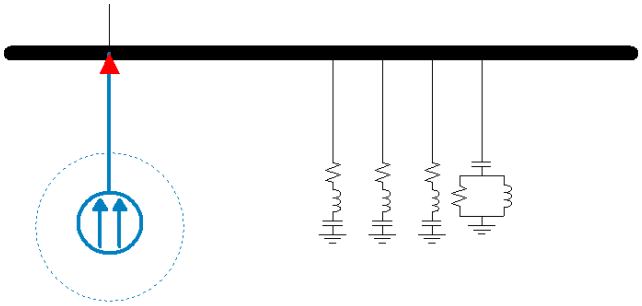

Figure 3-6 Multiple filter bank

3.3.5 Resonance problem

The parallel resonance produced by single tuned filters can interact with the frequency response of the system and cause a large resonance peak. At the parallel resonance frequencies, the harmonic current can amplify voltage distortion and cause harmonic problems within the system. The installation of several single tuned harmonic filters can provide several parallel resonances in the system.

3.3.6 Constraint

In order to achieve a suitable voltage at PCC, the following constraints should be considered in harmonic filter design:

A) Harmonic distortion limit by IEEE 519

The acceptable limits of voltage and current distortions according to IEEE 519 guideline is presented in Table 3-1 and table 3-2. IEEE 519 set limits for harmonic current injected into PCC as well as harmonic voltage at PCC.

Table 3-1 IEEE 519 voltage distortion limits

Voltage kV (L-L)		**IHD**	**THD**
>	< =		
0	69	3	5
69	161	1.5	2.5
161		1	1.5

Table 3-2 IEEE 519 current distortion limits

$\frac{\mathbf{I_h}}{\mathbf{I_L}}, \% -$ **General Distribution System (120 V – 69 kV)**						
$\frac{\mathbf{I_h}}{\mathbf{I_L}}$	$\mathbf{h < 11}$	$\mathbf{11 \leq h < 17}$	$\mathbf{17 \leq h < 23}$	$\mathbf{23 \leq h < 35}$	$\mathbf{h \geq 35}$	**TDD** (%)
< 20	4.0	2.0	1.5	0.6	0.3	5
20 50	7.0	3.5	2.5	1.0	0.5	8
50 - 100	10	4.5	4.0	1.5	0.7	12
100 – 1000	12	5.5	5.0	2.0	1.0	15
> 1000	15	7.0	6.0	2.5	1.4	20

B) Harmonic distortion limit by IEEE 18

The filter should be designed in a way to satisfy the IEEE 18 standard requirements. According to the IEEE 18 guideline "Capacitors shall be capable of operation under contingency system and bank conditions provided that none of the following limitations are exceeded":

1- 110% of rated RMS voltage.

2- 120% of rated peak voltage, i.e., peak voltage not exceeding 1.2 x √2 x rated RMS voltage, including harmonics, but excluding transients.

3- 135% of nominal RMS current based on rated kVAR and rated voltage.

4- 135% of rated kVAR.

It should be noted that in section 3.4, we will discuss how to choose a suitable rated voltage for a capacitor bank.

3.3.7 Quality factor

The ability of distributing the absorbed energy at tuned frequency is named quality factor. The quality factor in single tuned fitters should be large enough to trap the largest amount of the harmonic frequency; however, in high pass filters, the quality factor should be low to trap the large amount of harmonic frequency. Typical quality factor is between 20 and 120 for single tuned filters and between 2.5 and 5 for high pass filters.

3.3.8 Filter detuning factor

As can be seen from Figure 3-2, each single tuned filter provides series and parallel resonance in the system. Most of the times, there are multiple dominant harmonic components in the system and accordingly multiple single tuned filters are placed while the tuning frequencies of the filters due to the following conditions can be changed:

1- The temperature variations can cause aging in capacitors and accordingly it would cause decrement in capacitance value.

2- The manufacturing tolerance of the filter components can shift the tuning frequency in any directions.

3- Removing or adding a new load or any variation in topology or configuration of the system that changes the impedance of the system, can result in shifting of the tuning frequency.

Shifting of series resonant point to a higher frequency point can lead the harmonic filter to amplify the harmonic voltage distortion instead of reducing it. Therefore the harmonic filters are typically tuned a few percent below the harmonic frequency (3% to 5% lower than the harmonic frequency).

Detuning factor should be determined in a way to prevent interactions between the system impedance and the resonance peak of the single tuned filter.

3.3.9 K-Factors transformer

K-factor addresses the problems caused by non-linear loads (harmonic sources). Sometimes the harmonics cause overheating and subsequent insulation failure in transformer's winding insulation, and it is necessary to de-rate the transformer capacity. The K-Factor is given by the following equation:

$$K = \frac{\sum_1^h (I_h \times h)^2}{\sum_1^h I_h^{\,2}} \tag{3.1}$$

where

I_h : Harmonic current at h harmonic order

K : K-Factor

For transformer with K-Factor greater than 1, the transformer should be de-rated.

3.4 Algorithm of filter design

The algorithm of harmonic filter design adopted in this work is presented as follows:

Step 1 - Initialization

The input data required to carry out the passive filter design are detailed as follows:

- Select the bus
- Select the desired *PF*
- Select the filter detuning factor (δ)
- Select the quality factor (Q)

The load flow is run and following parameters at selected bus are calculated:

- Determine P (active power),
- Determine PF (power factor)
- Determine the Thevenin equivalent impedance

The Harmonic analysis is run and following parameters at selected bus are calculated:

- determine THDv and IHDv
- Measure the voltage at each bus (at fundamental frequency and harmonic frequencies separately)
- Measure the current at each bus (at fundamental frequency and harmonic frequencies separately)

Step 2 – Select the dominant harmonic components

According to IEEE 519, the dominant harmonic components are selected, e.g. for the nominal voltage between *0* and 69*kv*, harmonic components with IHDv greater than 3% are selected.

Step 3

The harmonic voltages *V(h)* and harmonic currents *I(h)* corresponding to the selected harmonic orders are measured.

Step 4 - Select type of filters

In this step, *n* numbers of harmonic orders are selected. For the first iteration *n* is equal to 1, and in each iteration one filter is added (*n = n+1*). Then, the suitable filters for each harmonic order are sized.

The types of harmonic filters are selected as follows:

- Single tuned filter for low frequencies. (recommended for $2 < \mathrm{h} < 17$)
- High pass filter for high frequencies. (recommended for $\mathrm{h} > 17$)

Step 3 - Determine the initial values of the filter components

The harmonic filters are also used to compensate the reactive power. The total reactive power needed to correct the power factor can be determined as:

$$Q_{Total} = P(\tan\theta_2 - \tan\theta_1) \quad (3.2)$$

$$\theta_1 = \arccos Pf_1 \quad (3.3)$$

$$\theta_1 = \arccos Pf_2 \quad (3.4)$$

where:

Q_{Total} : Reactive compensation of the bus

P : Active power of the bus

Pf_1 : Initial power factor of the bus

Pf_2 : Desired power factor of the bus

Step 4

Once the value of the reactive compensation is calculated in a way to improve the power factor to desired level then the parameters of filter are calculated. The capacitor corresponding to the *h'th* harmonic filter can be distributed approximately by:

$$Q_c = Q_{Total} \times \frac{I_i^h}{\sum_{i=1}^{j} I_i^h} \tag{3.5}$$

where:

Q_c : Reactive power of the filter

I_i^h : Harmonic current of the bus (at h harmonic order)

Step 5 - Select the size and the voltage of capacitor

According to the standard values of capacitor banks (appendix B), the rating voltage and the rating reactive powers of the capacitor bank are selected.

For the first iteration (i = 1), the rated voltage of capacitor bank is assumed to be equal to the nominal voltage of the bus. And, the capacitor is assumed to be close to the Q_c (size of capacitor should be selected from the standard values appendix B).

For i > 1, the rated voltage and the rated size of the capacitor bank should be greater than previous values (they should be selected from the standard values appendix B).

It has to be mentioned that the rated voltage of the capacitor bank should be equal or greater than the nominal voltage of the bus since the reactor increases the voltage on the capacitor bank.

Step 6

Since the rated voltage of the capacitor bank and the nominal voltage of the bus are not equal, the reactive power should be de-rated by using:

$$Q_{c\ derated} = Q_c \times \frac{V_n^2}{V_{rated}^2} \tag{3.6}$$

where:

$Q_{c\ derated}$: De-rated reactive power of the capacitor bank.

V_n : Nominal voltage of the bus.

V_{rated} : Rated voltage of the capacitor bank.

Step 7

The equivalent reactance of the capacitor bank is calculated as:

$$X_c = \frac{Q_{c\ derated}}{V_n^2} \tag{3.7}$$

$$C = \frac{1}{\omega X_c} \tag{3.8}$$

where:

X_c : Capacitor reactance.

V_n : Nominal voltage of the bus.

C : Capacitor in *uf*.

ω : Angular frequency measured in radians per second

Step 8

The harmonic filters are tuned at their harmonic frequencies. Detuning factor should be applied to the single tuned filter due to their sharp resonance.

The inductance of harmonic filter of single tuned filter at *h'th* harmonic order is calculated as:

$$L = \frac{1}{(\omega \times h \times \delta)^2 \times C} \tag{3.9}$$

where:

L : Inductance of the filter.

δ : Filter detuning factor

X_L : Impedance of reactor

h : Harmonic order

The inductance of harmonic filter of high pass filter at *h'th* harmonic order is calculated as:

$$L = \frac{\mathbf{1}}{(\omega \times h)^2 \times C} \tag{3.10}$$

$$X_L = \omega L \tag{3.11}$$

Step 9

The resistance of the filters can be determined as:

For single tuned filters

$$R = \frac{h\, X_L}{Q} \tag{3.12}$$

For high pass filter

$$R = Q \times \sqrt{\frac{L}{R}} \tag{3.13}$$

where:

R : Reactive compensation of the bus

X_L : Impedance of reactor

h : Harmonic order

Q : Quality factor of the filter

Step 10 - IEEE 18

The rated voltage and the rated size of capacitor bank should satisfy the IEEE 18 requirements, thus, the voltage and the current through the filter should be determined.

The impedance of the filter at the fundamental frequency and at the harmonic frequencies are calculated as follows:

For single tuned filter

$$Z_h = R + j(\omega L - \frac{1}{\omega C}) \quad (3.14)$$

For high pass filter

$$Z_h = \frac{-1}{j\omega C} + \frac{1}{(\frac{1}{R} + \frac{1}{j\omega L})} \quad (3.15)$$

Where:

Z_h : Impedance of the filter at h harmonic order.

The fundamental current through the filter is calculated as:

For single tuned filter

$$I_c = \frac{V_n}{\sqrt{3}(X_C - X_L)} \quad (3.16)$$

For high pass filter

$$I_c = \frac{V_n}{\sqrt{3}\ Z_h} \quad (3.17)$$

where:

I_c : Current of the capacitor bank at fundamental frequency.

Z_h : Impedance of the filter at fundamental frequency.

The reactance of the capacitor at *h'th* harmonic frequency is calculated as:

$$X_{ch} = \frac{X_C}{h \times \delta} \quad (3.18)$$

where:

X_{Ch} : Impedance of the capacitor bank.

The *h'th* harmonic current through a filter is given by:

$$I_{ch} = \frac{V_h}{Z_h} \quad (3.19)$$

where:

I_{ch} : Harmonic current at h harmonic order

V_h : Harmonic voltage at h harmonic order (line - phase)

The RMS voltage of the capacitor can be determined as follows:

$$V_{rms} = \sqrt{(X_c I_c)^2 + (X_{ch} I_{ch})^2} \tag{3.20}$$

$$V_{rms-pu} = \frac{V_{rms}}{V_{rated(LN)}} \tag{3.21}$$

where:

V_{rms} : RMS voltage of the capacitor bank.

V_{rms-pu} : RMS voltage of the capacitor bank (per unit)

$V_{rated\ (LN)}$: Rated voltage (line - neutral)

The peak voltage of the capacitor can be determined as follows:

$$V_{peak} = \sqrt{2} \times (X_c I_c + X_{ch} I_{ch}) \tag{3.22}$$

$$V_{peak-pu} = \frac{V_{peak}}{\sqrt{2} \times V_{rated(LN)}} \tag{3.23}$$

Where:

V_{peak} : Peak voltage of the capacitor bank.

$V_{peak-pu}$: Peak voltage of the capacitor bank (per unit)

The RMS current through the capacitor bank can be determined as:

$$I_{rms} = \sqrt{I_c^{\,2} + I_{ch}^{\,2}} \tag{3.24}$$

$$I_{rms-pu} = \frac{I_{rms}}{I_{rated}} \tag{3.25}$$

where:

I_{rms} : RMS current of the capacitor bank.

I_{rms-pu} : RMS current of the capacitor bank. (per unit)

I_{rated} : Rated current of the capacitor bank.

The reactive power of capacitor bank can be calculated as:

$$Q_{new} = \sqrt{(X_c I_c)^2 + (X_{ch}(1) I_{ch}(1))^2 + \ldots + (X_{ch}(h) I_n(h))^2} \quad (3.26)$$

$$Q_{new-pu} = \frac{Q_{new}}{Q_{derated}} \quad (3.27)$$

where:

Q_{new} : New reactive power of the capacitor bank.

Q_{new-pu} : New reactive power of the capacitor bank. (pu)

If any requirement is not met within the limitations of IEEE 18, the process is started over. The rated voltage and rated reactive power of the capacitor bank should be increased ($i = i+1$). Then the process is started form step 5. If all the requirements are satisfied, the process should move to next step.

Step 11 - IEEE 519

After placing the harmonic filters, the harmonic analysis is run, then afterward, the THDv[1] and IHDv[2] are determined.

If any requirement is not met within the limitations (of IEEE 519), the process is started over. And, another filter is added ($n = n+1$). . Then the process is started form step 4.If all the requirements are satisfied, the process should move to next step.

Step 12 - Check the parallel resonance

In this step, the resonance point of the system with inclusion of harmonic filter is checked.

$$f_{p-r} = \frac{1}{2\pi\sqrt{(L_s + L)C}} \quad (3.28)$$

where:

f_{p-r} : Parallel resonance of the filter.

[1] The equations of THD (Total Harmonic Distortions) are presented in the appendix A

[2] The equations of IHD (Individual Harmonic Distortions) are presented in the appendix A

L_s : Thevenin inductance of the bus.

3.5 Flowchart (1).of filter design

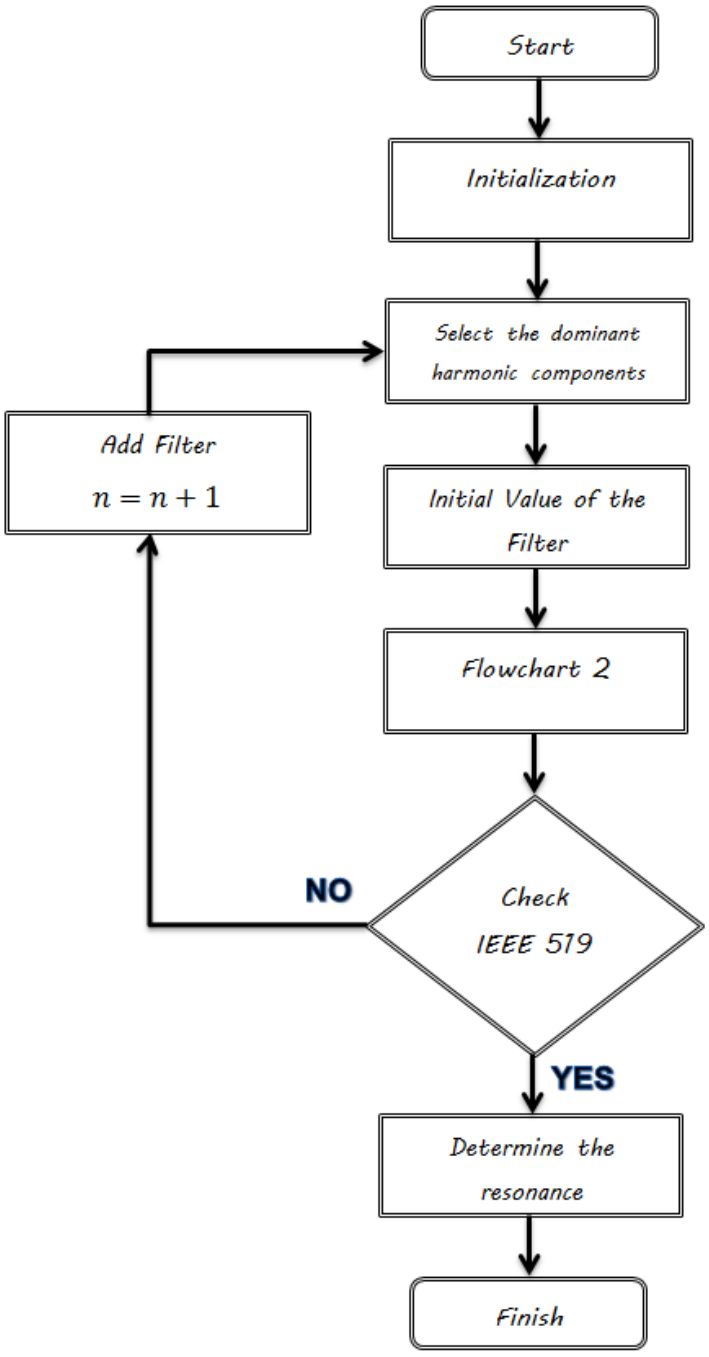

Figure 3-7 Flowchart 1 of Passive Filter Design

3.6 Flowchart (2).of filter design

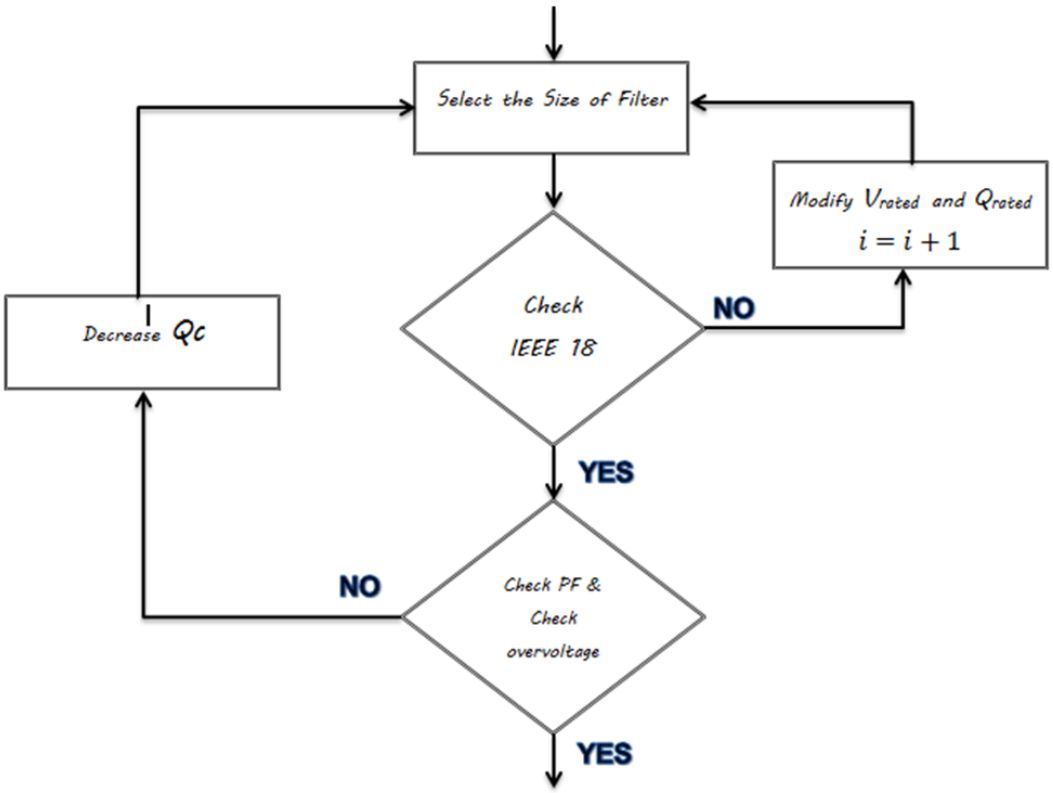

Figure 3-8 Flowchart 2 of Passive Filter Design

3.7 Harmonic filters allocation

As a rule of thumb, the harmonic filters should be installed close to the harmonic sources, however, in a system with multiple harmonic sources; this strategy may not give the best solutions since the harmonic flow will be altered by harmonic filters. The aim is to find efficient locations for placing the harmonic filters, the natural choices for the allocation of harmonic filter are at the bus with the highest harmonic distortion or bus with the large nonlinear device however as it can be seen later, the harmonic placement strongly depends on the impedance of the system and consequently the whole system need to be analyzed [36].Moreover the installation of harmonic filters is always costly, hence, optimization of the number of harmonic filters will result reduction in filtering cost [24]. In the proposed algorithm in this section, all possible configurations are simulated and the suitable configurations which can provide the maximum reductions in harmonic distortions are selected.

In order to find solutions to optimal harmonic allocation, the GA (genetic algorithm) is usually addressed [36], [35] and [37], however, it often looks like a never-ending process [38].

3.8 Algorithm of filter allocation

A simple algorithm for placing harmonic filters for medium size industrial networks is proposed in this study.

Step 1 - Initialization

The harmonic analysis is run (MANA harmonic analysis). THDv and IHDv are determined.

Step 2 - Identify the candidate buses

The candidate buses are identified as follows:

- The buses connected to the synchronous generator are ignored (the passive filter will decrease the power factor).
- The buses with very low distortions are ignored (according to IEEE 519).
- The buses required reactive power compensation are selected.

Step 3- Identify the sensitive load (optional)

The loads that need to be supplied by high quality of power is selected (optional)

Step 4 - Run proposed algorithm for sizing the suitable filters at each candidate bus

The following parameters at each simulation should be determined

- THDv and IHDv at all buses
- Voltages and PF at all buses
- K-Factor of transformer connected to the selected bus

Step 5 – Check maximum reduction in THDv and IHDv

The buses provided maximum reduction in THDv and IHDv are selected.

Step 6 – Check overvoltage

Filter placing at some locations can provide overvoltage at other buses. These buses should be ignored from filter allocation.

Step 7 – Check K-Factor

K-factor of the transformers should be checked. If filter placing at any location can cause the K-factor of any transformer be greater than 1, this placement is not acceptable. And accordingly this filter allocation should be ignored.

Step 8

Remaining buses are suitable locations for filters allocation.

3.9 Flowchart of filter allocation

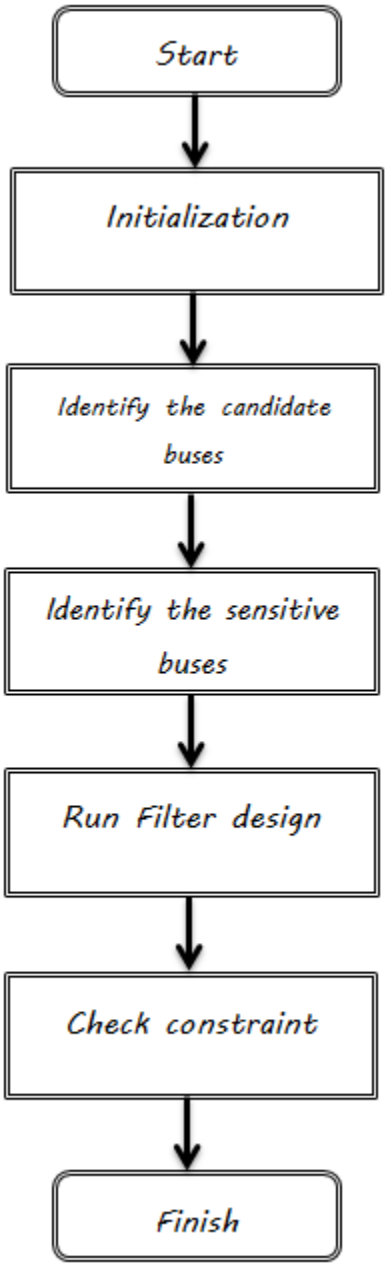

Figure 3-9 Harmonic filter placement

CHAPTER 4 TEST CASES

In this section, multiple benchmarks are tested to validate the proposed methods.

4.1 Validation of harmonic analysis based MANA

For the validation of the proposed method, a 34-bus distribution system is tested using a MATLAB code developed specifically for the scope of this thesis. The results are validated using EMTP-RV version 2.6.1.

4.1.1 Description of the study network

The test case is characterized by unbalanced loading of nonlinear “spot” and “distributed” loads. In this test case, the elements of the network are modeled as follows:

- Overhead lines are represented with PI harmonic model.
- Transformer is represented with a series RL while R and L are not frequency dependent. The magnetization branch is neglected. The phase shifts of voltages are automatically considered in MANA formulation.
- Spot loads and distributed loads are assumed as constant impedances. The RL parallel harmonic model is utilized in harmonic analysis. The distributed loads are divided to two equal loads and are placed at two ends of the lines.
- Regulators are considered to be ideal.

The spot load connected to the bus #830 is assumed to be a nonlinear load. The harmonic current produced by the nonlinear device is presented in Table 4-1. The harmonic source is defined at different frequencies: low frequency (300Hz), medium frequency (660 Hz) and high frequency (1260 Hz). The one line diagram of the system to be studied is illustrated in Figure 4-1.

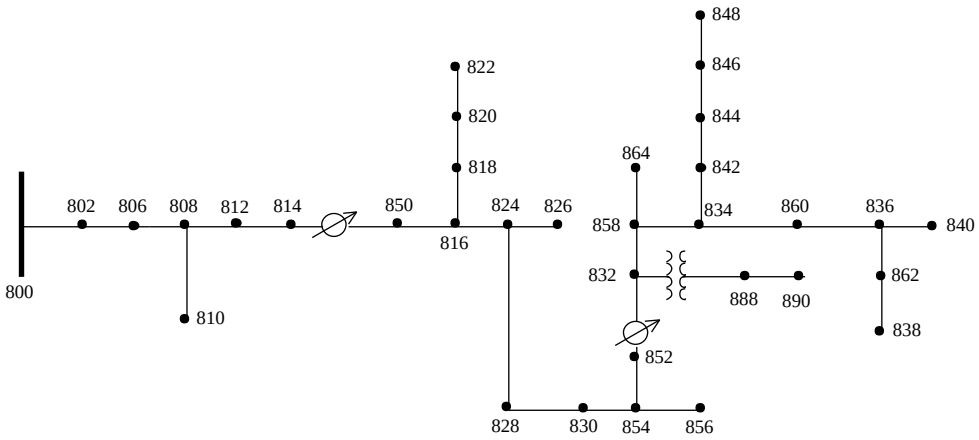

Figure 4-1 IEEE 34 bus distribution system

Table 4-1 Harmonic source

Harmonic order	Harmonic current (% of fundamental current)
5 (300 Hz)	22%
11 (660 Hz)	8%
21 (1260 Hz)	5%

4.1.2 Results and discussions

The harmonic distortions of the network are determined under following conditions:

1- IEEE 34 distribution system with capacitor banks

The results of the harmonic analysis in 34 bus distribution system are presented in Table 4-2. As can be seen from the results, the total harmonic distortion and individual harmonic distortions are not significant at certain buses; because, the lines are long and the network is lightly loaded. In addition to that, the capacitor bank connected to the node #844 provides filter action and suppresses the harmonic distortions produced by the harmonic source. The figure 4-3 shows the waveform of the voltage at Bus 800a. The voltage is sinusoidal since the large amount of the harmonic current is absorbed by the capacitor bank (placed at Bus #844).

Table 4-2 Harmonic analysis in 34 bus distribution system

Bus	h = 1		h = 5			h = 11			h = 21			THD
	V	***θ***	***V***	***θ***	**IHD**	***V***	***θ***	**IHD**	***V***	***θ***	**IHD**	
800a	21211.67	0.00	357.30	-71.79	1.68	77.25	-95.24	0.36	77.60	174.29	0.37	1.76
800b	21346.57	-120.02	376.22	168.26	1.76	87.08	148.33	0.41	85.08	44.60	0.40	1.85
800c	21483.67	120.01	382.22	46.63	1.78	81.95	32.89	0.38	154.85	-61.70	0.72	1.96
810b	20941.74	-120.93	376.14	168.56	1.80	86.19	149.05	0.41	81.70	46.20	0.39	1.88
822a	19348.84	-2.01	354.65	-74.63	1.83	72.13	-101.72	0.37	54.51	157.52	0.28	1.89
826b	20182.14	-122.84	370.38	170.03	1.84	75.63	152.89	0.37	46.55	60.17	0.23	1.89
838b	19824.31	-124.28	364.37	173.02	1.84	56.82	161.88	0.29	22.35	170.37	0.11	1.86
840a	19366.29	-2.75	369.11	-66.14	1.91	56.79	-77.67	0.29	23.75	-65.52	0.12	1.93
840b	19827.42	-124.27	364.40	173.05	1.84	56.82	161.92	0.29	22.33	170.46	0.11	1.86
840c	19862.34	116.54	371.98	48.87	1.87	58.12	38.32	0.29	21.72	59.24	0.11	1.90
848a	19379.10	-2.84	374.14	-66.23	1.93	60.06	-77.78	0.31	30.69	-66.21	0.16	1.96
848b	19835.92	-124.36	368.51	173.08	1.86	59.68	162.34	0.30	29.81	173.64	0.15	1.89
848c	19876.73	116.45	376.76	48.69	1.90	61.55	37.75	0.31	29.42	62.64	0.15	1.93
864a	19434.62	-2.70	369.19	-66.63	1.90	57.83	-79.36	0.30	20.44	-73.91	0.11	1.93
890a	2850.72	-4.87	51.38	-85.18	1.80	6.81	-117.61	0.24	1.34	-132.46	0.05	1.82
890b	2956.09	-126.86	52.66	151.87	1.78	7.33	119.95	0.25	1.58	80.67	0.05	1.80
890c	2931.57	114.33	52.62	28.99	1.79	6.94	-0.35	0.24	1.61	-31.29	0.05	1.81

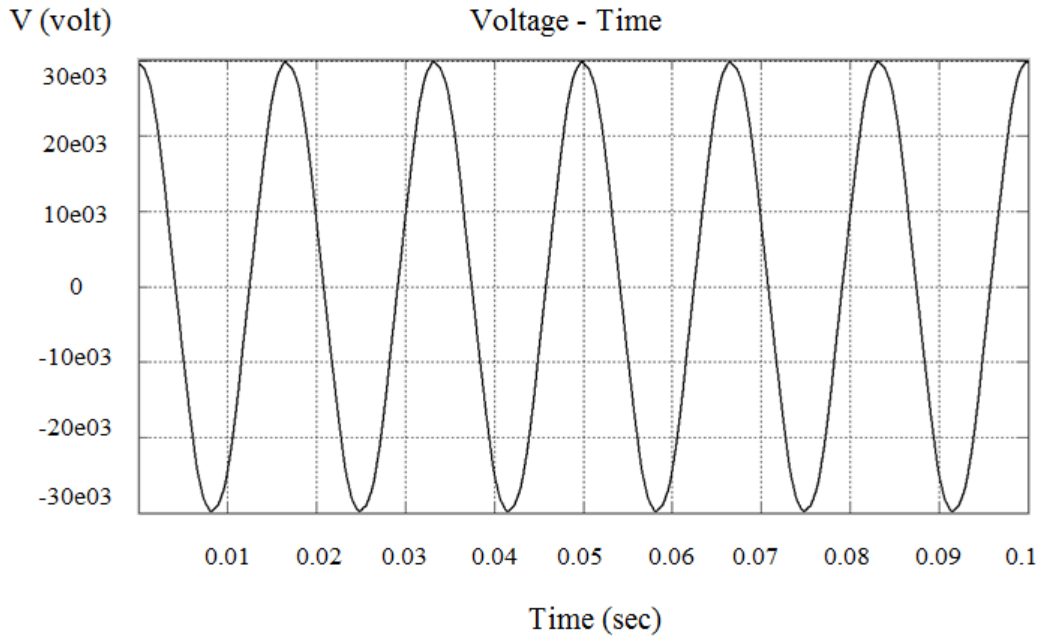

Figure 4-2 Voltage waveform at Bus 880a (from MATLAB code)

2- IEEE 34 distribution system without capacitor banks

The aim of harmonic filters is to push harmonic currents in a low impedance circuit, to suppress them from flowing in the network. The results of harmonic analysis are illustrated in Table 4-3. The results confirm that the capacitor bank placed at Bus #844 works as a passive harmonic filter. As can be seen from Figure 4-3, in the absence of the capacitor banks, the voltage at Bus 800a is considerably distorted.

Table 4-3 Harmonic analysis in 34 bus distribution system

Bus	h = 1		h = 5			h = 11			h = 21			THD
	V	θ	V	θ	IHD	V	θ	IHD	V	θ	IHD	
800a	21211.67	0.00	856.34	-11.46	4.04	293.26	-48.76	1.38	161.13	-88.21	0.76	4.33
800b	21346.57	-120.02	895.08	-140.06	4.19	304.51	-171.87	1.43	186.96	146.44	0.88	4.51
800c	21483.67	120.01	1210.25	100.73	5.63	420.12	65.62	1.96	239.78	23.93	1.12	6.07
810b	20941.74	-120.93	895.26	-139.78	4.28	301.77	-171.20	1.44	178.84	147.87	0.85	4.59
822a	19348.84	-2.01	847.92	-14.38	4.38	271.58	-55.50	1.40	112.62	-103.13	0.58	4.64
826b	20182.14	-122.84	883.00	-138.32	4.38	266.72	-167.48	1.32	99.33	160.01	0.49	4.60
838b	19824.31	-124.28	871.37	-135.42	4.40	203.65	-158.99	1.03	44.86	-81.42	0.23	4.52
840a	19366.29	-2.75	881.61	-6.08	4.55	211.20	-32.26	1.09	55.25	33.32	0.29	4.69
840b	19827.42	-124.27	871.46	-135.40	4.40	203.63	-158.94	1.03	44.82	-81.33	0.23	4.52
840c	19862.34	116.54	1175.22	103.37	5.92	296.46	73.04	1.49	30.65	134.28	0.15	6.10
848a	19379.10	-2.84	883.14	-5.86	4.56	210.59	-31.56	1.09	57.45	35.54	0.30	4.69
848b	19835.92	-124.36	870.98	-135.18	4.39	201.83	-158.35	1.02	46.84	-78.30	0.24	4.51
848c	19876.73	116.45	1175.24	103.53	5.91	294.68	73.42	1.48	32.05	139.86	0.16	6.10
864a	19434.62	-2.70	881.54	-6.54	4.54	215.25	-33.85	1.11	48.10	25.86	0.25	4.68
890a	2850.72	-4.87	114.85	-25.04	4.03	21.26	-70.18	0.75	3.99	-15.73	0.14	4.10
890b	2956.09	-126.86	131.79	-159.18	4.46	28.61	151.53	0.97	1.81	169.80	0.06	4.56
890c	2931.57	114.33	168.79	85.99	5.76	37.47	39.61	1.28	3.75	40.92	0.13	5.90

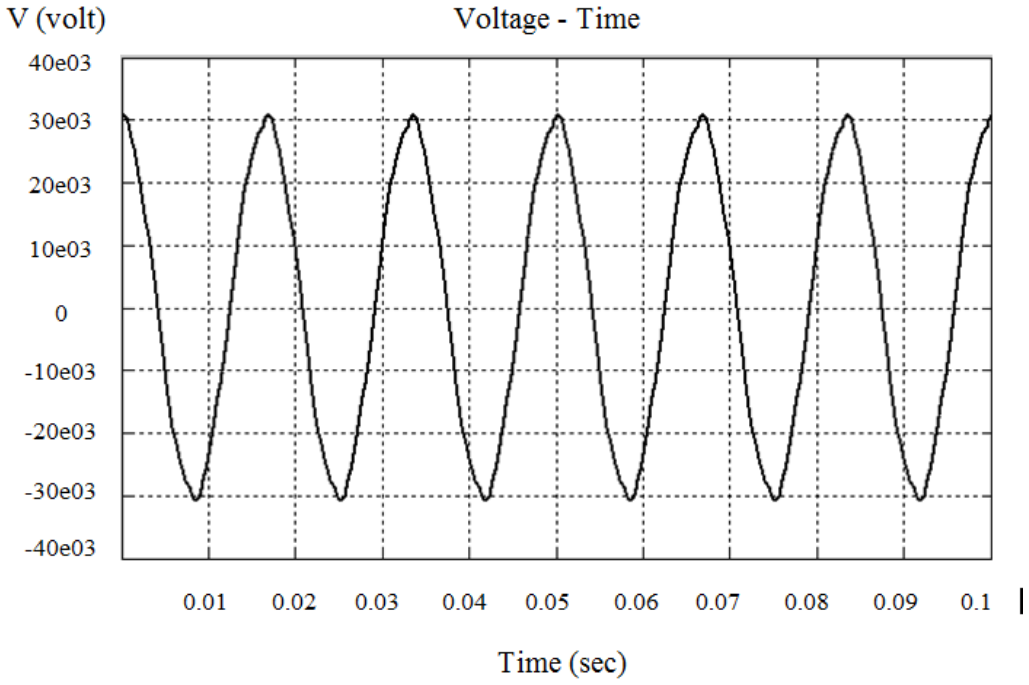

Figure 4-3 Voltage waveform at Bus 880a (from MATLAB code)

3- IEEE 34 distribution system without spot loads

The results of harmonic analysis without the spot loads are presented in Table 4-4. The distortions increase slightly due to the removal of spot loads. As the results confirm that the loads have a damping effect on harmonic distortions. The waveform of the voltage at Bus 880a is illustrated in Figure 4-4. The harmonic flow depends on the impedance of the system and accordingly any modification in the impedance of the network can change the direction of harmonic currents flowing in the network.

Table 4-4 Harmonic analysis in 34 bus distribution system

Bus	h = 1		h = 5			h = 11			h = 21			THD
	V	***θ***	***V***	***θ***	**IHD**	***V***	***θ***	**IHD**	***V***	***θ***	**IHD**	
800a	21211.67	0.00	361.37	-83.97	1.70	77.18	-99.44	0.36	80.46	171.58	0.38	1.78
800b	21346.57	-120.02	379.15	156.22	1.78	86.58	144.24	0.41	87.01	43.17	0.41	1.87
800c	21483.67	120.01	382.17	34.54	1.78	81.38	28.83	0.38	162.80	-63.40	0.76	1.97
810b	20941.74	-120.93	379.07	156.51	1.81	85.70	144.96	0.41	83.59	44.77	0.40	1.90
822a	19348.84	-2.01	358.69	-86.80	1.85	72.06	-105.92	0.37	56.55	154.81	0.29	1.91
826b	20182.14	-122.84	373.25	157.99	1.85	75.20	148.79	0.37	47.72	58.76	0.24	1.90
838b	19824.31	-124.28	365.53	160.64	1.84	56.00	157.12	0.28	22.37	168.69	0.11	1.87
840a	19366.29	-2.75	370.77	-78.62	1.91	55.96	-82.51	0.29	24.06	-67.29	0.12	1.94
840b	19827.42	-124.27	365.57	160.67	1.84	56.00	157.17	0.28	22.35	168.79	0.11	1.87
840c	19862.34	116.54	370.13	36.36	1.86	57.23	33.42	0.29	21.97	58.31	0.11	1.89
848a	19379.10	-2.84	375.49	-78.75	1.94	59.08	-82.70	0.30	31.07	-67.95	0.16	1.97
848b	19835.92	-124.36	369.44	160.65	1.86	58.74	157.50	0.30	29.80	171.98	0.15	1.89
848c	19876.73	116.45	374.55	36.12	1.88	60.51	32.74	0.30	29.80	61.89	0.15	1.91
864a	19434.62	-2.70	371.79	-79.00	1.91	57.29	-84.04	0.29	20.74	-75.92	0.11	1.94
890a	2850.72	-4.87	62.27	-79.35	2.18	9.78	-85.32	0.34	3.11	-85.58	0.11	2.21
890b	2956.09	-126.86	61.76	160.27	2.09	9.99	155.54	0.34	3.08	145.35	0.10	2.12
890c	2931.57	114.33	62.27	36.25	2.12	10.01	33.04	0.34	3.11	17.20	0.11	2.15

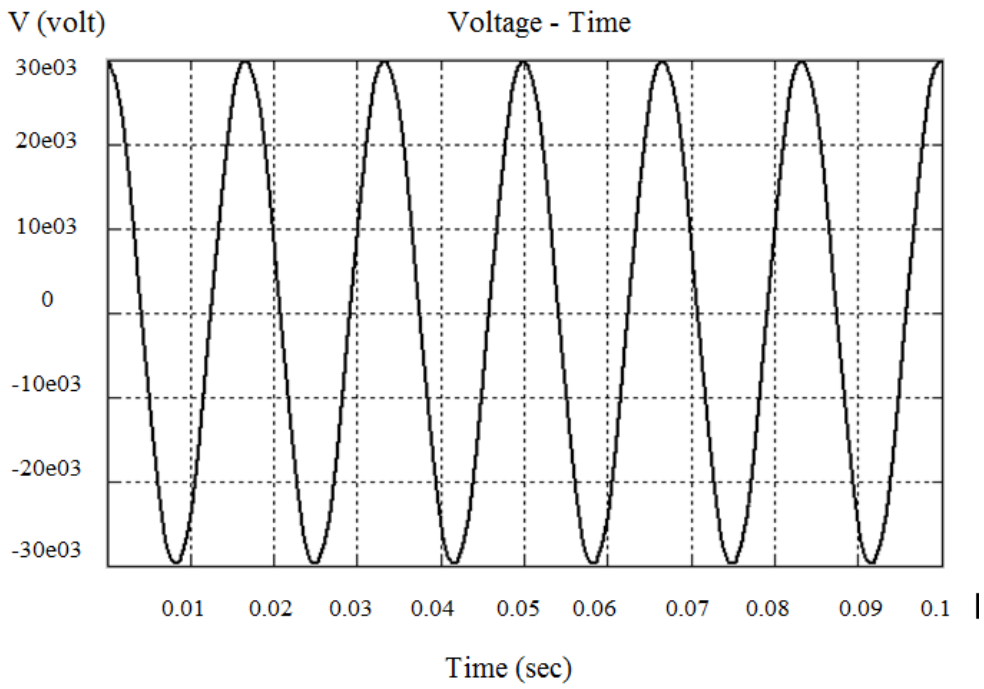

Figure 4-4 Voltage waveform at Bus 880a (from MATLAB code)

4- IEEE 34 distribution system with a rotating load (induction machine) connected to the node # 888

In this test case, a synchronous motor is connected to the Bus # 888. Synchronous machine is represented with equivalent sequence impedance. The positive and negative sequence impedances of the Synchronous machines are presented in equations 2.92 to 2.96. The results of harmonic analysis with a rotating load are shown in Table 4-5. As already mentioned, loads can provide damping to the impedance of the system. Due to this fact, THD and IHD of the Bus 890 are slightly decreased.

Table 4-5 Harmonic analysis in 34 bus distribution system

Bus	h = 1		h = 5			h = 11			h = 21			THD
	V	***θ***	***V***	***θ***	**IHT**	***V***	***θ***	**IHT**	***V***	***θ***	**IHT**	
800a	21211.67	0.00	361.37	-83.97	1.70	77.18	-99.44	0.36	80.46	171.58	0.38	1.78
800b	21346.57	-120.02	379.15	156.22	1.78	86.58	144.24	0.41	87.01	43.17	0.41	1.87
800c	21483.67	120.01	382.17	34.54	1.78	81.38	28.83	0.38	162.80	-63.40	0.76	1.97
810b	20941.74	-120.93	379.07	156.51	1.81	85.70	144.96	0.41	83.59	44.77	0.40	1.90
822a	19348.84	-2.01	358.69	-86.80	1.85	72.06	-105.92	0.37	56.55	154.81	0.29	1.91
826b	20182.14	-122.84	373.25	157.99	1.85	75.20	148.79	0.37	47.72	58.76	0.24	1.90
838b	19824.31	-124.28	365.53	160.64	1.84	56.00	157.12	0.28	22.37	168.69	0.11	1.87
840a	19366.29	-2.75	370.77	-78.62	1.91	55.96	-82.51	0.29	24.06	-67.29	0.12	1.94
840b	19827.42	-124.27	365.57	160.67	1.84	56.00	157.17	0.28	22.35	168.79	0.11	1.87
840c	19862.34	116.54	370.13	36.36	1.86	57.23	33.42	0.29	21.97	58.31	0.11	1.89
848a	19379.10	-2.84	375.49	-78.75	1.94	59.08	-82.70	0.30	31.07	-67.95	0.16	1.97
848b	19835.92	-124.36	369.44	160.65	1.86	58.74	157.50	0.30	29.80	171.98	0.15	1.89
848c	19876.73	116.45	374.55	36.12	1.88	60.51	32.74	0.30	29.80	61.89	0.15	1.91
864a	19434.62	-2.70	371.79	-79.00	1.91	57.29	-84.04	0.29	20.74	-75.92	0.11	1.94
890a	2850.72	-4.87	62.27	-79.35	2.18	9.78	-85.32	0.34	3.11	-85.58	0.11	2.21
890b	2956.09	-126.86	61.76	160.27	2.09	9.99	155.54	0.34	3.08	145.35	0.10	2.12
890c	2931.57	114.33	62.27	36.25	2.12	10.01	33.04	0.34	3.11	17.20	0.11	2.15

4.1.3 Comparison of harmonic analysis using MANA with harmonic analysis in EMTP-RV (v 2.6.1)

The results of harmonic analysis of 34 bus distribution system calculated by EMTP-RV (v 2.6.1) are shown in Table 4-6. The comparisons of the results are presented in the column titled "ERROR". The validation results show that the algorithms and device MANA models provide accurate results.

Table 4-6 EMTP-RV results of harmonic analysis

Bus	h = 5				h = 11				h = 21			
	EMTP-RV		ERROR (%)		EMTP-RV		ERROR (%)		EMTP-RV		ERROR (%)	
	V	θ	V	θ	V	θ	V	θ	V	θ	V	θ
'832a'	370.10	-67.18	0.30	0.17	58.70	-81.19	0.08	0.46	18.03	-85.66	-0.24	2.60
'834a'	370.71	-66.15	0.34	0.09	57.30	-77.62	0.76	0.10	23.67	-65.35	-0.45	0.16
'836a'	370.34	-66.20	0.33	0.09	57.22	-77.74	0.74	0.10	23.63	-65.62	-0.51	0.16
'840a'	370.33	-66.20	0.33	0.09	57.22	-77.75	0.74	0.10	23.63	-65.63	-0.51	0.16
'842a'	370.77	-66.12	0.34	0.09	57.27	-77.50	0.78	0.09	23.85	-64.92	-0.42	0.10
'844a'	371.07	-65.95	0.35	0.08	57.15	-76.95	0.88	0.05	24.72	-62.93	-0.29	-0.20
'858a'	370.37	-66.72	0.32	0.14	58.05	-79.59	0.38	0.29	20.31	-75.03	-0.66	1.49
'862a'	370.33	-66.20	0.33	0.09	57.21	-77.74	0.74	0.10	23.63	-65.62	-0.51	0.16
'888a'	57.63	-75.33	0.32	0.15	8.24	-96.03	0.22	0.48	2.14	-101.78	0.97	2.16

The results of harmonic analysis of 34 bus distribution system with synchronous motor calculated by EMTP-RV (vs 2.6.1) are shown in Table 4-7. The synchronous motor is connected to the Bus #888. Since the harmonic model of synchronous machines in EMTP-RV is different, the differences in the angle of the voltages are more significant than the previous test case.

Table 4-7 EMTP-RV results of harmonic analysis

Bus	h = 5				h = 11				h = 21			
	EMTP-RV		ERROR (%)		EMTP-RV		ERROR (%)		EMTP-RV		ERROR (%)	
	V	θ	V	θ	V	θ	V	θ	V	θ	V	θ
'812a'	354.90	-69.94	-0.66	-12.16	70.37	-98.25	-3.75	-1.36	65.60	178.40	3.02	4.80
'814a'	351.05	-69.90	-0.61	-12.14	66.73	-97.99	-3.27	-1.46	50.86	175.54	3.04	3.97
'836c'	375.89	50.09	1.53	12.41	58.46	38.31	2.10	12.77	22.35	58.03	1.72	-0.50
'842b'	367.98	174.97	0.63	8.12	56.98	162.63	1.93	3.20	21.98	172.80	-2.04	1.81
'842a'	371.71	174.86	0.61	8.13	59.71	162.80	1.63	3.25	28.98	175.07	-2.82	1.76
'852a'	359.75	-64.34	0.22	-12.31	56.95	-80.44	1.22	-6.07	17.58	-85.59	-0.78	0.03
'858a'	373.93	-63.85	0.57	-12.73	58.60	-78.79	2.23	-6.66	20.37	-75.07	-1.83	-1.13
'860c'	375.90	50.10	1.53	12.40	58.45	38.34	2.10	12.77	22.34	58.08	1.71	-0.48
'888a'	375.90	50.09	1.53	12.41	58.46	38.31	2.10	12.77	22.36	58.03	1.72	-0.49

4.2 Validation of the method of passive filter design

4.2.1 Description of the study network

In this section, the solution algorithm is tested on the 5-bus industrial system. This program is written in MATLAB and the performances of the filters are tested using the commercial harmonic analysis package CYME Harmonic module.

The system serves the small industrial plant which has an AC motor fed by a 6 pulse converter. The figure 4.5 depicts a single diagram for this system. The industrial plant has an AC generator, two Ygyg transformers and nonlinear loads. The details of the system data are as follows:

Synchronous Generator, P = 5000 kW, V = 13.8 kV

Transformer 1 (connected between Bus 1 and Bus 2), S = 20000 kVA, 138 kV/13.8 kV

Transformer 2 (connected between Bus 4 and Bus 5), S = 5000 kVA, 13.8 kV/4.2 kV

Line 1 (between Bus 3 and Bus 2), length = 0.061 km, Cable

Line 2 (between Bus 2 and Bus 4), length = 0.1528 km, Cable

Nonlinear load, P = 3500 kW, Q = 1000 kVAR,

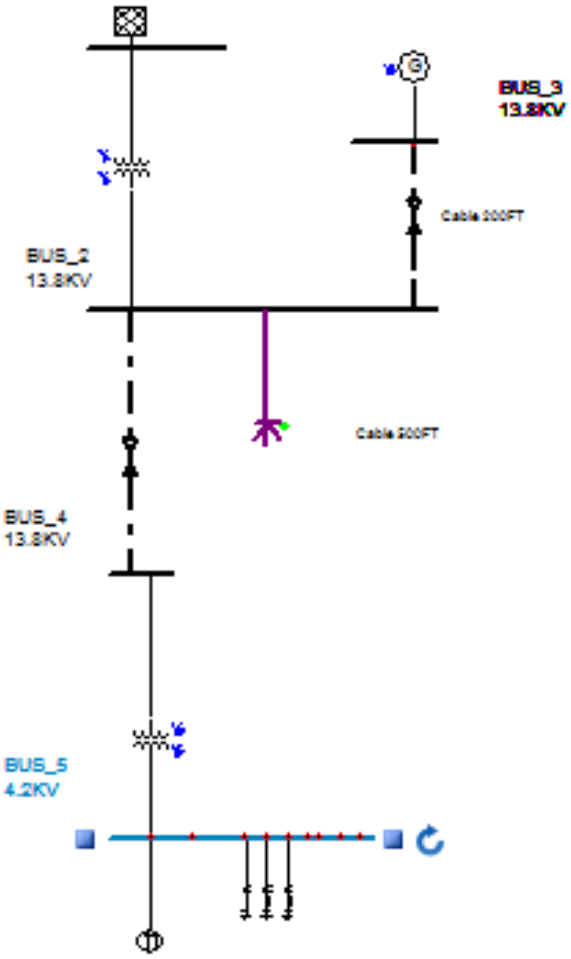

Figure 4-5 5-Bus industrial system with multiple harmonic filters at bus 5

The harmonic currents produced by the 6 pulse converter are shown in Table 4-8; the dominant harmonic components at drive bus are 5, 7, 11, 13 and 19. The magnitudes of the harmonic currents are based on the full load operation (The worst case condition is taken into account).

Table 4-8 Harmonic distortion of a typical 6 pulse converter PWM

harmonic order	**current magnitude (in % of the fundamental current magnitude)**	**current magnitude (degree)**
1	96.98	-15
3	0.57	106
5	22.81	96
7	5.9	94
9	0.09	176
11	4.43	-173
13	4.0	167
15	0.06	22
17	1.75	-109
19	1.33	-107
21	0.03	179
23	0.73	-85
25	0.54	-85

The system data is presented in Table 4-9:

Table 4-9 System data

Parameters	**Value**
Sload	3.64 MW
Isc	8252 A
IL	152 A
Isc / IL	54.23

The distorted voltage and current before the installation of harmonic filters are shown in Figures 4-6 and 4-7. The voltage IHD, voltage THD and current THD are shown in Figures 4-8, 4-9 and 4-10 respectively, and Figure 4-11 presents the impedance scan of the network seen from the bus #5. As can be seen from the figures, the voltage THD at bus #5 is over the maximum allowable limits. And also the 5^{th} order harmonic voltage at bus #5 is over the limitations. In terms of current, current THDs at bus #2, #4 and #5 do not satisfy the standard requirements. Therefore the harmonic filters should be connected to decrease harmonic distortion within the IEEE requirements.

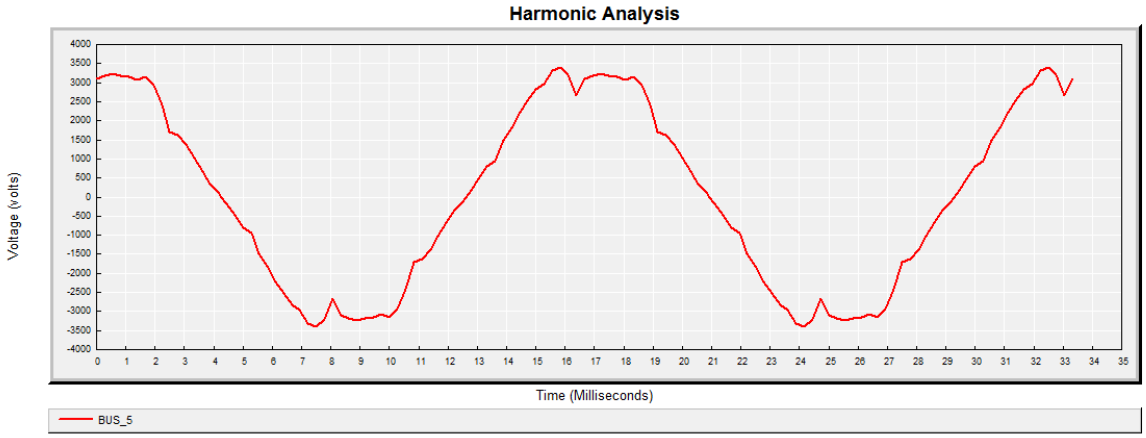

Figure 4-6 Voltage waveform at bus 5 (from CYME Harmonic module)

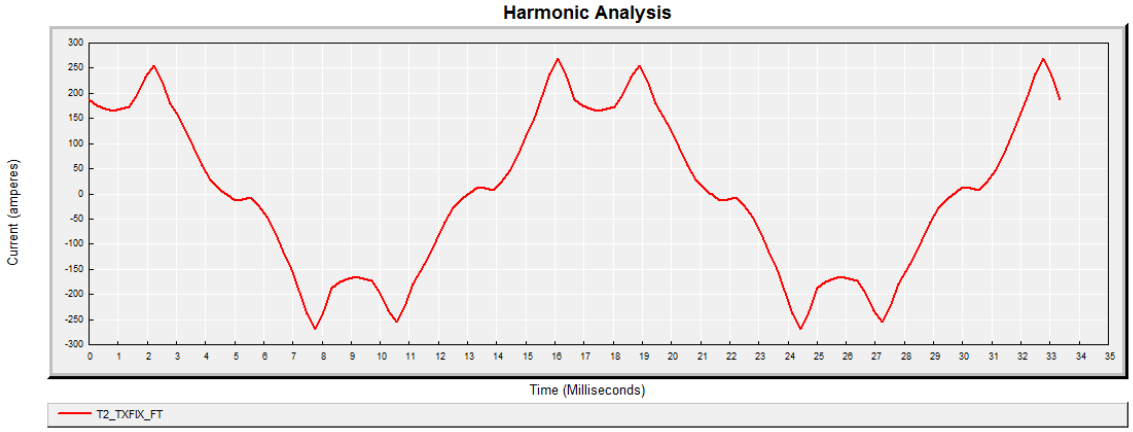

Figure 4-7 Current waveform at bus 5(from CYME Harmonic module)

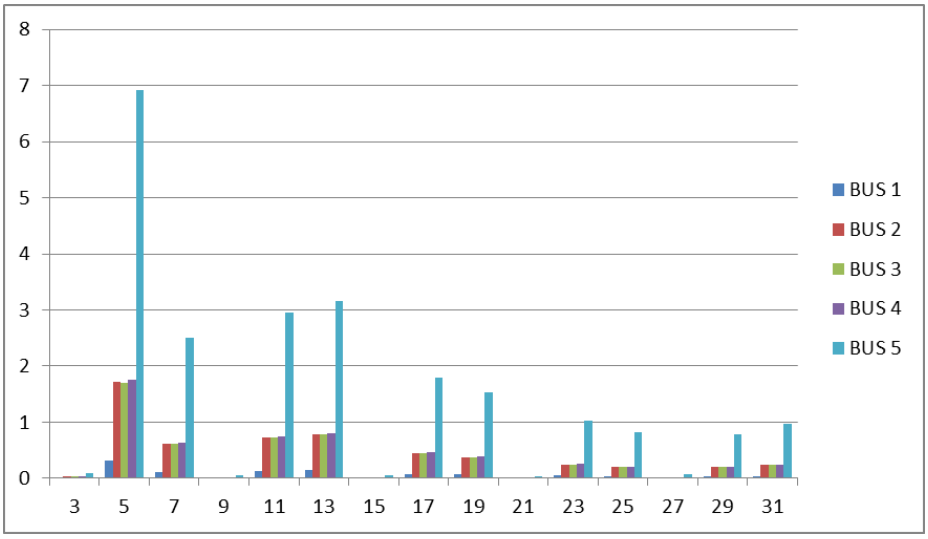

Figure 4-8 Voltage Individual Harmonic Distortions (Voltage IHD)

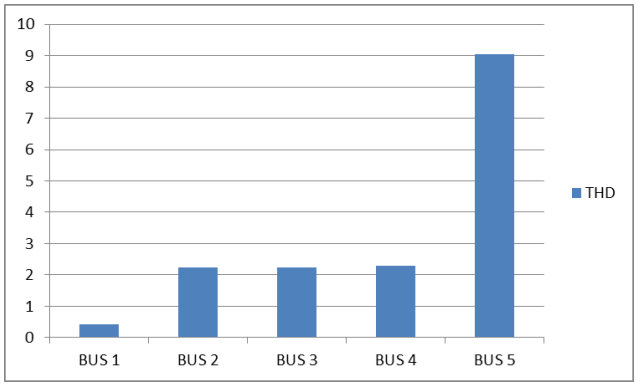

Figure 4-9 Voltage Total Harmonic Distortions (Voltage THD)

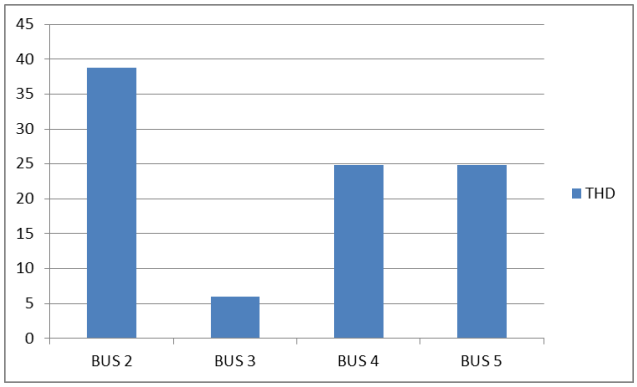

Figure 4-10 Current Total Harmonic Distortions (Current THD)

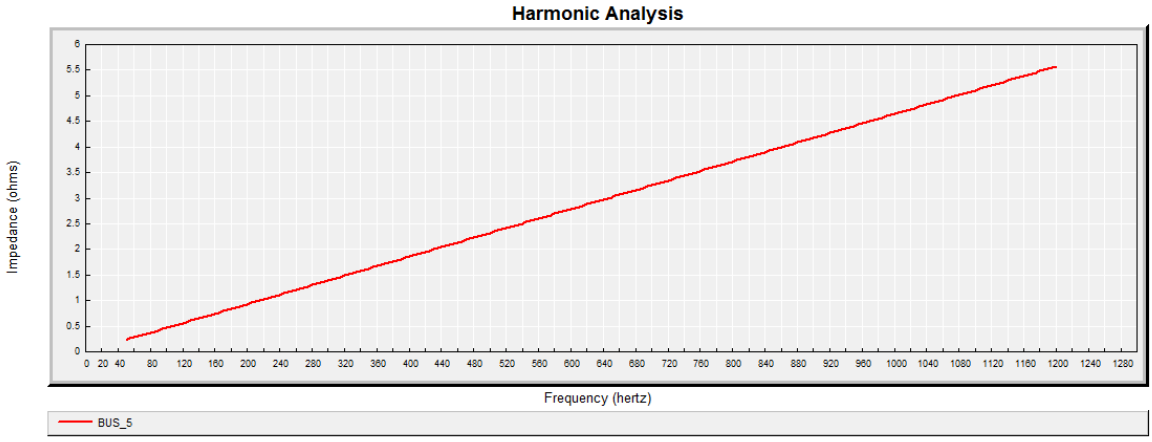

Figure 4-11 Impedance characteristic waveform before filtering at bus 5 (from CYME Harmonic module)

4.2.2 Results and discussions

The proposed algorithm is applied to determine the appropriate filters for the system. The desired power factor is assumed to be 0.99.

From the solution of the proposed algorithm, three single tuned filters (5^{th}, 7^{th} and 11^{th}) are designed. As mentioned above, in order to avoid the parallel resonance between the lower harmonics and the filter designed for the suppression of higher order harmonic, the frequency of the resonance points should be checked, and if they are nearby the frequencies of the dominant harmonics, filter should be detuned. In this case, filters are tuned three percent lower than their harmonic frequencies. These filters' parameters are as follows:

Table 4-10 Parameters of harmonic filters measured by proposed method for 5 Bus industrial system

	Filter 1	**Filter 2**	**Filter 3**
Type	Single tuned	Single tuned	Single tuned
Qc	900 kVar	300 kVar	300 kVar
Vc3	7200 v	7200 v	7200 v
C	0.22 uf	0.76 uf	0.76 uf
L	0.0130 H	0.0081 H	0.0080 H
R	0.24 ohm	0.52 ohm	0.33 ohm
Quality factor	100	100	100
Filter detuning factor	0.97	0.97	0.97
Filter tuned at	291 Hz	407.4 Hz	640.2 Hz

The graphs of the voltage, current, voltage THD, voltage IHD, current THD and impedance scan at bus #5 after installation of harmonic filters are presented as follows:

[3] rated voltage of the capacitor bank

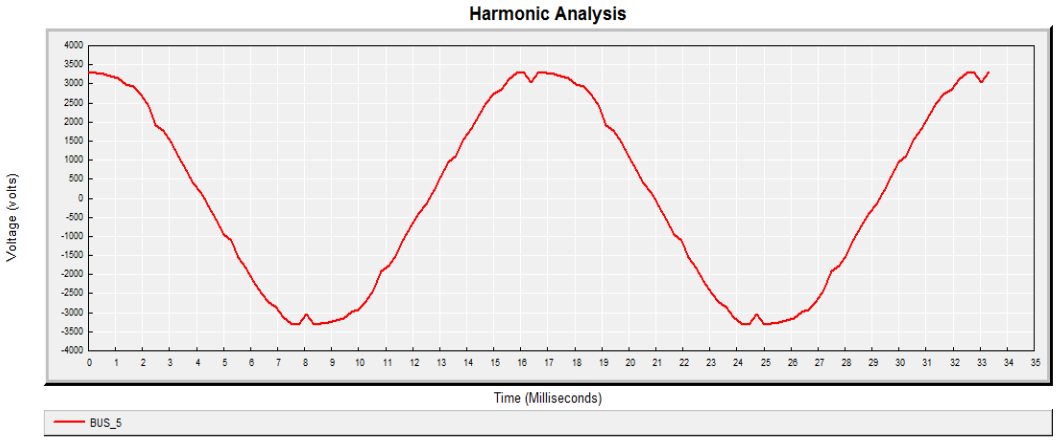

Figure 4-12 Voltage at bus 5 (from CYME Harmonic module)

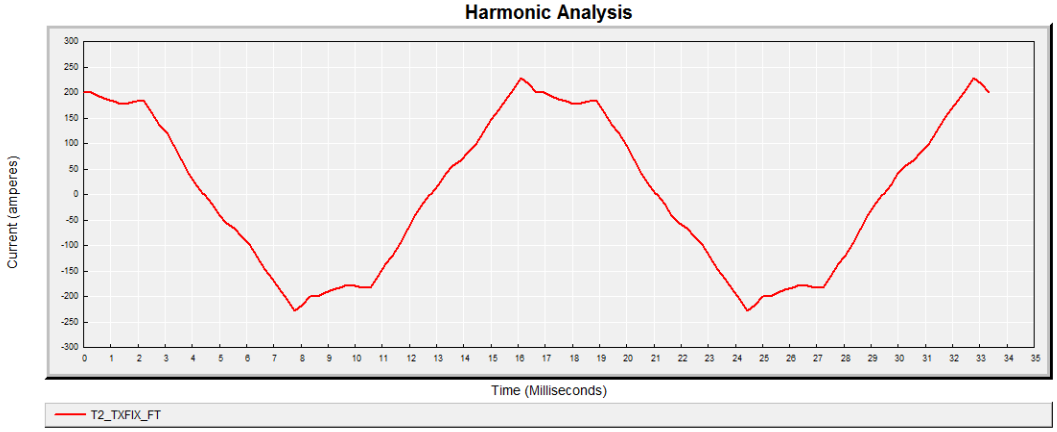

Figure 4-13 Current waveform at bus 5(from CYME Harmonic module)

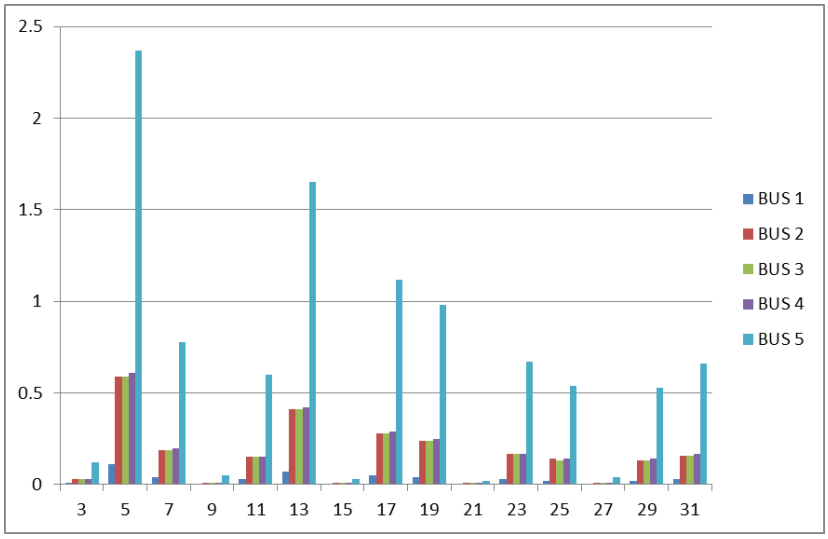

Figure 4-14 Voltage Individual Harmonic Distortions (Voltage IHD)

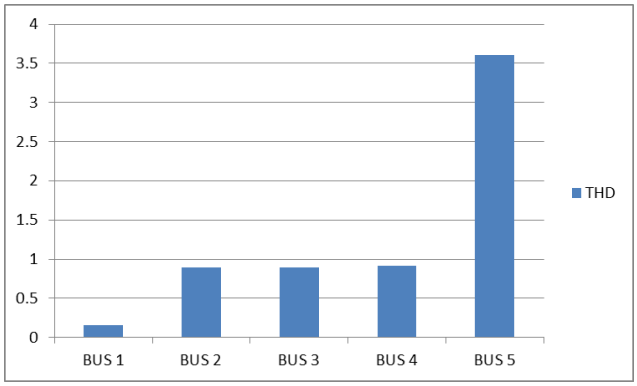

Figure 4-15 Voltage Total Harmonic Distortions (Voltage THD)

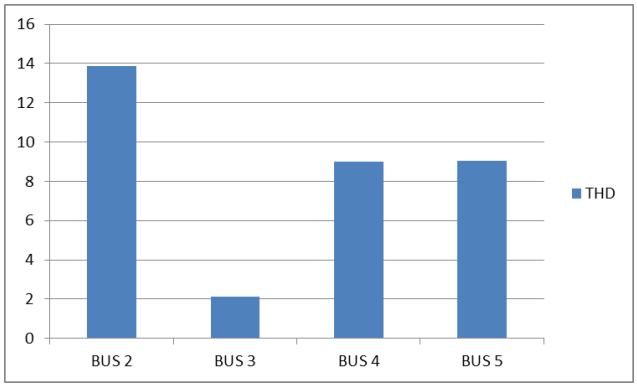

Figure 4-16 Current Total Harmonic Distortions (Current THD)

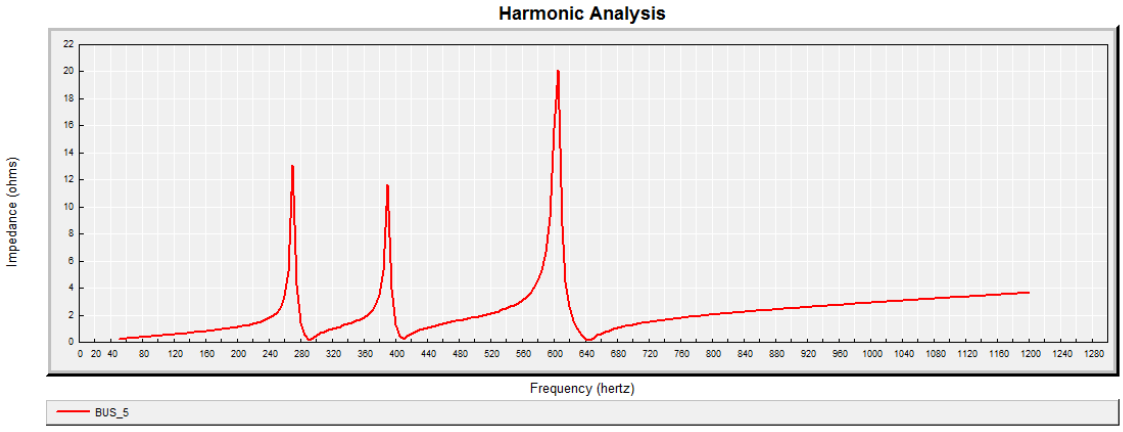

Figure 4-17 Impedance characteristic waveform after filtering at bus 5 (from CYME Harmonic module)

The filters satisfy the IEEE 18 limits. Table 4-11 presents the mathematical solutions.

Table 4-11 Values required to satisfy IEEE 18

Filter Type	$f\ (Hz)$	$Q_c\ (kVar)$	$Q_c\ (kVar)$	$Q_c\ (kVar)$	$Q_c\ (kVar)$	$Q_c\ (kVar)$	$Q_c\ (kVar)$
Single tuned filter	300	900	7200	0.61	0.99	0.63	0.77
Single tuned filter	420	300	7200	0.71	1.18	0.61	0.74
Single tuned filter	660	300	7200	0.41	0.72	0.58	0.62

4.3 Validation of harmonic filter allocation

In order to demonstrate the performance of the proposed methodology, the solution is tested on the 13-bus industrial system. This program is written in MATLAB and the performances of the filters are tested using CYME Harmonic module.

4.3.1 Description of the study network

The study considers three harmonic sources connected to the BUSES bus #5, bus #9 and bus #13. Given the harmonic current introduced by the 12 pulse converter as mentioned in Table 4-12, the one line diagram of the system to be studied is illustrated in Figure 4.18. Figure 4.19 shows the harmonic distortion at each bus before placing the harmonic filters. As can be seen from the figure, bus #9 and bus #13 have the highest harmonic distortion in the system.

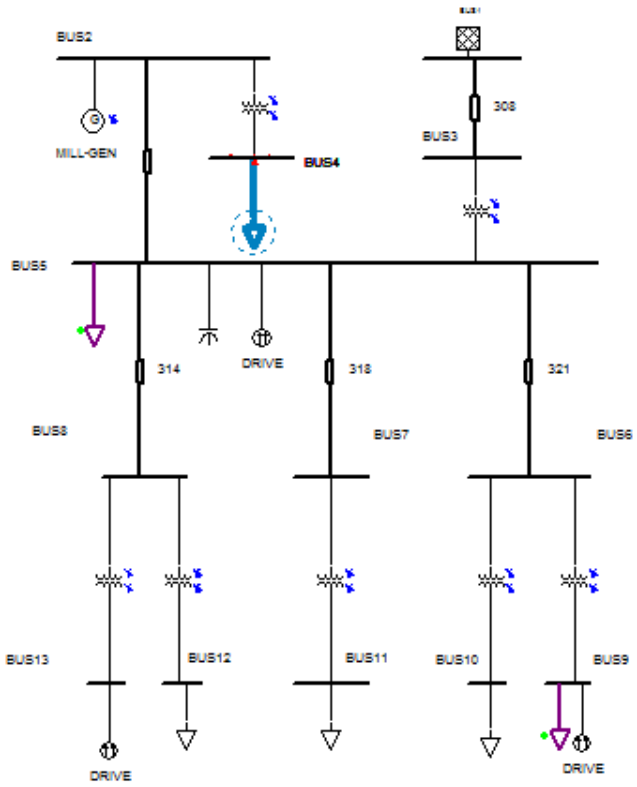

Figure 4-18 13 Bus industrial system

Table 4-12 Harmonic distortion of a typical 12 pulse converter

harmonic order	**current magnitude (in % of the fundamental current magnitude)**	**current magnitude (degree)**
1	99.22	-11
3	3.59	-146
5	4.41	89
7	1.65	-132
9	0.43	146
11	6.49	45
13	4.91	53
15	0.24	-118
17	0.47	115
19	0.42	-135
21	0.28	84
23	0.85	55
25	1.08	62
27	0.09	-131
29	0.12	171
31	0.4	176

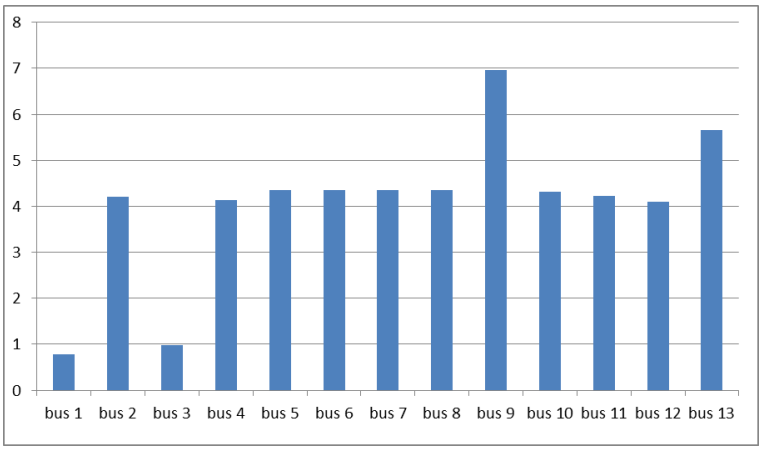

Figure 4-19 Voltage THD weight of the 13 bus system (before filters placement)

4.3.2 Results and discussions

As can be seen from the one line diagram, system shows thirteen buses and hence presents thirteen possible placements for harmonic filters. According to the proposed algorithm, all busses except bus #1, bus #2 and bus #3 are candidates for harmonic filter placements.

According to the simulation results, from ten possible allocations for harmonic filters at this system, two of them result in considerable reduction at harmonic distortion level (bus #6 and bus #9). The simulation result is summarized in Table 4-13. Figures 4.20 to 4.29 illustrate the resultant harmonic voltages when the filters are placed. In simulation of all configurations, over voltages are taken into account and filters are design in the way to satisfy the IEEE 519 and IEEE 18 requirements.

Table 4-13 THD voltage at each bus after installation of filters (%)

Bus Number	Filters placed at:										
	-	4	5	6	7	8	9	10	11	12	13
1	0.77	0.76	0.3	0.42	0.37	0.33	0.39	0.83	0.76	0.8	0.62
2	4.1	4.01	1.6	2.22	1.96	1.75	2.07	4.43	4.04	4.26	3.32
3	0.99	0.94	0.37	0.52	0.46	0.41	0.49	1.03	0.94	0.99	0.77
4	4.1	1.6	1.58	2.15	1.91	1.7	2.03	4.36	3.98	4.19	3.27
5	4.28	4.16	1.65	2.29	2.03	1.82	2.14	4.58	4.18	4.4	3.44
6	4.3	4.16	1.67	2.24	2.01	1.79	2.13	4.57	4.18	4.4	3.43
7	4.2	4.16	1.65	2.29	2.02	1.82	2.14	4.58	4.17	4.4	3.44
8	4.3	4.16	1.66	2.29	2.03	1.8	2.14	4.58	4.18	4.4	3.43
9	6.9	7.09	7.3	4.91	5.52	5.13	3.38	7.2	7.08	7.26	6.6
10	4.3	4.14	1.66	2.22	1.99	1.77	2.12	3.06	4.16	4.38	3.41
11	4.2	4.05	1.62	2.17	1.93	1.72	2.07	4.46	0.96	4.29	3.34
12	4.1	3.92	1.59	2.05	1.85	1.6	2.00	4.32	3.94	0.82	3.22
13	5.78	5.75	5.55	3.38	3.93	3.53	4.39	5.92	5.75	5.94	2.71

The harmonic filters installed at bus #9 require lower total power than the harmonic filters installed at bus #6; therefore, bus #9 is suitable location for harmonic filter allocation.

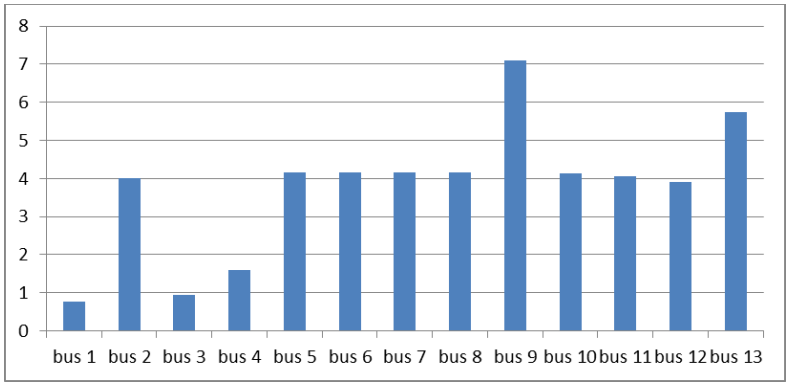

Figure 4-20 Voltage THD weight of 13 bus system (Filter at bus 4)

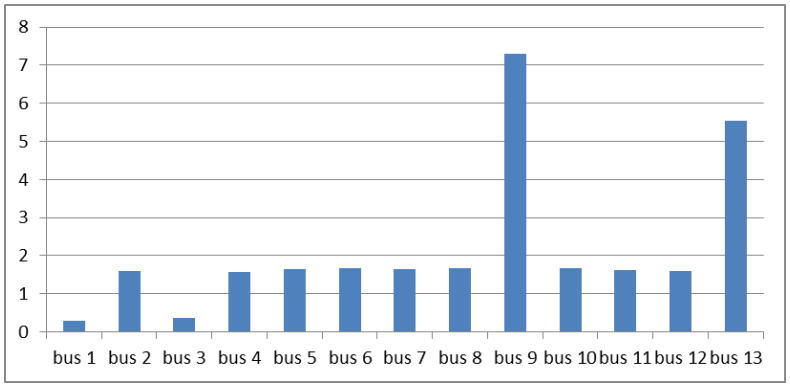

Figure 4-21 Voltage THD weight of 13 bus system (Filter at bus 5)

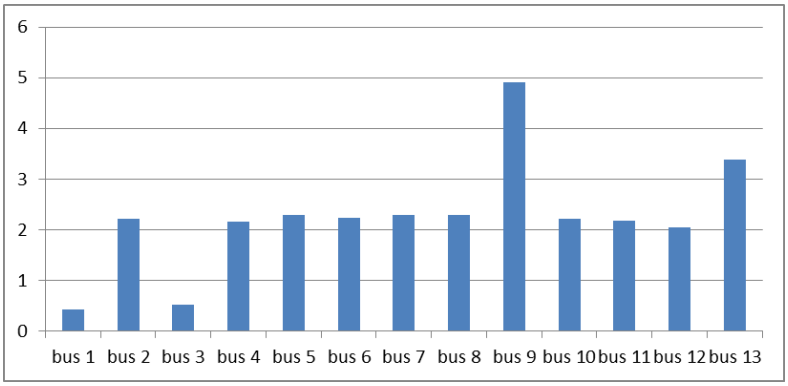

Figure 4-22 Voltage THD weight of 13 bus system (Filter at bus 6)

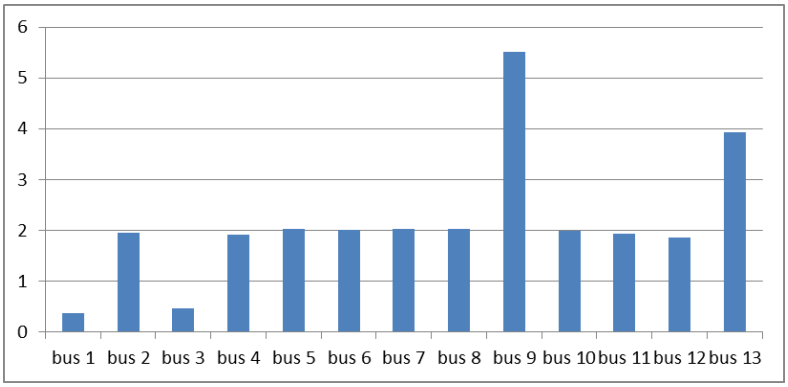

Figure 4-23 Voltage THD weight of 13 bus system (Filter at bus 7)

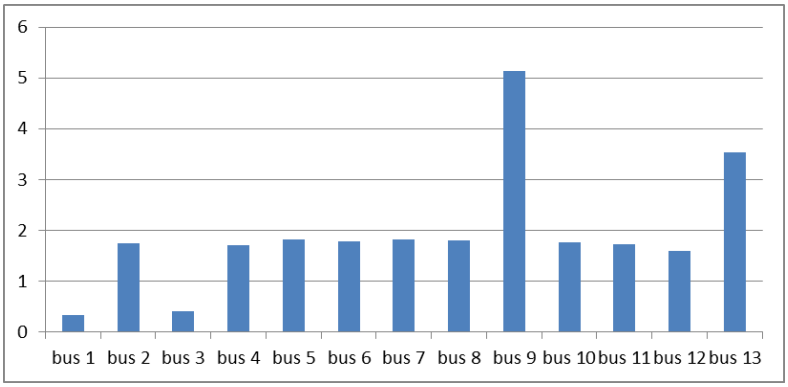

Figure 4-24 Voltage THD weight of 13 bus system (Filter at bus 8)

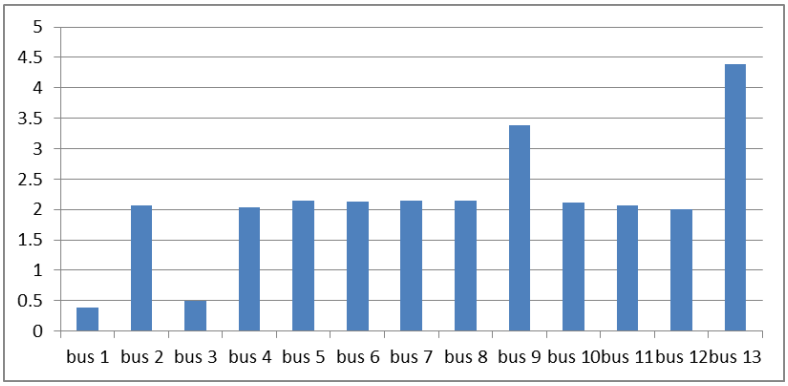

Figure 4-25 Voltage THD weight of 13 bus system (Filter at bus 9)

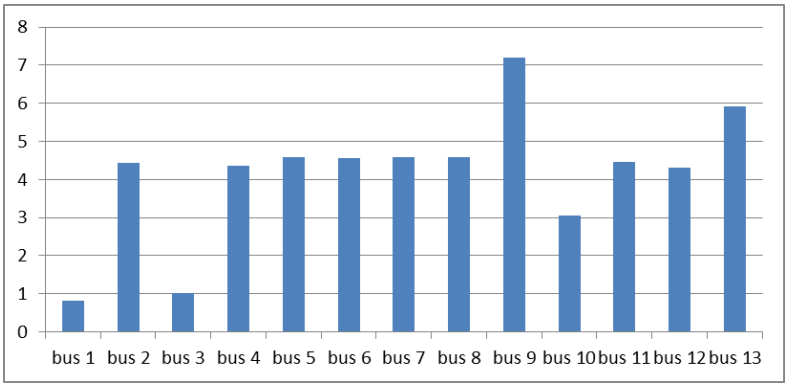

Figure 4-26 Voltage THD weight of 13 bus system (Filter at bus 10)

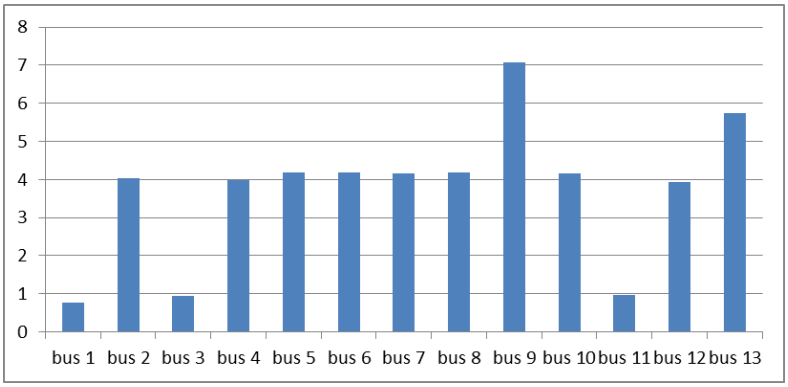

Figure 4-27 Voltage THD weight of 13 bus system (Filter at bus 11)

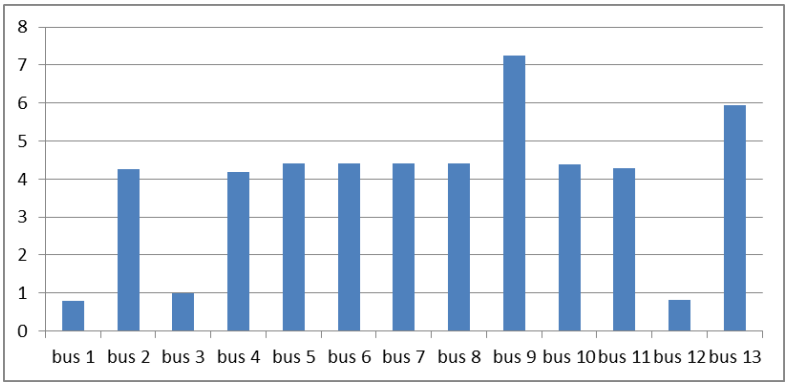

Figure 4-28 Voltage THD weight of 13 bus system (Filter at bus 12)

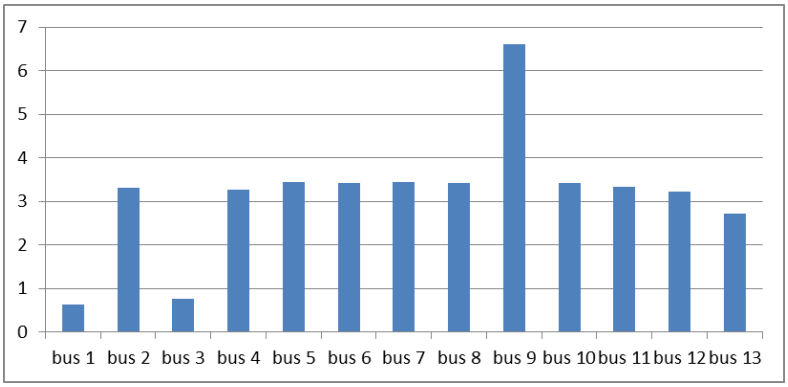

Figure 4-29 Voltage THD weight of 13 bus system (Filter at bus 13)

CHAPTER 5 CONCLUSION AND RECOMMENDATIONS

This thesis presents the harmonic models of system components under balanced and unbalanced conditions in phase frame and uses them in the MANA formulation. Certain models are obtained from their equivalent circuits in sequence frame. In the case of multi-phase transmission lines, it is possible to obtain the admittance matrix from different line models directly in phase frame. It is shown that using simplified models, such as equivalent pi model, changes the frequency response of the line.

Harmonic analysis based on the MANA formulation and which can be applied to balanced or unbalanced electric networks is described, In addition, this methodology was implemented in a computer program which allows the analysis of characteristic and non-characteristic of the complex harmonic quantities. The purpose of this research work is to provide a reliable method to determine harmonic distortion in large networks. The comparison with EMTP-RV confirms that the method yields precise results. The difference observed between the results of EMTP-RV and the results of the proposed method was less than three percent in magnitude of voltages, which is due to the differences between harmonic models and detailed EMTP-RV models for certain devices. For example, in EMTP-RV, the models used for rotating loads are based on dynamic equations and models while in the proposed method, the steady state models are employed for them.

The following conclusions and recommendations can be made for harmonic analysis:

- MANA methodology significantly simplifies the harmonic models of transformers and other components under unbalanced conditions.
- Norton equivalent provides a straightforward solution and can speed up harmonic analysis computations when compared to the Thevenin equivalent which requires the evaluation of the Thevenin impedance of the bus connected to the harmonic source.
- Harmonic studies and reduction of harmonic distortions using capacitor banks, as well as harmonic filters, can be performed in a straightforward manner without addressing heuristic methods given the complexity and size of industrial networks and due to the simple fact that the mitigation of harmonic distortions can be achieved by placing filters close to the harmonic sources

- Capacitor banks can change the direction of harmonic flow in the system. Hence, in the harmonic polluted system, the capacitor banks should be taken into account.

This thesis proposes practical solution strategies for passive filter design and filter allocation. The objectives are to determine the parameters of harmonic filters and also to find efficient locations for harmonic placement. The proposed methods are successfully implemented as a computer program. The results show that the proposed method forms an efficient tool for designing and placing harmonic filters in industrial systems. It has to be mentioned that the proposed method for filter allocation has a limitation and it cannot be applied to large networks. The following conclusions and recommendations can be made for harmonic filters:

- In multiple filters branch, due to parallel resonance generated by single tuned filters, the tuning frequencies of the harmonic filters should be taken into account.
- The rated voltage of capacitor banks should satisfy IEEE 18 requirements. Otherwise the harmonics can cause failure in capacitor banks (as shown with the 5 bus industrial system).
- The natural choice for the allocation of harmonic filters is at the bus with the highest harmonic distortion or bus with the largest nonlinear device. When there are multiple harmonic sources, this strategy may not give the optimal solution and further trials may be required by considering the electrically close buses (as shown with the 13 bus industrial system).

BIBLIOGRAPHY

[1] Roger C dugan, Mark F. Mcgranghan, Surya Santoso,H. Wayne Beaty, Electrical Power Systems Quality, McGraw-Hill, 2004.

[2] Alexander Kusko, Marc Thompson, Power Quality in Electrical Systems, McGraw Hill Professional, 2007.

[3] Philip E. C. Stone, Jingjiang Wang Yonge June Shin, Roger A. Dougal, "Efficient Harmonic Filter Allocation in an Industrial Distribution System," *IEEE transactions on industrial electronics*, vol. 59, no. 2, p. 740, 2012.

[4] I. Kocar, J. Mahserdedjian, U. Karragace, G. Soykan, O. Saad, "Multiphase Load Flow Solution For Large Scale Distribuation system using MANA," *IEEE TRANSACTIONS ON POWER DELIVERY*, vol. 29, no. 2, p. 908, 2014.

[5] Task Force on Harmonics Modeling and Simulation, "Modeling and Simulation of the Propagation of Harmonics in Electric Power Networks," *IEEE transaction on Power Delivery*, vol. 11, no. 1, p. 452, 1996.

[6] J. Arrillaga, D. Bradley and P. Bodger, Power System Harmonics, Jhon Wiley& Sons Ltd, 1989.

[7] G. J. Wakileh, Power Systems Harmonics, New York: Springer , 2001.

[8] J. Pedra, , L. Sainz, F. Córcoles, "Harmonic Modeling of Induction Motors," *Electric Power System Research*, vol. 76, p. 936, 2004.

[9] Vikas Singhvi, Student Member, IEEE and, S. Mark Halpin, Fellow, IEEE, "Synchronous Machine Modeling for Low-Frequency Harmonic Studies," in *39th Southeastern Symposium on System Theory*, Macon, 2007.

[10] Wilsun W. Xu Hermann W. Dome1 Jose R. Marti, "A SYNCHRONOUS MACHINE MODEL FOR THREE-PHASE HARMONIC ANALYSIS AND EMTP INITIALIZATION," *Transactions on Power System*, vol. 6, no. 4, p. 1530, 1991.

[11] "Impact of Aggregate Linear Load Modeling on Harmonic Analysis: A Comparison of Common Practice and Analytical Models," *IEEE TRANSACTIONS ON POWER DELIVERY,*, vol. 18, no. 2, p. 625, 2003.

[12] Sergio Herraiz, Luis Sainz, and Jordi Clua, "Review of Harmonic Load Flow Formulations," *IEEE TRANSACTIONS ON POWER DELIVERY*, vol. 18, no. 3, p. 1079, 2003.

[13] W. Xu, Jose R. Marti, Hermann W. Dommel, "A MULTIPHASE HARMONIC LOAD FLOW SOLUTION TECHNIQUE," *IEEE "axions on Power Systems*, vol. 6, no. 1, p. 174, 1991.

[14] Keyhani,A. Abur, Member, S. Hao, "Evaluation of Power Flow Techniques for Personal Computers," *IEEE Transactions on Power Systems*, vol. 4, no. 2, p. 817, 1989.

[15] Vinay Sharma, R.J. FleminG, Leo Niekamp, "An Iterative Approach for Analysis of Harmonic Penetration in the Power Transmission Networks," *IEEE Transmission and Distribution Committee of the IEEE Power Engineering Society* , p. 1698, 1991.

[16] E. Thunberg, L. Soder, Member, "A NORTON APPROACH DISTRIBUTION NETWORK MODELING FOR HARMONIC STUDIES," *IEEE Transactions on Power Delivery*, vol. 14, no. 1, p. 272, 1999.

[17] A. A. Girgis, W. H. Quaintance III, J. Qiu, E. B. Makram, "A TIME-DOMAIN THREE-PHASE POWER SYSTEM IMPEDANCE MODELING APPROACH FOR HARMONIC FILTER ANALYSIS," *IEEE Transactions on Power Delivery*, vol. 8, no. 2, p. 504, 1993.

[18] A. Medina, J. Segundo-Ramirez, P. Ribeiro, W. Xu, K. L. Lian, G. W. Chang, V. Dinavahi, and N. R. Watson, "Harmonic Analysis in Frequency and Time Domain," *IEEE*

TRANSACTIONS ON POWER DELIVERY, vol. 28, no. 3, p. 1813, 2013.

[19] M.A. Moreno Lope de Saa and J. Garcia, "Three Phase Harmonic Load Flow in Frequency and Time domain," *IEE Proc- Electric. Power Appl,* vol. 150, no. 3, p. 295, 2003.

[20] J. R. Carson, "Wave Propagation in Overhead Wires with Ground," *Bell Syst. Tech. J.,* vol. 5, pp. 539-554, 1926.

[21] W. H. Kersting, Distribution System Modeling and Analysis, CRC, 2012.

[22] A. Deri, G. Tevan, A. Semlyen, A. Castanheira, "The Complex Ground Return Plane a Simplified Model for Homogeneous and Mult-Layer Earth Return," *IEEE Transactions on Power Apparatus and Systems,* vol. 100, no. 8, 1981.

[23] R. Horton, W. G. Sunderman, R. F. Arritt, R. C. Dugan,, "IEEE Transactions on Power Apparatus and Systems Earth Voltage Analysis of Multi-Grounded Distribution Feeders," *IEEE,* vol. 1, no. 1, p. 1.

[24] Enrique Acha, Manuel Madrigal, Power Systems Harmonics, Jhon WILEY and Sons, Ltd, 2001.

[25] J. M. Roldan-Fernandez, Francisco M. Gonzalez-Longatt, José Luis Rueda, H. Verdejo, PowerFactory Applications for Power System Analysis, Springer, 2014.

[26] Elham B. makram E.V. Subramaniam Adly A.Girgis, "Harmonic Filter design usung actual recorded data," in *IEEE,* 1992.

[27] Kun Ping Lin, Ming Hoon Lin, and Tung Ping Lin, "An Advanced Computer Code for Single Tuned Harmonic Filter," *IEEE Transactions on industry applications,* vol. 34, no. 4, p. 640, 1998.

[28] Kun-Ping Lin, Ming-Hoon Lin, and Tung-Ping Lin, "An Advanced Computer Code for Single-Tuned Harmonic Filter Design," *IEEE TRANSACTIONS ON INDUSTRY*

APPLICATIONS, vol. 34, no. 4, p. 640, 1998.

[29] Young-Sik Cho, Bok-Ryul Kim, Hanju Cha, "Transfer Function Approach to a Passive Harmonic Filter Design for Industrial Process Application," in *International Conference on Mechanics and Automation* , Xi an, 2010.

[30] Chia-Nan Ko, Ying-Pin Chang, and Chia-Ju Wu, Senior Member, IEEE, "A PSO Method With Nonlinear Time-Varying Evolution for Optimal Design of Harmonic Filters," *IEEE TRANSACTIONS ON POWER SYSTEMS,,* vol. 24, no. 1, p. 437, 2009.

[31] Alexander Kusko, Marc T. Thompson, Power Quality in Electrical System, The McGraw-Hill Companies, 2007.

[32] F. C. D. L. Rosa, Harmonic and Power System, 2006: CRC.

[33] R. Natarajan, Computer-aided Power System Analysis, New york: Marcel Dekker Inc., 2002.

[34] Yong Zhao, Hongying Deng, Jianhua Li, Daozhi Xia, "Optimal Planning of Harmonic Filters on Distribution System by Chance Constrained Programming," *Electrical power system research,* vol. 68, p. 149, 2004.

[35] Gary W. Chang, Hung Lu Wang, and Shou Yung Cgu, "Strategic Placement and Sizing of Passive Filters in a Power System for Controlling Voltage Distortion," *IEEE transaction on power delivery,* vol. 19, no. 3, p. 1204, 2004.

[36] A.M Variz, F. M. Niquini, J.L.R Pereira, P.G. Barbosa, S. Carneiro and P.F. Rebeiro, "Allocation of the Power Harmonic Filters using Genetic Algorithm," in *IEEE international conference on harmonic and quality of power- ICHQP 2012*, 2012.

[37] GaryW. Chang, Shou-Yung Chu and Hung-LuWang, "A New Method of Passive Harmonic Filter Planning for Controlling Voltage Distortion in a Power System," *IEEE TRANSACTIONS ON POWER DELIVERY,* vol. 21, no. 1, p. 305, 2006.

[38] Mohammad A. S. Masoum, Marjan Ladjevardi, Akbar Jafarian, and Ewald F. Fuchs, "Optimal Placement, Replacement and Sizing of Capacitor Banks in Distorted Distribution Networks by Genetic Algorithms," *IEEE TRANSACTIONS ON POWER DELIVERY,* vol. 19, no. 4, p. 1794, 2004.

APPENDIX A – DISTORTION FACTORS

Total Harmonic Distortion is calculated as

$$THD = \frac{\sqrt{V_2^2 + V_3^2 + V_4^2}}{V_1}$$

Individual Harmonic Distortion is given by:

$$IHD = \frac{V_h}{V_1}$$

Where

V_1 : Voltage at fundamental frequency

V_i : Voltage i harmonic order

APPENDIX B – COMMON VOLTAGE AND REACTIVE POWER RATING BASED ON IEEE 18

Volt, rms Line to line	Kvar	Number of phases
216	5, 7 ½, 13 1/3, 20 and 25	1 and 3
240	5, 7 ½, 13 1/3, 20, 25 and 50	1 and 3
480	5, 7 ½, 13 1/3, 20, 25, 50, 60 and 100	1 and 3
600	5, 7 ½, 13 1/3, 20, 25, 50, 60 and 100	1 and 3
2400	50, 100, 150 and 200	1
1770	50, 100, 150 and 200	1
4160	50, 100, 150 and 200	1
4800	50, 100, 150 and 200	1
6640	50, 100, 150, 200, 300 and 400	1
7200	50, 100, 150, 200, 300 and 400	1
7620	50, 100, 150, 200, 300 and 400	1